DEVELOPMENT OF A SYSTEM FOR EXCIMER LASER CORNEAL SURGERY*

BY *George O. Waring III*, MD, FACS

INTRODUCTION

SINCE THE LATE 19TH CENTURY, OPHTHALMIC SURGEONS HAVE CREATED and refined an increasing number of refractive corneal surgical procedures, so that in 1988, more than a dozen different techniques are being used on humans (Table I).[1,2] All of these refractive surgical procedures share two weaknesses, the inability to predict accurately the outcome of surgery for an individual patient and lack of adjustability. The less than desirable predictability stems from variability in surgical techniques and variability in corneal biomechanical properties and wound healing among patients.

The development of pulsed lasers, particularly the argon fluoride (ArF) (193 nm) excimer laser, offers a potential solution to the first of these two problems, because these lasers can create accurate and precise excisions of corneal tissue to an exact depth with minimal disruption of the remaining tissue. Laser surgery can also excise tissues in almost any conceivable configuration. Using computers to control these lasers may create robotic corneal refractive surgery, removing the art from the procedure and allowing the surgeon to perform the exact desired operation, case after case.[3-6]

Since 1983, when excimer lasers were first suggested as instruments for refractive surgery, researchers in laboratories around the world have raced to define the conditions that might make this technology a clinical reality. Depending on one's perspective, progress has moved either rapidly—approximately five systems of varying sophistication currently being available for laboratory and clinical experimentation, or slowly—many fundamental technical and biological questions about the process remaining unanswered.

*From the Refractive Surgery Research Laboratory, Department of Ophthalmology, Emory University School of Medicine and Yerkes Regional Primate Center, Atlanta, Georgia. This research was supported by National Eye Institute grant EY07388, Emory University Biomedical Research Support grant; Grants-in-aid from Emory University, Coherent Radiation Corporation, Research to Prevent Blindness, Inc, and Fight For Sight, Inc.

TABLE I: CLASSIFICATION OF REFRACTIVE CORNEAL SURGERY TECHNIQUES

I. Keratomileusis with microkeratome for myopia, hyperopia, aphakia
   A. Barraquer microkeratome excision and cryolathe carving of lenticule
   B. Nonfreeze, planar, microkeratome carving of lenticule on mold
   C. Keratokyphosis—microkeratome with mold for carving of lamellar bed*
   D. In situ microkeratome excision of tissue from lamellar bed for myopia
   E. Removal and resuturing of lamellar lenticule without excision of tissue for hyperopia
II. Epikeratoplasty
   A. Human donor lenticule
      1. Cryolathe and lyophilization
      2. Nonfreeze, planar microkeratome
      3. With power: myopia, hyperopia, aphakia, astigmatism*
      4. Without power: keratoconus
   B. Synthetic lenticule*
      1. Collagen
      2. Alloplastic
III. Intracorneal lens (keratophakia)
   A. Human donor for hyperopia, aphakia
   B. Hydrogel for aphakia, myopia,* hyperopia*
   C. Fenestrated polysulfone lenticule* for aphakia, myopia, hyperopia
   D. Intracorneal ring* for myopia, hyperopia, aphakia
IV. Lamellar keratoplasty
   A. Central for keratoconus
   B. Peripheral for marginal thinning
V. Keratotomy
   A. Radial for myopia
   B. Transverse with or without radial for astigmatism (many patterns)
   C. Crescentic relaxing incision for astigmatism after penetrating keratoplasty with or without compression sutures
   D. Circumferential (hexagonal) for hyperopia)
VI. Keratectomy—manual
   A. Crescentic wedge resection for astigmatism after penetrating keratoplasty
   B. Crescentic lamellar for marginal thinning
VII. Laser photorefractive keratectomy
   A. Keratomileusis (surface area ablation) for myopia, hyperopia, aphakia
   B. Transverse linear keratectomy for astigmatism
   C. Radial linear keratectomy for myopia*
VIII. Penetrating keratoplasty and cataract surgery (refractive aspects)
   A. Incision technique to create symmetrical, regular wounds
   B. Wound closure techniques to reduce astigmatism
      1. Running sutures
      2. Selective removal of interrupted sutures
   C. Calculations of intraocular lens power
   D. Transverse keratotomy and keratectomy for astigmatism
IX. Thermokeratoplasty
   A. Central heat probe or microwave* for keratoconus
   B. Peripheral radial intrastromal for hyperopia

*Procedures not now in clinical use.
Modified and updated, Waring GO: Development and evaluation of refractive surgical procedures. *J Refract Surg* 1987; 3:142-157.

In this thesis, I summarize the efforts of our research group to develop an excimer laser system for refractive keratoplasty. After considering the terminology of this surgery and a few basic principles of lasers, I present the problems that face the creation of such a system and the solutions found by others, including the selection of an appropriate laser, the design of an effective delivery system, the coupling of the delivery system to the eye, the interaction of the laser with the cornea, the patterns of excisions to alter corneal curvature, and the effect of wound healing on these excisions. Then I describe the approach to solving these problems in our collaborative laser corneal surgery research program, including modifications of an ArF excimer laser, creation of a moving slit delivery system, design of a suction cone coupling and surface condition system, calibration of the ablation curve for the cornea, and characterization of the response of corneal tissue to laser surface keratomileusis in both rabbits and monkeys.

TERMINOLOGY FOR LASER CORNEAL SURGERY

The terminology used in laser corneal surgery can be confusing. Fundamental to all designations is the fact that pulsed laser light removes tissue from the cornea. Therefore, a cut made with the laser is an excision—a keratectomy that leaves a defect, not an incision—a keratotomy that leaves only a dehiscence. A term such as "excimer laser radial keratotomy" is inappropriate.

The fundamental effect of a pulsed excimer laser on tissue is a photochemical one, the breaking of molecular bonds with enough energy that tissue fragments fly from the surface at supersonic speeds; this process has been designated photoablative decomposition—"photoablation" or "ablation" for short. This process contrasts with the more familiar photocoagulation of an argon laser and photodisruption of a neodynium:yitrium-aluminum-garnet (Nd:YAG).[7]

For clinical use, "laser refractive keratoplasty" has the appeal of simplicity, but the generic term photorefractive keratectomy (PRK) is more accurate.[8] "Photo" signifies the laser source; "refractive" alludes to the purpose of the procedure; "keratectomy" indicates corneal tissue removal. Appropriate descriptors easily modify the term, such as "argon fluoride photorefractive keratectomy."

Linear excisions should be designated laser radial keratectomy, laser transverse keratectomy, or simply laser linear keratectomy. This is a bit of a tongue twister, because we are so accustomed to talking about radial keratotomy, but the precisions required of refractive surgery should be reflected in our terminology.

The process of removing tissue from the surface of the central cornea with the laser has been labeled corneal reprofiling, corneal etching, surface area ablation, refractive keratectomy, and laser keratomileusis. The term laser keratomileusis is most appealing, because keratomileusis means "carving or chiseling the cornea," a process that involves removal of tissue from the center of the cornea as part of a lamellar refractive keratoplasty procedure.

Laser circular trephination designates the use of a laser to cut out a corneal button. Laser epikeratoplasty describes using a laser to make an epikeratoplasty lenticule and maybe the groove into which it fits.

Table II presents a proposal for conventional terminology for laser corneal surgery.

TABLE II: PROPOSAL FOR CONVENTIONAL TERMINOLOGY FOR LASER CORNEAL SURGERY

I. Generic terms designating all types of laser corneal surgery
   - A. Laser corneal surgery
   - B. Laser refractive keratoplasty
   - C. PRK

II. Removal of tissue from central cornea
   - A. Terms to designate both refractive or therapeutic surface excisions:
     1. Laser lamellar keratectomy
     2. Surface area ablation
   - B. Term to designate refractive surface ablation: Laser keratomileusis ("carving the cornea"); five types in current use:
     1. Anterior excimer laser keratomileusis
     2. Barraquer cryolathe keratomileusis
     3. BKS,* planar, nonfreeze keratomileusis
     4. Ruiz in situ keratomileusis
     5. Intrastromal dye laser keratomileusis
   - C. Colloquial terms for refractive surface ablation
     1. Reprofiling
     2. Recontouring
     3. Sculpting
     4. Photoetching

III. Linear, arcuate, or circular excisions
   - A. Laser radial keratectomy for myopia
   - B. Laser transverse keratectomy for astigmatism (straight or arcuate)
   - C. Circular keratectomy for penetrating keratoplasty

IV. Removal of lamellar disk of cornea with laser

*BKS, Barraquer-Krumeich-Swinger.

PRINCIPLES OF LASERS

To understand the use of lasers in PRK, it is helpful to review briefly the basic principles of lasers. Details are presented in textbooks.[6,9] We use the ArF excimer laser to illustrate these principles.[5,6,10-12]

Light has both wave-like and particle-like properties. Wave-like properties explain optical phenomena such as refraction and interference; parti-

cle-like properties explain how tissues acquire and release energy—the absorption and emission of light by atoms and molecules. Therefore, we use the terms wave and photon interchangeably, depending on the phenomena that we want to explain.

The electromagnetic spectrum is composed of a broad range of wavelengths, from long ratio waves to short gamma waves. Our interest is in the wavelengths in the invisible ultraviolet range (approximately 100 to 300 nm) to the infrared range (approximately 3000 μm). Each wavelength of the electromagnetic spectrum interacts with the cornea in a specific way. The cornea absorbs well the ultraviolet and infrared radiation and transmits effectively the radiation between 300 to 1300 nm. Numerous wavelengths have been tested for PRK: 193, 248, 308, 2900 to 3000, and 10,600 nm.

SPECIFIC CHARACTERISTICS OF LASER LIGHT AS APPLIED TO CORNEAL SURGERY

Monochromaticity

Light of a single wavelength forms a specific color in the visible spectrum and a specific invisible "color" outside that spectrum. Absolute monochromaticity is an unobtainable goal—even our best laser light is a mixture of some wavelengths. It is this characteristic that determines the amount of laser energy absorbed or transmitted by the cornea.

Directionality

Laser light is essentially collimated light that has a small divergence or spread as it leaves the laser cavity; the spread may vary in different directions. This characteristic allows laser light to be directed at a very small spot a relatively long distance from the laser itself and is the characteristic that allows laser light transmission through the delivery system to the eye. The directionality is measured by the full angle beam divergence in radians. The typical laser beam increases in cross-section about 1 mm for every meter of travel but divergence varies among lasers. For example, the divergence of an excimer laser beam is relatively large; that of a solid state infrared laser relatively small.

Brightness

The intense brightness of the laser light is an expression of the energy contained in the laser beam; because the energy is concentrated in a single wavelength moving in one direction, the radiant energy (measured in joules) is extraordinarily high. This absorbed energy in the cornea is responsible for the ablation of tissue. This radiant exposure of the tissue (sometimes called fluence) is measured in joules/cm^2 (mJ/cm^2); the radiant power is measured in watts; the irradiance is measured in watts/cm^2.

Coherence

Coherence occurs when the light waves in the laser are in phase and there is a predictable and constant correlation between the peak and the rough of the waves. The great regularity of coherence is dependent on the laser's monochromaticity and directionality and is measured by interferometry. Coherence is not a very important characteristic in the use of lasers for corneal or ophthalmic surgery, where the major emphasis is on absorption of specific wavelengths and the energy of the beam. Indeed, excimer lasers emit relatively incoherent beams. Coherence becomes important, however, in the use of lasers for communication, holography, and measurement.

Mode Structure

The distribution of energy in the laser beam is characterized as the mode of the beam, the energy distribution across the beam being called the transverse mode and that along the beam being called the longitudinal mode. The mode structure of the laser beam is important in determining its potential uses, based upon the divergence and coherence of the beam. The transverse mode (more specifically, the transverse electromagnetic mode-TEM) can have a number of patterns and configurations. When there is more power in the center of the beam than at the edge of the beam the mode is designated TEM_{00}. If there is less power in the center and the distribution is bimodal, the designation is TEM_{10}. The simpler the mode structure of the beam the more homogeneous it is. Depending on the resonant properties in the laser cavity, laser beams can acquire many different mode structures, becoming multimode. Excimer lasers produce a multimode beam which is more difficult to render homogenous than are the beams of solid state or dye lasers. A homogeneous beam creates a smoother surface on the cornea.

CREATION OF LASER LIGHT

To create laser light, three basic conditions must exist (Fig 1). First, there must be an active medium—a collection of atoms, molecules, or ions that emit radiation in the optical part of the electromagnetic spectrum. The medium can be (1) a gas such as krypton, carbon dioxide (CO_2), or those in an excimer, (eg, Arf), (2) a solid such as neodynium-doped YAG crystal, or (3) a liquid such as a dye laser. Second, there must be a source of energy for the laser—a pump that can cause a population of atoms to undergo the transition from their ground state to the higher energy level—a population inversion. The pumping may be achieved with an electrical discharge, as in an argon or excimer laser, with a flash lamp as in a Nd:YAG or

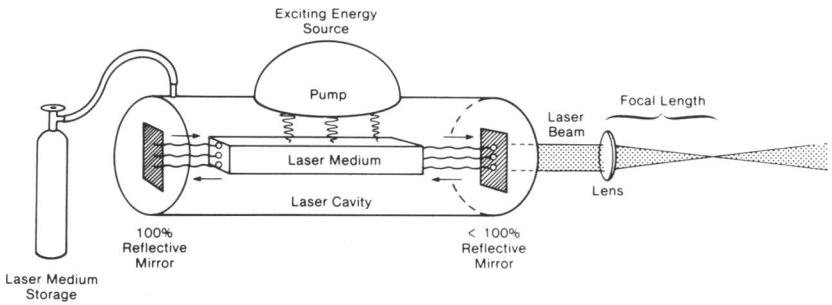

FIGURE 1
Basic configuration of excimer laser demonstrates the active laser medium as gas in the storage tank and in the laser cavity, the exciting energy pumping source illustrated as a bank of electrical capacitors whose discharge can create a population inversion in the laser medium, and the laser cavity with its mirrors at each end to amplify the laser beam before it is emitted through a delivery system containing lenses.

Er:YAG laser, or with an optical source as in dye lasers. The third necessary element is the optical resonator that allows the emitted light beam to feed back by being reflected between two mirrors, stimulating other atoms to a higher energy level in the process, thereby amplifying the light and creating a much more powerful beam. The number of feedback or resonating cycles varies greatly among lasers, from many in the argon to few in an excimer. A more detailed examination of these three components will provide a basis for understanding the development of a system for laser corneal surgery.

Active Medium

The basis for understanding laser action is our current conception of how atoms behave. In an atom, the nucleus of protons and neutrons is surrounded by clouds of electrons at different energy levels—electron orbitals. An atom in its ground state of energy is at rest, but the addition of external radiation can induce it to make a transition to a higher energy level, the electrons being moved from their ground state inner orbital to a higher energy outer orbital. This is a less stable condition, and the electron returns almost immediately to the less energetic resting state, emitting a photon (wavelet) of surplus energy in the process (Fig 2). This photon with its specific wavelength is the basis for creating laser light. When the photon is liberated spontaneously, the process is called spontaneous emission. In reality, however, the emission of photons is stimulated by the external energy source and by the other photons that have been

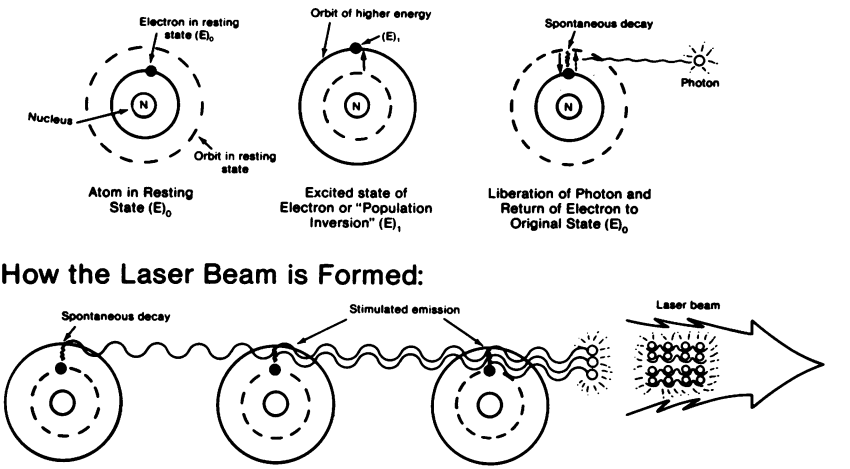

FIGURE 2
Process of photon formation and stimulated emission of radiation from active laser medium is illustrated here and explained in text.

emitted in the active medium. The atoms that undergo stimulated emission radiate their photons (waves) of energy in phase with each other (coherence), so that the waves add energy to each other on a constructive basis, creating the powerful laser light. This circumstance is the basis for the acronym LASER (Light Amplification by Stimulated Emission of Radiation).

Laser Pumping and Population Inversion

To initiate the lasing process, an external source of energy must be pumped into the active medium, so that the atoms can be excited to the higher energy state, a condition known as population inversion. Once this population inversion is achieved, the light amplification by stimulated emission can take place. Many sources of energy can be used. In gas lasers, an electric discharge is commonly used and the electrons in the discharge are accelerated by the electric field between the two electrodes so that they collide with the atoms, ions, or molecules in the gas medium, inducing transitions to higher energy states. In solid state lasers such as the Nd:YAG, the discharge is from a flash lamp. Dye lasers are optically pumped. Most commonly light from another laser that has a peak emission near the dye absorption band creates a continuous wave dye laser. A flash lamp can also be used to create a pulsed dye laser.

The transition of electrons from one energy level to another is not simple, and many transitions can occur in an atom, creating emissions of different wavelengths. Control of this process is part of the sophistication of laser design.

Optical Feedback and Amplification in a Resonating Chamber

The active medium is contained within a resonating chamber, into which the pumping energy is discharged. The resonating chamber consists of mirrors at each end, so that the stimulated emitted photons are reflected back and forth within the resonating cavity. This increases the distance that they travel and insures that the photons strike other atoms of the active medium and stimulate them to higher energy levels, with the production of more photons. This feedback between the mirrors is the basis for the amplification process that creates the great power of a laser beam.

The mirror at one end of the laser cavity is completely reflective, but the mirror at the other end is only partially reflective, allowing the emission of the laser beam. A laser with 98% reflective mirror at the emitting end has an effective length roughly 50 times the actual separation distance between the mirrors. The number of feedback trips varies from laser to laser. In an excimer, for example, the number of oscillations are very few, approximately two in an 80 cm long cavity.

The configuration of the mirrors at either end of the resonating cavity determines the portion of the reflected waves that remain close to the optical axis of the cavity and those that diverge from the axis. Greater divergence creates lower power output. These configurations are called "stability conditions" (Fig 3). A stable resonator cavity has two concave mirrors or one concave and one planar mirror, so that the feedback paths are focused close to the optical axis. An unstable resonator cavity has a central convex mirror at the partially reflective end, so that much of the diverging beam emerges around this mirror. In a stable cavity, less of the light within the cavity is used for the lasing and the emergent beam contains more of the total light. In the unstable resonator, more of the reflected light is used for lasing within the cavity, and a smaller percent of the total light is emitted in the beam. These considerations become important in dealing with excimer lasers in corneal surgery, where higher energy outputs are more difficult to achieve.

Emission of Laser Light

Laser light is emitted either continuously or in pulses (Fig 4). With continuous wave (CW) lasers, a constant pumping of the laser medium

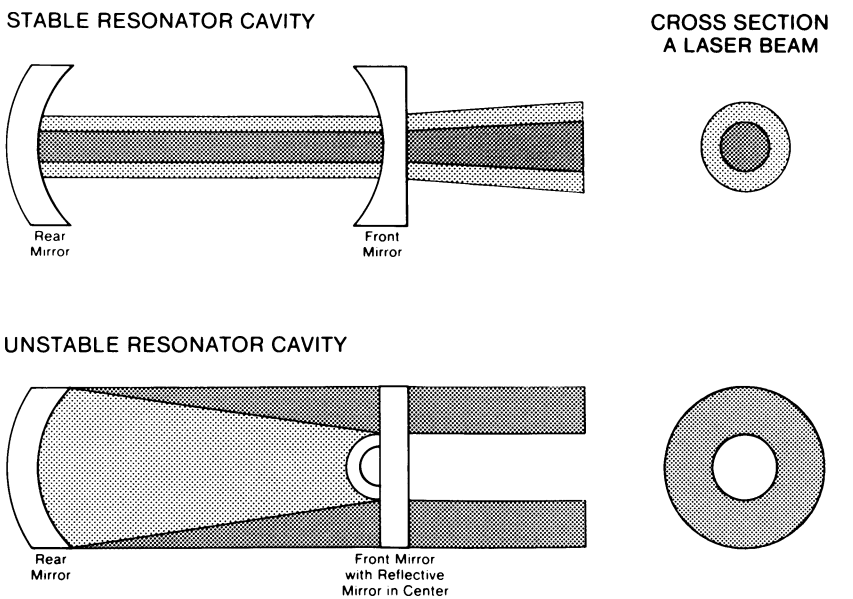

FIGURE 3
Stability conditions in resonating chamber of a laser. In the stable configuration, two concave or a concave and planar mirror are used, resulting in a beam of higher power but more divergence. In an unstable configuration, the transmitting mirror has a convex mirror in the center of it, creating a beam with less power and less divergence and a less regular beam profile.

leads to a stationary emission of light, such as in the familiar argon laser. With pulsed lasers, excitation of the laser medium is achieved by single events, such as the flash from a flash lamp or a periodic electrical discharge, leading to a single short emission of light—the laser pulse. This is familiar in the pulsed Nd:YAG laser. The power of a pulsed laser is on the order of 1 thousand to 1 million times higher than that of a CW laser. Only pulsed lasers are useful in refractive corneal surgery. The power emitted from a pulsed laser can be increased by assuring that the longitudinal modes of the laser beam within the laser cavity are in phase and are emitted in brief spikes-mode locking. Alternatively, an opaque shutter can be placed at the end of the laser cavity to allow a buildup of very high energy within the cavity, so that when the shutter is opened briefly a large amount of energy is dissipated in a single cycle as a high energy pulse—Q-switching. These methods can be used with a Nd:YAG laser, but not with excimer lasers.

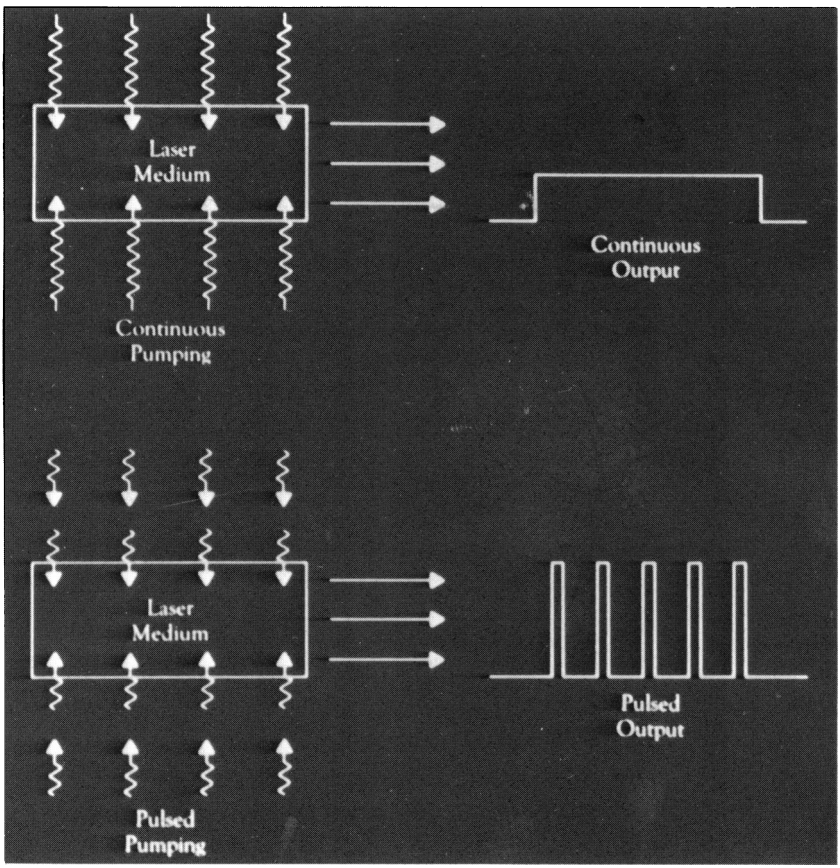

FIGURE 4
Pattern of emission of laser light can be either as a CW from continuous pumping of the laser medium or as individual pulses from intermittent pulsing of the laser medium.

INTERACTION OF LASER LIGHT WITH THE CORNEA

There are four interactions that laser light may have with the cornea: transmission, scattering, reflection, and absorption (Fig 5). Which of these four occurs depends on the laser characteristics and the tissue characteristics.

Transmission of laser light through the normal human cornea generally occurs between wavelengths of 300 and 1600 nm.[12] Thus, lasers such as the argon and the Nd:YAG pass through the cornea without difficulty. Laser light can also be scattered by the tissue if the beam is distributed

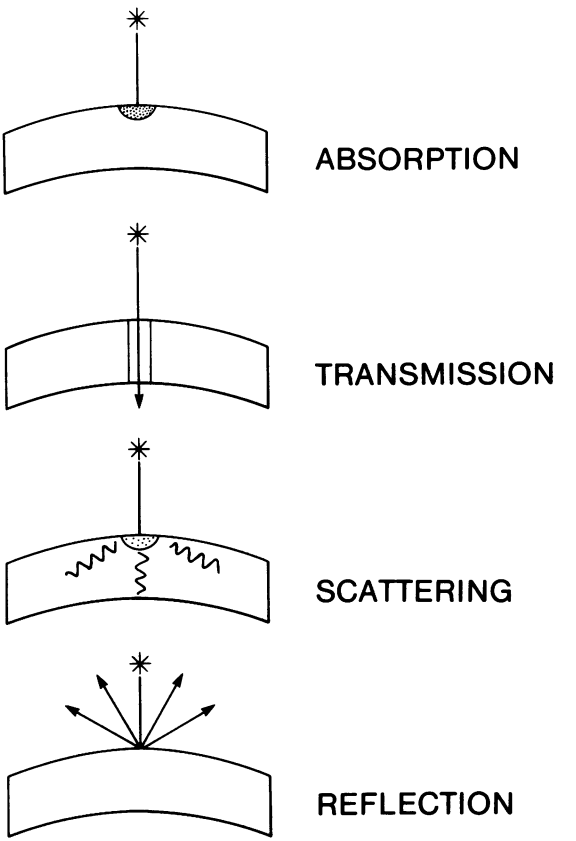

FIGURE 5
Four types of interaction of laser light with the cornea.

over a large area, increasing the extension of thermal and other side effects and decreasing the efficiency of the laser. Reflection of the laser beam seldom occurs from the cornea.

The most important interaction is absorption of the laser energy by the cornea.

ABSORPTION

The greater the absorption, the more "opaque" the cornea is to a given wavelength and the easier the process of surface ablation. Therefore, the key to understanding the appropriate selection of lasers for keratectomy lies in the absorption spectra of chromophores in corneal tissues[13-18]

TABLE III: ABSORPTION BANDS FOR COMPONENTS OF CORNEA

CORNEA COMPONENT	ABSORPTION WAVELENGTH (nm)	LOCATION OF MAJOR CONCENTRATION	OPTICAL RADIATION
Protein[13]	190, 248	Stroma	Ultraviolet
Glycosaminoglycans[14]	190	Stroma	Ultraviolet
Collagen[15]	240	Stroma	Ultraviolet
Nucleic acid[16]	248	Epithelium	Ultraviolet
Ascorbic acid[17]	250	Epithelium	Ultraviolet
Water[18]	2900	Stroma	Infrared
	1000		

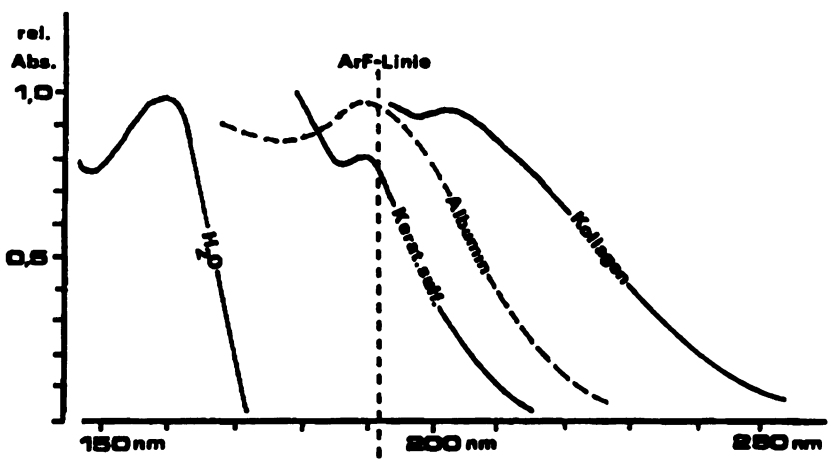

FIGURE 6
Absorption spectrum for molecules in the cornea. The X axis indicates wavelength in nanometers and the Y axis the relative absorption. The *wavy dotted line* shows the reference point for albumin. The *vertical dotted line* shows ArF at 193 nm, where there is a relatively high absorption for collagen, keratin sulfate (courtesy of Theo Seiler, MD).

(Table III) (Fig 6). Light absorption in the cornea occurs in the far ultraviolet region at wavelengths less than 300 nm (absorbed by macromolecules) in both the middle infrared region near 3000 and 6000 nm and the far infrared region above 10,000 nm (absorbed by water).

A good way to conceive of absorption is in terms of the penetration depth of the laser light: the greater the absorption, the less the penetration, the better the potential for surface ablation, and the less chance of thermal damage to the tissue. Table IV lists the penetration depths of

TABLE IV: LASERS POTENTIALLY USABLE FOR KERATECTOMY*

LASER	WAVELENGTH (nm)	PULSE DURATION (nsec)	PENETRATION DEPTH (μm)
Excimer (ArF)	193	10	2
Excimer (KrF)	248	10	10
Excimer (XeCl)	308	10	300
Nd:YAG (5th harmonic)	212	20	2
HF	2870-2910	50	1.5
Er:YAG			
non-Q-switched	2940	200,000	1.5
Q-switched		100	1.5
Raman shifted YAG	2800	10	1.5
CO_2 TEA	10,600	Variable	30

*Courtesy of Theo Seiler, MD, PhD.

lasers that have been used for keratectomy. Ultraviolet lasers have small penetration depth and therefore are best suited for corneal surgery. The hydrogen fluoride (HF), Er:YAG are also well absorbed. Wavelengths absorbed by nucleic acids such as the 248 nm and 308 nm excimers may be mutagenic and therefore are not appropriate for clinical use.

When laser light is absorbed by the cornea, there are three types of effects that can occur: (1) photothermal, (2) photodisruption, and (3) photochemical.

PHOTOTHERMAL EFFECTS

Photothermal effects occur when the energy absorbed by photons produces molecular vibration. This vibration produces heat and increases the temperature enough to break weaker bonds, such as hydrogen bonds, producing protein denaturation.

There are two types of thermal effects: (1) photocoagulation and (2) photovaporization. Photocoagulation is the most common use of CW lasers ophthalmology, such as argon and krypton laser photocoagulation of the retina and choroid. The laser needs to elevate temperature only 10° to to 20°C to coagulate the tissue. Variables set by the surgeon are power, duration of exposure, and spot size.

In photovaporization, very high radiant densities are used and tissue temperature rapidly reaches the boiling point of water, where both coagulation and excision of tissue occur. Photovaporization is the mechanism for keratectomy by the infrared lasers, such as HF and CO_2. The higher the irradiances, the greater the amount of tissue removed and the less the coagulation. For example, a CO_2 laser can ablate corneal tissue with less thermal damage if a pulsed rather than a CW laser is used.

PHOTODISRUPTION EFFECTS

Photodisruption by means of ionization occurs at a very high irradiance with pulse durations shorter than 20 nsec. The high energy density tears electrons from their atomic orbitals and disintegrates the tissue into a gaseous collection of ions and electrons called plasma. The effect produces microexplosions followed by mechanical shock waves. This is the mechanism used by the Nd:YAG laser and the pulsed dye laser.

PHOTOCHEMICAL EFFECTS

Photochemical effects usually occur at shorter wavelengths with low to moderate radiant exposures. There are two basic types of photochemical reactions: photoradiation and photoablation. Photoradiation is used in photoradiation therapy (PRT) in which a hematoprophyrin derivative is selectively taken up by active tumor cells and the laser radiation produces an excited state of the porphyrin which triggers chemical reactions that destroy the cell.

The process most commonly utilized in refractive corneal surgery is ablative photodecomposition (photoablation for short) and is accomplished with ultraviolet radiation. The ultraviolet photons are almost completely absorbed near the surface of the cornea. They also have an extremely high photon energy (6.4 electron volts [ev] at 193 nm), an energy that is in excess of the intermolecular bond energy of approximately 3.5 ev. Thus, the absorption of this energy at the surface breaks up the molecules with such energy that the fragments leave the surface at supersonic velocities of 1000 to 3000 m/sec. The excess energy is carried off and there is minimal thermal damage in the residual tissue.[8,12,19-33] This process is described in detail below.

LASERS USED FOR REFRACTIVE CORNEAL SURGERY

As laser refractive corneal surgery continues to develop and expand, an increasing number of lasers are being used for the process (Table IV). Presently, five types of lasers are under active investigation.

EXCIMER LASERS

Excimer lasers are discussed in detail in this thesis and are briefly defined here. In an excimer laser, the active medium is most commonly the combination of an excited rare gas atom (such as argon or krypton) with a diatomic halogen molecule (such as fluorine or chlorine). The laser is pumped by a high-voltage electrical discharge across the laser cavity and the ultraviolet light beam is emitted with megawatt power and a wave-

length of 190 to 350 nm, which is absorbed by the macromolecules (proteins, nucleic acids, proteoglycans) in the cornea. Excimer lasers have the potential advantage of precisely removing very small amounts of tissue with each pulse, leaving behind minimal thermal or mechanical damage.

Excimer lasers were first developed in 1975.[33] Extensive research on the excimer-polymer interactions was performed by Dyer and Srinivasan,[19] Lazare and Srinivasan,[21] Sutcliffe and Srinivasan,[25] and others,[31] who demonstrated that because the ultraviolet wavelengths were useful for etching silicones and other polymers[29] they might be used for manufacturing microcircuits. Reed and co-workers[34] were the first to use the excimer laser on the cornea; they observed that the corneal epithelium is very sensitive to the wavelengths of krypton fluoride at 248 nm.

The first application for refractive corneal surgery occurred when Srinivasan of the IBM Research Center in Yorktown, New York, and Trokel of Columbia University in New York, reasoned that if excimer lasers could be used to etch and carve polymers, they might be used also to etch and carve the cornea. This resulted in their 1983 publication demonstrating exquisite linear excisions in the cornea and suggesting the use of these lasers for refractive corneal surgery.[32]

Around the same time, L'Esperance filed broad "methods patents" that covered all types of laser corneal surgery using wavelengths less than 400 nm, including excimers. Trokel contended that he was the first person to come up with the idea of corneal laser surgery, and this led the Patent and Trademark Office to begin a legal proceeding known as an interference to determine who was the first to create the idea. IBM joined the legal fray, receiving a broad patent that covers the fundamental use of lasers in the far ultraviolet spectrum to remove human tissue. At the time of this writing, the legal issues are unresolved.[35,36]

CARBON DIOXIDE LASER

In a CO_2 laser, the lasing medium is a mixture of nitrogen, helium, and CO_2. Pumping is usually done by a high-voltage electric current that excites the nitrogen atoms, whose electrons are rapidly transferred to the CO_2 atoms. The excited CO_2 atoms decay, emitting infrared light, most commonly at a wavelength of 10,600 mm. This is amplified within the resonance cavity at high efficiency, and can produce tremendous amounts of output power. Thermal interaction relies on water content to determine the effect produced by the CO_2 laser. The intracellular and extracellular water undergoes an abrupt phase change, creating steam and vaporizing the tissue. The dispersed energy can be absorbed by the tissue

adjacent to the ablation, resulting in coagulation and carbonization of the remaining tissue. However, reducing the exposure time can minimize the thermal effect.

The features of the pulsed CO_2 laser that make it particularly suitable for corneal surgery are: (1) CO_2 laser is strongly absorbed by water molecules, and (2) the thermal relaxation time of water is different than other biological tissues. Since the cornea is composed of 78% water, the corneal endothelium as well as other portions of the eye may be protected from thermal damage from transmitted energy delivered with short exposure times. In other words, it should be possible to vaporize tissue without creating damage to adjacent areas. A large amount of power will need to be delivered during the short pulse duration, creating high power densities. The poor hemostatic ability of the laser utilized in this fashion may be of concern in other tissues, but in an avascular tissue like the cornea, this is not relevant.

The first laser incisions in the cornea were done with a CW CO_2 laser by Fine and colleagues in 1967.[37,38] The deep penetration of about 25 μ caused large zones of thermal damage adjacent to the incision, resulting in inflammation and corneal scarring with a need for penetrating keratoplasty. Beckman and colleagues[39] used a pulsed CO_2 laser, reducing thermal damage to the cornea, but still leaving enough damage to render its use impractical for corneal surgery. Keates et al[40] used a pulsed CO_2 laser and a specially designed delivery system to create a narrow cut into the cornea. The edges of the excised tissue were ragged compared to those achieved with an excimer laser. We have used a pulsed TEA CO_2 laser for experimental corneal surgery, as described elsewhere.[41]

HYDROGEN FLUORIDE LASERS

The lasing medium consists of hydrogen and sulphurhexafluoride gases. The laser is pumped by an electrical discharge into vibrationally excited HF molecules that have a number of emission lines, ranging from 2740 to 2960 nm. These wavelengths are absorbed by water in the cornea.

Two groups have reported on the use of HF lasers for surgery. Seiler and colleagues[42] observed that the excisions of tissue made with the laser created more thermal damage and a more irregular margin than those made with an ArF (193 nm) excimer laser. However, with more careful design of the delivery system and more careful focusing of the laser, sharp-edged excisions with less thermal damage can be achieved.

Loertscher and co-workers[43,44] have used the HF laser to perform penetrating laser circular trephination using an axicon lens delivery system with a narrowly focused beam. Trephinations performed in eye bank

eyes demonstrated vertical excisions with reasonably smooth edges, but not as smooth as those obtained with an ArF excimer.

The experiments performed by these two groups have produced somewhat contradictory results, Seiler and co-workers[42] using lower radiant exposures of 100 mJ/cm^2 while Loertscher and colleagues[45] operated with higher fluences between 0.7 and 2.3 J/cm^2, identifying an ablation threshold of 400 mJ/cm^2 and an optimal radiant exposure to minimize thermal damage of 2 J/cm^2. Both groups have found thermal damage extending at least 10 to 30 μ laterally from the excision. This can be achieved only under optimal conditions. Many ablations show more damage.

The advantages of a HF laser are the simplicity of the laser itself, and the greater possibility of creating delivery systems using fiberoptics and the absence of toxic gases, such as the fluorine in an ArF excimer laser.

ERBIUM:YAG LASER

Very similar to the Nd:YAG laser, this type of a solid state laser uses a YAG crystal doped with erbium ions as a lasing medium. The emitted wavelength is 2.94 μm, very near by the maximal absorption of water. Commercial devices include a Q-switch that is able to create pulses with an energy of 100 mJ and a pulse duration of 100 nsec. Unfortunately, only repetition rates of less than 10 Hz are available.

Early experiments indicate that the ablation threshold of corneal tissue is at about 750 mJ/cm^2, obtained by a pulse length of 600 nsec. The thermal damage zone extends less than 3 to 5 μm into corneal stroma. (Seiler and Bende, oral communication, Gordon conference, 1988).

The advantages of this laser include its small size, easy technical handling, and its transmission through optical fibers, making both direct application to the cornea and intraocular surgery possible. Manufacturing difficulties include the need for special optical elements that contain no absorbed water.

DYE LASERS

In general, lasers that emit visible light are not used for corneal surgery, because they are not absorbed by the cornea. However, if a high enough energy density can be applied in a short enough pulse, a keratectomy can be achieved by tissue disruption or ionization.

In a dye laser, an organic dye dissolved in a solvent is irradiated with a strong light source, such as an argon laser, which causes the dye to fluoresce over a broad spectrum of colors. A specific wavelength can be made to lase by inserting a birefringent crystal into the laser cavity. By turning this crystal, an appropriate angle can be found that will transmit

only a narrow wavelength of light, allowing the operator to turn the crystal and dial up the desired wavelength.

Troutman and co-workers[46] have used a pulsed dye laser to perform intrastromal keratectomies by focusing the laser in the center of the stroma. The rationale behind this approach to laser refractive surgery is to preserve an intact Bowman's layer and anterior corneal stroma so that the all-important anterior corneal surface is essentially undisturbed. The dye laser emitted a wavelength of 595 nm (yellow) which allowed the investigators to obtain radiances of up to 10^{15} watts/cm^2 when in focus, using picosecond pulses. Histological examination of animal and human eye bank eyes showed creation of space within the stroma with damage to the adjacent tissue extending 20 to 40 μ from the wound.

For such an approach to be successful, it must not only produce negligible stromal scarring and opacification from the intrastromal ablation, but it must also change the anterior corneal curvature. Since Bowman's layer and the anterior cornea are reasonably rigid compared to Descemet's membrane and the posterior cornea, and since there is a pressure differential across the cornea from the posterior side (the intraocular pressure exceeding atmospheric pressure), it seems more likely that the posterior layers of the cornea will collapse forward, leaving the anterior layers in their preoperative configuration with minimal change in refraction. It seems that this approach will have more impact in linear excisions rather than in the central surface type of excisions.

EXCIMER LASERS

The term excimer is a contraction of the terms excited dimer, which describe the lasing medium that consists of an atom of an inert gas combined with a molecule of a halide gas, a dimer that exists in an excited state after pumping. Understanding basic features of excimer lasers is helpful for the clinician who uses these systems. Details are available in the literature.[47]

PHYSICS OF EXCIMER LASERS

Lasing Medium

The two gases, inert gas such as argon and a diatomic halide gas such as fluorine, left to their own devices, do not interact; but under the impact of the energy from a high-powered electrical discharge, the electrons are moved to a higher energy state and the atoms become excited and form an unstable molecule, such as ArF. When the molecules delay, they emit highly energetic photons of ultraviolet light.[10]

Within the excimer laser cavity are three gases. The first is a buffer gas that simply mediates the transfer of energy. It is helium or neon and fills 88% to 99% of the cavity. The rare gas (argon, krypton, or xenon) constitutes 0.5% to 12% of the mixture. The halogen (fluorine or chlorine) contributes approximately 0.5% of the mixture. The combination of the rare gas and halogen gas produces photons of a specific wavelength (Table III). Modulation of the buffer gas affects the quality of the laser beam.

Electrical Pumping

Pumping of the laser is produced by an electrical discharge, up to 5% of the energy being converted into laser energy. Electron beam pumping is achieved with a series of high voltage potentials that accelerate electrons to high energies that are transmitted to the laser cavity at beam currents on the order of 100 kAmp. Lasing action is obtained parallel to the electrodes, perpendicular to the electric discharge path. With multiple uses, the gases deteriorate and need to be refilled to maintain the high energy and the quality of the laser beam.

Optics and Resonator Cavity

If the gain produced by the population inversion is so large that lasing occurs without feedback between the mirrors, the laser is termed superradiant. Excimer lasers are almost superradiant but still have a resonator configuration. The back mirror of the laser resonator cavity is completely reflective and the front mirror has a reflectivity of about 4%, which is quite enough because of the high gain of the laser. The partial transmission of the front mirror allows the laser beam to escape in nanosecond pulses. The shape of the emergent beam is determined by stable or unstable configuration of the mirrors of the resonator cavity, as described above.

Effect of Excimer Laser on Materials and Tissue

The mechanism of ablative photodecomposition achieved by this laser is illustrated in Fig 7.[48] Puliafito and colleagues[49] used high speed photography to chronicle the ejection of fragments from the surface, as explained in Fig 8.

EXCIMER LASER VARIABLES

Three types of variables control the effect of an excimer laser on the cornea. (1) The variables in the laser include wavelength, pulse duration, pulse energy, radiant exposure, and peak power. (2) The variables that the surgeon can easily change include the pulse repetition rate, the total number of pulses, the configuration of the laser beam as it emerges from

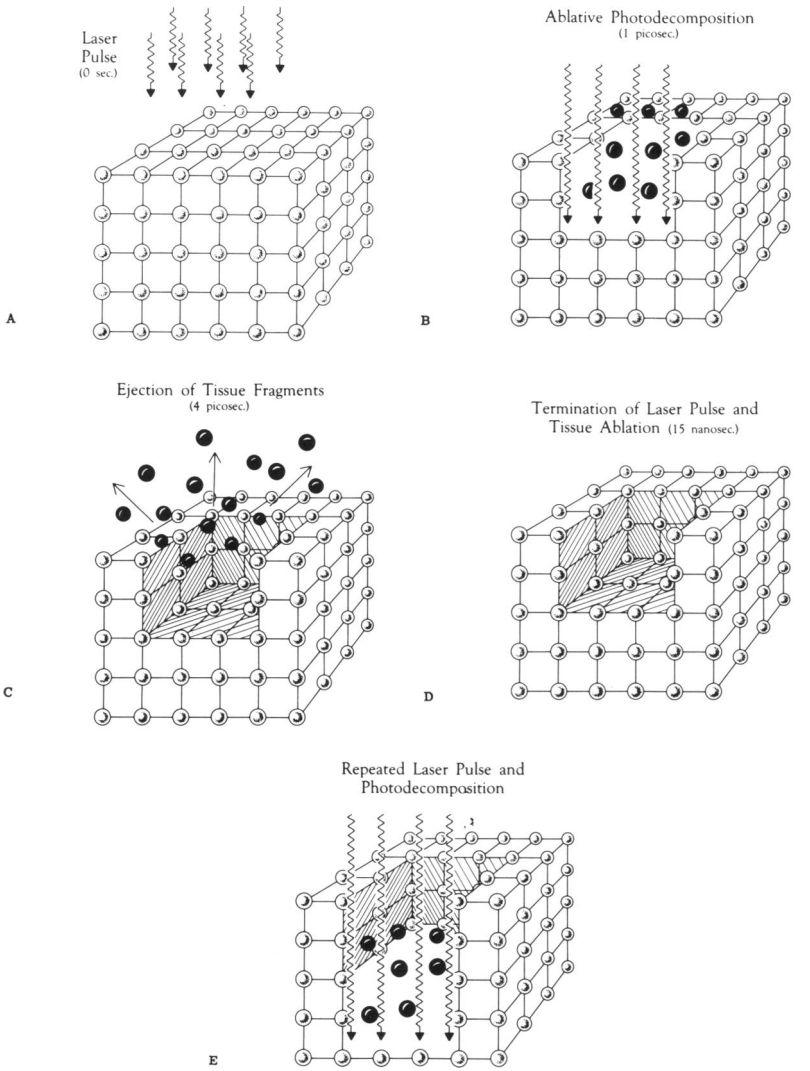

the delivery system, the pattern and sequence in which the pulse hit the cornea. (3) The interaction between the laser and the tissue are determined by the hydration of the cornea, the conditions at the surface of the cornea (eg, disposition of the photofragments) on the depth of penetration of a pulse, the depth of ablation achieved by a single pulse, and the depth of the total excision of tissue. Gaster and colleagues[50] have demonstrated

FIGURE 7

Model for the ablative photodecomposition of the cornea by ArF (193 nm) laser ultraviolet radiation. A: The highly energetic (approximately 6.4 ev) ultraviolet photons head toward the organic material, with the intermolecular bond strength of approximately 3.5 ev. B: The photons break the intermolecular bonds, creating smaller molecular species, such as H^2, CO, CH3, H_2. The entire laser pulse is absorbed in approximately 0.1 to 0.5 μm of the material. C: Because of excess energy from photons and the concentration of this energy in a thin layer of material at the surface, there is an intense build-up of energy and pressure that ejects fragments off the surface at speeds approximating 1500 m/sec. Fragments leave tissue perpendicularly and clear the surface in times of picoseconds to a few nanoseconds. D: Laser pulse terminates at approximately 15 nsec, leaving the surface clear of the fluent and allowing time for dissipation of any thermal energy that may have accumulated. E: Repeated laser pulses ablate successive layers of material, requiring that the fragments travel further to clear the surface and allowing fragments to fall back into ablated area, possibly interfering with successive pulses if they are fired at a rapid rate. (Adapted from Garrison BJ, Srinivasan R: Microscopic model for the ablative photodecomposition of polymers by far ultraviolet radiation [193 nm]. *Appl Phys Lett* 1984; 44:849-851.)[48]

TABLE V: VARIABLES OF PULSED LASERS USED FOR KERATECTOMY

VARIABLE	TYPICAL VALUE FOR DIMENSION	EXPERIMENTAL USE
In the laser		
Wavelength	nm	200 (UV) 3000 (IR) 10,000 (IR)
Pulse duration	nsec	10–100
Pulse energy	mJ	200–2000
Fluence or radiant energy density	mJ/cm^2	100–300 (UV) 1000–3000 (IR)
Peak power	watts	10^8
Beam profile and spatial regularity	% deviation from mean	± 5% to 10%
Adjusted by the surgeon		
Repetition rate	Hz	5–50
Total no. of pulses	N	500–5000
Laser-tissue interactions		
Penetration depth	μm	1–5
Ablation depth	μm/pulse	0.1–0.5 (UV) 0.1–2.0 (IR)
Excision depth	μm	30–400

the effects of laser variables on the rabbit cornea. Table V lists the typical values for these variables. Table VI summarizes the findings of selected studies of the effect of these variables on the cornea.[22,23,32,49-60]

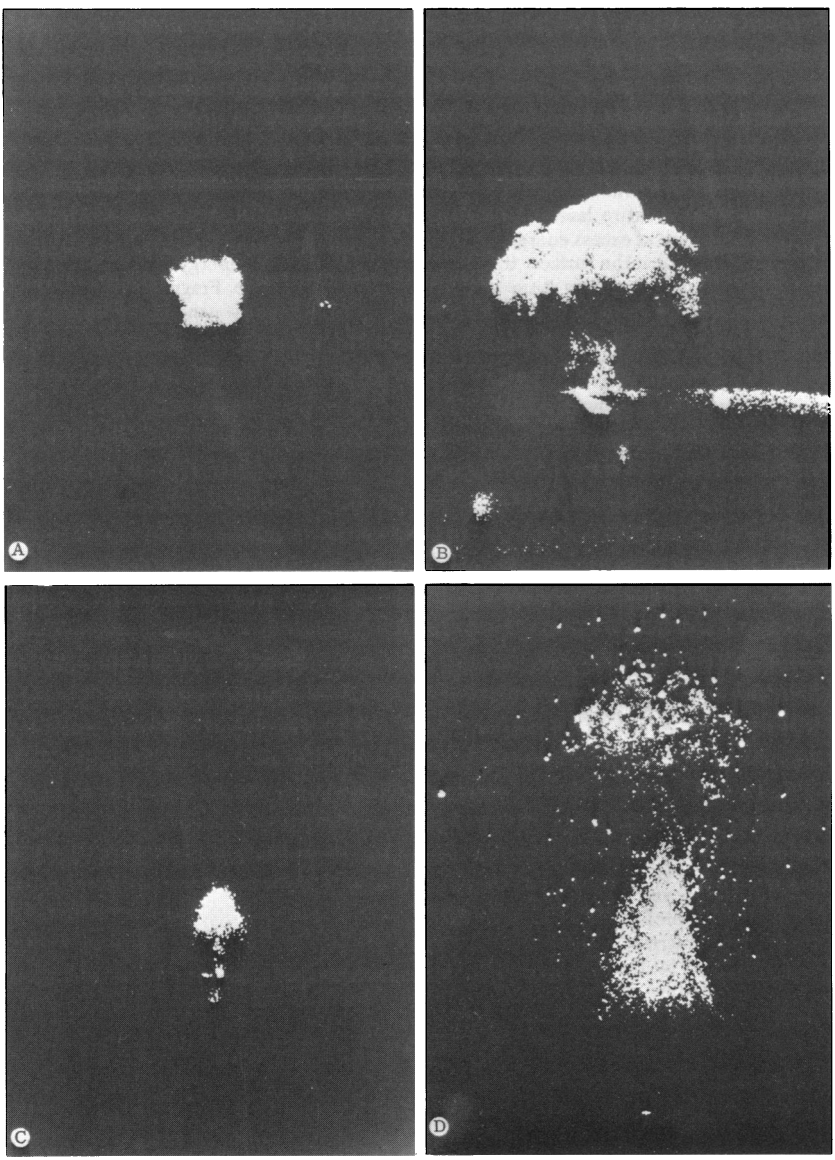
A
B
C
D

FIGURE 8
High speed photography of the excimer laser ablation plume. Ablated fragments of tissue are leaving the surface in a vertical direction at speeds of approximately 2000 m/sec. A: Plume with 193 nm laser approximately 5 microseconds after ablation shows cloud of tissue fragments immediately above the surface. B: Plume from 193 nm laser approximately 50 microseconds after ablation resembles a nuclear mushroom cloud, with fragments expanding away from the surface. C: Plume from 248 nm laser approximately 5 microseconds after ablation shows fragments farther from the surface with expansion into a larger cloud than that seen with 193 nm. D: Plume from 248 nm laser approximately 150 microseconds after ablation shows tissue fragments leaving central cloud. Ablations with 193 nm were performed at 900 mJ/cm^2. Ablations with 248 nm were performed at 500 mJ/cm^2. (Courtesy of Carmen Puliafito, MD) (Puliafito CA, Wong K, Steinert RF: Quantitative and ultrastructural studies of excimer laser ablation of the cornea at 193 and 248 nanometers. *Lasers Surg Med* 1987; 7:155-159.)[49]

Wavelength

Many ultraviolet wavelengths can be generated by excimer lasers (Table IV); laboratory experiments and histopathologic studies have demonstrated that the ArF laser emitting at 193 nm creates the most regular margin of the excision with the least damage to residual tissue.[8,24,32,51,61,62] Presumedly, this is because the shorter wavelengths have the higher photon energies and small penetration depths, and achieve a more purely photochemical process of ablative photodecomposition near the surface, whereas the longer wavelengths of krypton fluoride (9248 nm) and xenon chloride (308 nm) have more energy dissipated in the adjacent tissue, causing thermal damage.

Specifically, Puliafito and colleagues[24] compared in human and bovine corneas the quality of the ablation achieved with ArF at 193 nm and kryptoride at 248 nm. They found a better quality of ablation with the 193 nm laser. The zone of condensation and thermal damage was 0.1 to 0.3 μm thick with 193 nm but it extended 2.5 μm for the 248 nm. The 248 nm wavelength also created more disorganization of the residual stromal tissue. They concluded that the 193 nm excision was similar to the incision made with the diamond knife and that this was the preferred wavelength. Similar findings resulted from studies of Krueger et al[62] using 193 nm, 248 nm and xenon chloride laser emitting at 308 nm. The walls of the remaining tissue at 193 nm showed only a thin layer of condensed tissue at the surface, but at 248 nm the residual tissue was irregular and vacuolated and at 308 nm there was a wide area of cornea necrosis and coagulation, suggesting thermal damage. Similar findings were reported by Peyman et al[63] using 308 nm excimer wavelength. Indeed, the 308 nm wavelength may pass through the cornea and damage intraocular structures. Marshall and colleagues[8] demonstrated that 193 nm could create a smooth ablation surface in contrast to 248 nm, where

TABLE VI: SUMMARY OF SELECTED PUBLISHED STUDIES OF ArF (193 nm) EXCIMER LASER ABLATION OF THE CORNEA

AUTHORS (YR)	RADIANT EXPOSURE (FLUENCE) (mJ/cm²)	REPETITION RATE (Hz)	FINDINGS
Trokel SL, Srinivasan R, Braren B, (1983)[32]	100–200	1–20	Define 193 nm as preferable wavelength for corneal surgery; demonstrated discrete linear excisions; proposed laser keratomileusis
Krueger RR, Trokel SL (1985)[51]	Range of fluences	NR	Ablation profile has sigmoidal shape with 3 different areas: (1) slow, (2) rapid increase, (3) level off; threshold is > 50 mJ/cm²; etching rate varies with fluence: 100 mJ/cm² = 0.1 mm, 200 mJ/cm² = 0.45 mm; most efficient fluence is 200 mJ/cm²
Marshall J, Trokel S, et al (1985)[22]	150, 300	10	Description of "pseudomembrane" condensate on ablated surface, 20 to 100 nm thick; endothelial cell damage beneath excision when < 40 μm from the posterior surface
Marshall J, Trokel S, Rothery S, et al (1986)[23]	150, 300, 450	NR	Very smooth surface when compared with diamond knife incisions; no mention of difference of tissue quality with different parameters
Seiler T, Wollensak J (1986)[52]	100–300	30	Uniform ablation up to 50 Hz, but less uniform at ≥ 60 Hz; ablation depth proportional to exposure time (no. of pulses)
Lieurance RC, Patel AC, Wan WL, et al (1987)[53]	15–30	NR	Good quality, clean lamellar keratectomies by histology, TEM & SEM
Puliafito CA, Wong K, Steinert RF (1987)[49]	95, 306, 612	20	Levels ablation profile off approx 600 mJ/cm²; suggested fluences above this level for less variation between pulses; TEM at 95, 306, and 612 mJ/cm² showed no difference among specimens
Trentacoste J, Thompson K, Parrish RK, et al (1987)[54]	3.5–13.4	1	Fibroblasts and tissue culture did not undergo transformation or mutagenesis after exposure to 193 nm radiation
Munnerlyn CR, Kooms SJ, Marshall J (1988)[55]	200–214	20	Calculation of depth of ablation required for optical correction of varying diameters of optical zone: 3 mm = 3 μm/D; 4 mm = 5.3 μm/D; 5 mm = 8.3 μm/D; rotation of beam for spatial averaging

Marshall J, Trokel SL, Rothery S, et al (988)[56]	140, 310	5–10	3 mm diameter ablation in monkeys 40–130 μm deep showed faint haze up to 6 mos with later clearing grossly but persistent haze biomicroscopically; epithelium and epithelial basement membrane healed normally by 1 mo; subepithelial fibroplasia occurred with good remodeling by 8 mos
Serdarevic ON, Hanna K, Gribomont A, et al (1988)[57]	110	15–20	Rotating slit excimer laser circular trephination wound were more uniform in human eye bank eyes and in rabbits than those achieved with mechanical trephines; more endothelial damage occurred with mechanical trephination; there were no differences in rates of wound healing in rabbits up to 3 mos
Tenner A, Neuhann T, Schroder E, et al (1988)[58]	NR	NR	Three human eyes received 8-incision linear radial keratectomy to about 50% of corneal depth; with a 5 mm clear zone, mean keratometric flattening of approx 1.75 D was achieved in two eyes at 6 mos
Hanna K, Chastang JC, Pouliquen Y, et al (1988)[59]	200	20	Each 4.5 mJ pulse ablated at 0.17 μm in stroma; slit of calculated shape rotating at 0.03 Hz created minus lens surface contour
L'Esperance FA, Warner JW, Telfair WB, et al (1989)[60]	80–125	10	Eleven humans with severe ocular disease had 3–5 mm diameter, 30–150 μ deep, circular superficial keratectomy; slit-lamp examination showed fine fibrillar subepithelial haze; delivery system using a rotating disc with varying sized circular apertures, a keratoscope imaging system and a beam homogenizing and measuring system is described
Gaster RN, Binder PS, Coalwell K, et al (1989)[50]	23–178	10–40	Unmodified ArF excimer laser used to ablate 6 mm diameter central area of rabbit corneas using a variety of radiant exposures and repetition rates showed the laser beam to be nonuniform, and demonstrated best epithelial and stromal healing at a low fluence of 23 mJ/cm^2 and repetition rate of 40 Hz when examined up to 3 mos after surgery

NR, not reported.

edges and surface of the ablated zone were rougher with a 2 to 3 μm-wide area of disruption of residual stromal tissue.

Thus, the experience of all researchers seems consistent at this point: 193 nm ArF lasers produce the most acceptable wounds in the cornea. As mentioned above, the proteins and proteoglycans of the cornea have a peak absorption at 190 nm, making the ArF laser ideal. Collagen and nucleic acids have absorption at slightly higher wavelengths of 240 to 250 nm.

However, these wavelengths and their high energies impose limitations on the design of laser delivery systems. For example, excimer lasers cannot be transmitted through fiberoptic bundles and they damage lenses and mirrors that do not have special nonabsorbing coatings.

Pulse Duration

The duration of a single excimer laser pulse depends on the short lifetime of the excited dimer molecule—10 to 20 nsec. The longer the wavelength, the shorter the pulse required to enhance the ablative action and minimize thermal effects. For example, at the 248 nm wavelength, a pulse duration as low as 300 femtoseconds can be achieved to improve the uniformity of the remaining surface.

Pulse Energy

Interestingly, the total energy delivered in a single excimer laser pulse is not very great, usually a few hundred millijoules. However, because the pulses are of such short duration, a high power is achieved, more than 10 million watts. This power may produce some plasma along with the ejected tissue fragments but is far below the threshold for optical breakdown. There must be a uniform energy in each pulse, so that the total ablation of the tissue can be calculated and so that a uniform surface will result. Using a 193 nm excimer, the fluctuation of individual pulse energy is on the order of 5% to 10%,[10] a level too high to obtain refractive corrections of ± 0.25 diopter accuracy. However, when using a pulse train of about 1000 pulses, this fluctuation averages out to less than ± 0.3%.

Radiant Exposure (Fluence)

Radiant exposure or "fluence" is a measure of the energy flux per unit area at the surface of the material ablated. It is usually expressed as millijoules per square centimeter (mJ/cm^2). An ablation curve plots the amount of tissue removed and the cornea experiences only surface photochemical changes. Tissue removal begins at the ablation threshold, which is approximately 50 to 75 mJ/cm^2 for 193 nm in the cornea. The curve rises slowly, as the radiant exposure increases, until it reaches a level-off point, where

it flattens at approximately 600 mJ/cm^2. After this point, increasing fluences are not associated with increased tissue ablation.[8,28,49,62,64] The ablation threshold and the inflection on the curve vary with corneas from different species.[8,64] Human cadaver eyes have shown an inflection point in the curve as high as 1000 mJ/cm^2.[64]

The rate of tissue ablation and consequently the location of the inflection point on the ablation curve varies with the hydration and thickness of the cornea (Fig 9). This can be important in calculating the number of pulses used for a given refractive procedure in individuals with corneas of varying thickness and may have its greatest effect if excimer lasers are used in a therapeutic setting, such as the treatment of corneal infections or of superficial opacities such as band keratopathy. Thus, in calibrating a laser on corneal tissue to determine its rate of ablation and the number of pulses necessary for a surgical procedure, the cornea must be dehydrated to a normal thickness.

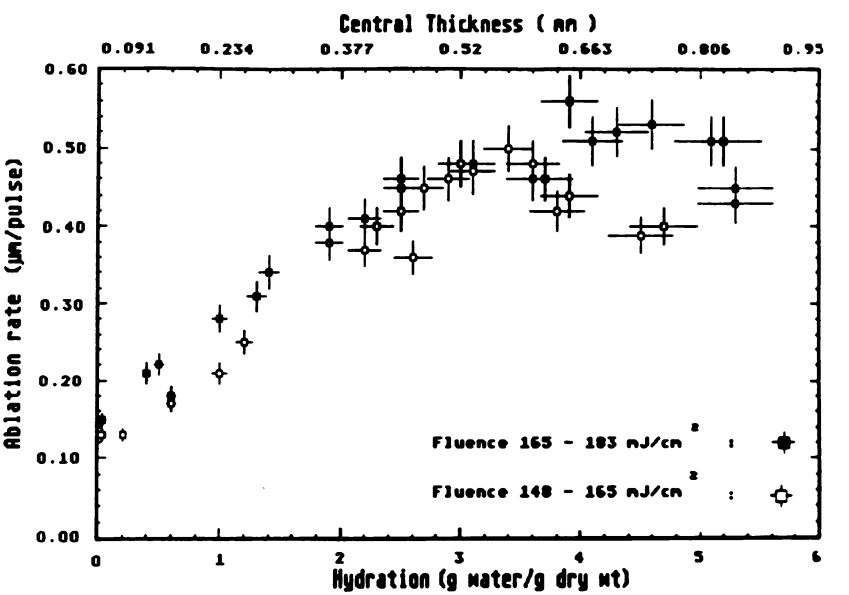

FIGURE 9

Effective corneal hydration on ablation rate demonstrates that below normal corneal thickness, a marked effect is present. In the range of normal corneal thickness from approximately 0.50 to 0.60, the ablation rate is reasonably constant. However, swollen corneas demonstrate some fall off the ablation rate, which can substantially alter the number of pulses needed to remove a specific amount of tissue to affect a given refractive change.

As the radiant exposure increases, an optimal fluence is reached where for a minimum exposure, tissue is most effectively removed. The exact location of this point is not known, although most studies have been done between 150 and 250 mJ/cm^2.[27,51,64,65] This is in the middle of the steepest part of the curve, but the value has been commonly derived from experiments on enucleated eyes, that may have been swollen. At this fluence, the laser ablates approximately 0.45 μ of tissue per pulse. It is difficult to work on this ascending part of the ablation curve at values of approximately 200 mJ/cm^2 because small differences in the energy density will create larger differences in the amount of tissue removed. Therefore, the beam must have a homogeneous energy profile and be uniform from pulse to pulse. Variations in these factors will produce a rougher surface. Working at higher fluences of 600 mJ/cm^2 or above may obviate this problem, because in this flat part of the curve, the same amount of tissue is removed regardless of the energy density, so the technical demand for homogeneous beam and uniform pulse is not as great.[12,55] Electromicroscopic studies have not demonstrated differences in the amount of residual tissue damage when fluences of 95, 306, and 612 mJ/cm^2 were used.[49] Indeed, ablations of cornea tissue have been performed up to 30,000 mJ/cm^2, still showing minimal disruption of residual tissue.[53] A possible explanation for this lack of tissue damage at higher fluences is that the superficiality of the ablation allows heat to escape from the surface with the ejected tissue fragments and a repetition rate slow enough allows time between pulses for the heat to dissipate, so that it does not penetrate the remaining tissue.

The fact that the amount of tissue removed can be precisely determined for a single pulse at a given fluence is the basis for the exquisite accuracy and precision promised by excimer lasers for PRK.

Homogeneity of the Laser Beam and Uniformity of the Ablated Surface

Beam uniformity is important, because the energy profile of the beam is projected onto the surface of the cornea, leaving its fingerprint. If the beam has more energy concentrated in the center, the ablated area will have a central depression, whereas a beam with more energy concentrated at the periphery will create a doughnut configuration in the tissue. Since one of the goals of PRK is to create as smooth a surface as possible, it is desirable to have as homogeneous a beam as possible. The laser beam at 193 nm is not homogeneous as it emerges from the resonating cavity, the energy density being greater in the center. Furthermore, the beam does not have a defined mode structure, and therefore is characterized only as a profile of energy density transversely and longitudinally. The beam profiles can change between pulses and have a tendency to become less

uniform as the gases in the active medium degrade.

Adjustments can be made to improve the homogeneity of the laser beam. Inside the resonating cavity, the electrodes that provide the pumping energy can be kept clean and smooth for a uniform discharge. The gases can be kept in a pure state by refilling the cavity periodically. The resonating mirrors can be aligned to improve the lasing process. The cavity can be configured as a stable resonator to improve beam uniformity. In the delivery system, clean coated optical elements can be used to avoid degradation of the image by erosion of the surface. Masks can be used to "scrape off" the less homogeneous edges of the laser beam. Beam homogenizers can be employed to fold the beam on itself, and "smooth out" the inherent inhomogeneities. The beam can be moved over the surface of the cornea so that the same shape beam does not strike the same location sequentially, avoiding the effect of imprinting inhomogeneities on the tissue. The environment over the tissue can be conditioned by removing air particles and water vapor which tend to absorb the laser energy irregularly and by removing the ejected photofragments which tend to irregularly block the laser beam on its way to the tissue.

Pulse Repetition Rate

The rate of delivery of the laser pulses to the cornea is measured as the number of pulses per second, expressed in Hertz (Hz). Ideally, laser corneal surgery should be completed as rapidly as possible to decrease the chances of patient movement and instrument malfunction. Therefore, a higher repetition rate is most desirable. However, there are marked limitations to the use of higher repetition rates (> 60 Hz) with excimer lasers because the rapid sequence of pulses creates a thermal effect in the tissue and damages the optical components of the delivery system. In addition, the consistency of the pulse energy and beam profile may decline at higher rates.[52]

The time for diffusion of heat in the cornea is on the order of 1 second, and therefore repetition rates higher than 1 Hz allow heat to accumulate. In repetition rates higher than 60 Hz, the temperature may rise more than 10°C adjacent to the area of excision, depending on the fluence. In addition, pulses delivered in rapid succession may create an accumulation of ejected fragments that block the effectiveness of successive pulses.

Currently, repetition rates from 5 to 30 Hz are being used,[8,24,32,59,66,67] the most common being around 10 Hz.

Number of Pulses

The most important factor that the surgeon controls is the number of pulses, because this determines the amount of tissue removed. Poten-

tially, this allows the surgeon to make a radial or transverse linear excision of an exact known depth uniform from end to end or perform laser keratomileusis by ablating a profile on the cornea of exact contour. The surgeon would compute the overall excision depth prior to surgery by multiplying the ablation depth per pulse times the total number of pulses. For example, if the surgeon wants to excise 100 μm of the cornea at 0.45 μm per pulse, a value of 222 pulses (100/45 = 222) would be entered into the operation terminal of the laser before surgery.

The simplicity of this data is confounded by a number of problems. First, the consistency of the pulse energy and the spatial uniformity of the beam profile can vary 5% to 10%, creating some inherent irregularity of the surface. Second, different tissues ablate at different rates, the epithelium and Bowman's layer ablate differently than the stroma depending on the radiant exposure, for example. This would have been taken into consideration in preoperative calculations for the amount of tissue removed. Third, laser keratomileusis requires removal of different amounts of tissue in different areas of the cornea to create a new optical profile, and this presents a challenge in the design of the delivery system. Fourth, changes in conditions during the surgery such as movement of the eye, variation in corneal thickness from changes in hydration and contamination of the surface with fluid, make the exact determination of the number of pulses needed to remove a calculated amount of tissue more difficult.

One method to empirically determine the ablation rate is to use a human donor eye of normal thickness as a calibration scale immediately prior to performing surgery. The thickness of the cornea is measured by ultrasonic pachometry and the cornea is then exposed to the laser beam until the cornea perforates. The ablation rate can be calculated by dividing the corneal thickness by the total number of pulses needed. This approach will obviate variability in the laser and delivery system, assuming the laser works the same on the test cornea as on the patient's cornea. However, it assumes that the test cornea and the patient's cornea are similar enough to have similar ablation rates. For example, a swollen test cornea may give inaccurate results.

EXCIMER LASER DELIVERY SYSTEMS

Between the time the laser beam emerges from the resonating cavity and the time it strikes the surface of the cornea, it must be modulated and shaped by a delivery system. In general, the delivery systems required for excimer lasers are more complex than those needed for the more familiar CW argon or pulsed Nd:YAG lasers. This requires a combination

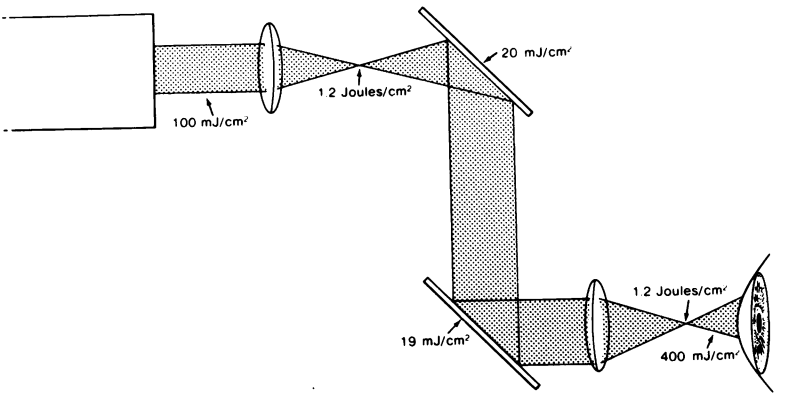

FIGURE 10
General depiction of the elements of an excimer laser delivery system. Cylindrical and spherical lenses can shape the beam and mirrors can direct the beam. In general, the optical elements should be placed at a distance from the focal point where the energy density is high, to decrease damage caused by laser beam. Not depicted are other elements of a delivery system, such as the mask to shape the beam, moving prisms or mirrors or masks to homogenize the beam and detectors to measure the beam.

of lenses, mirrors, masks, homogenizers, motors, computers, and detectors—all assembled in a clinically useful device that must be simple to use, versatile, and able to withstand the impact of the excimer beam itself (Fig 10).[59,68]

A variety of delivery systems have been designed by ophthalmologists, engineers, and commercial firms, and it is not possible to review each of these designs here, because of lack of space and because some of the information has been kept proprietary. Most companies work closely in conjunction with ophthalmologists. Active companies at the time of this writing include IBM, General Electric, Summit Technologies, Visx Corporation, Taunton Technologies, Meditech, as well as French and Soviet concerns.

Optical Elements

The high energy excimer laser will easily damage conventional lenses, mirrors and prisms, even if made of quartz. To solve this problem, the optics should be made of magnesium fluoride or calcium fluoride. In addition, the beam can be optically expanded so that the energy density is less at the optical interface and then re-focused by an objective lens at the end of the system. At every optical interface, some of the energy is lost, so that the more complex the delivery system and the less efficient its components, the more powerful the laser required to deliver a beam of

useful energy to the cornea, especially if there is a need to work at higher fluences along the upper part of the ablation curve.

The optical elements must be well aligned with the emergent beam and with each other for efficient transmission. The easiest "alignment system" is to transmit the beam through a fiberoptic bundle, but no optical fiber material is available that can withstand the power of the 193 nm ultraviolet excimer laser, so helium neon lasers are commonly used for alignment.

Control of Beam Uniformity

The energy profile of the beam as it is emitted from the laser must be improved as it travels through the delivery system to present the most homogeneous beam to the tissue. All optical elements must have smooth, nondegraded surfaces, so that they do not disrupt the beam. Masking the peripheral part of the beam and using only its more homogeneous central part will enhance uniformity. Rotating prisms or lenses and beam integrators can make the beam more homogeneous.

A variety of beam homogenizers can be designed into the delivery system, including prisms or mirrors that rotate or fold the beam, to time average the multiple pulses delivered to the cornea such that hot spots and cold spots in different pulses cancel each other out, and the result is a relatively homogeneous beam.

One way to test the homogeneity of the beam as it emerges from the delivery system is to fire a few pulses onto black photographic paper. A series of shots will gradually ablate the black emulsion to reveal the white material beneath, and this will easily reveal the inhomogeneities of the beam as lack of uniformity in the black and white ablated paper. Hot spots become totally white; cold spots remain black.

Shaping the Beam for Refractive Ablation

The shape of the ablated area on the cornea is determined by the shape of the beam that strikes the cornea. The ideal shape is selected based upon the ametropia to be corrected and the refractive surgical technique used,[2] as discussed in subsequent sections on laser linear keratectomy and laser keratomileusis.

Two methods are available for shaping the beam: masks and lenses. The principle of using a mask is to create an aperture that will ablate a desired profile on the cornea. Lenses project a beam of desired configuration on the cornea.

Slit Masks—The simplest method is a rectangular narrow slit to make a linear radial keratectomy to correct myopia or linear transverse or arcuate excision to correct astigmatism. If enough is available, four or eight radial slits could be superimposed on the surface of the cornea and all irradiated

at the same time to make simultaneous radial excisions, but this would waste a lot of energy impacting the areas between the slits in the mask. Therefore, a cylindrical lens can be used to shape the beam into a narrow rectangle that is then imaged onto the slit apertures in the mask and each of the four or eight slits is irradiated in turn. Such systems have been designed by Meditech[69] (Seiler and colleagues[65]) and by IBM as described by Hanna et al.[59] It is also possible to use an optical system of cylindrical lenses alone to create a slit-shaped beam and deliver it to the cornea without a mask. Slit-shaped masks can also be applied directly to the cornea to shape the beam immediately before it contacts the tissue. A foil-coated contact lens designed by Seiler in conjunction with Summit Technology can be laid directly on the surface of the cornea, the slit being aligned in the desired direction. A suction ring with slit masks in the middle has been designed by Meditech to attach to the limbus, with the slits being oriented in the proper direction over the cornea.

Diaphragm Masks—For laser keratomileusis (surface area ablation) a circular mask can be used. Obviously, if a simple circle is used, a cylindrical depression with steep edges will appear without predictable refractive effect. However, if a slowly constricting diaphragm is used to ablate a fixed circular area of the central cornea (ie, 6 mm in diameter) the outer portion of the ablation will be shallower than the continuously exposed inner portion. The profile of this ablation can be controlled by the rate of constriction of the diaphragm and the number of steps during the constriction, the central area achieving the greatest ablation. This would create a minus lens effect on the surface of the cornea to treat myopia. The diaphragm would be under mechanical control and could be linked to a feedback system for fine control. This approach has been used in the Visx (formerly Cooper) system.[67]

Advantages of the diaphragm are its relative simplicity and ease of centration. Another advantage is the rapid rate at which an area ablation can be accomplished—less than 1 minute. Disadvantages include the limitation of treating only myopia. In addition, the central cornea is exposed to all successive pulses, possibly elevating the temperature there and requiring that the ejected fragments be removed from the surface by suction or blowing air. As the diaphragm closes in steps, the edges of each circle are etched on the corneal surface, creating some irregularity; the more steps, the smoother the surface. The Visx delivery system uses this method.

Multiple Disc Masks—Another type of mask delivery system involves the use of a single circular disc with different sized apertures in it. For example, a sequence of circular apertures, from large (7 mm diameter)

down to small (1 mm diameter) can be used to make a series of progressively constricting, stepped excisions of tissue by first exposing the large mask, then the next smallest, then the next, etc. This will create a negative lens effect to correct myopia. A similar approach can be used to correct hyperopia, using translucent glass to block the central unablated zone and create annular apertures. A sequence of slits of different widths and orientation can be used to correct astigmatism. This system has been employed by Taunton Technologies.[60]

Moving Slit Mask—Another type of masking involves creating a slit image that moves over the surface of the cornea either rotating around a central point or translating across the surface.[59,66] The shape of the slit can be designed to correct virtually any ametropia. Linear slits create radial or transverse keratectomies. A slit wider near its central portion would ablate more central tissue from the cornea to correct myopia. A slit wider near the ends would ablate more of the paracentral cornea and correct hyperopia. Astigmatism could be corrected by using variations in the rate of movement of the slit, so that one meridian was exposed to more pulses than another or by passing the slit more frequently over one meridian than the other. Uniformly shaped linear slits can create radial or transverse linear keratectomies. A moving slit system has been designed by Hanna and colleagues[59,66] and is described in detail below.

A moving slit has some advantages. It can be modified to treat any ametropia. It does not ablate the same area of the cornea successively, so there is less thermal effect. The slit shape is infinitely modifiable, so that the pattern or laser ablation of the cornea can be tailored to the patient's need. A moving slit has disadvantages, including the irregular junction between each of the slit-shaped ablated areas and the need for more precise alignment and mechanical stability. In addition, it may be a slower method of ablation, depending upon the rate of the movement of the slit, requiring a few minutes.

Any moving mask system whether diaphragm, disc or slit, will require control of the rate of movement to govern the number of pulses that strike the cornea in a given area and to insure an accurate ablation profile. This requires accurate mathematical calculations that take into account the configuration of the aperture in the mask, the rate of movement of the aperture over the surface of the cornea and the repetition rate as well as computer controlled servomotors to move the mask or the optical elements.

Optical Shaping of Beam—A cylindrical lens can be placed in the delivery system to create a linear beam configuration that will ablate radial or transverse linear keratectomies in the cornea. This is one of the

earliest methods used to test the different wavelengths of excimer lasers.[24]

An axicon lens can be used to create a circular pattern. The axicon lenses are cone-shaped and refract the laser light from the original central axis out to the edge of the ring-shaped lens, projecting a circle onto the cornea. This system has been used by Loertscher, Thompson, and colleagues at the Bascom Palmer Eye Institute for circular corneal trephination. This system could be modified to create two parallel surfaces that would image two transverse slits simultaneously for the correction of astigmatism.

Properly coated optical systems transmit more energy than masks which block considerable areas of the laser. If the beam is optically shaped to conform to the size of the mask aperture, less energy is wasted on the edge of the mask.

To date, an optical system has not been developed to perform laser keratomileusis, because the design of such a system would require novel lens profiles for each refractive effect.

Measuring the Beam Intensity and Configuration

All of the processes that modify the beam will affect its energy profile. The surgeon needs the confidence that the pulse impinging on the cornea meet the calculated specifications. This requires detectors built into the system that can measure the final pulse energy, and beam homogeneity and shape. Ideally, this detecting system would be linked to a computer-controlled feedback mechanism that could modulate both the output from the laser and the beam management in the delivery system to insure that each pulse meets exact specifications. The Taunton Technologies system incorporates a beam intensity profilometer with computer software that generates color-coded images of the energy distribution across the beam as it emerges from the delivery system[60] but with no integrated feedback to regulate the laser system.

SYSTEMS TO COUPLE LASER AND EYE

Because PRK is done within micrometer accuracy, the demands for stability of the eye are greater than those required during other ophthalmic laser procedures. For example, during argon laser photocoagulation of the retina or Nd:YAG photodisruption of the posterior lens capsule, the eye can move between laser shots, because the interaction between the laser and a single spot on the tissue is brief and because the location of the laser shot needs to be controlled only within tenths of a millimeter. In PRK, even though interaction between the laser and the tissue lasts only

nanoseconds, the train of pulses must be delivered with submicron accuracy to the same or exactly adjacent areas of the cornea during the entire 30-second to 5-minute procedure. Therefore, the eye must be kept in a fixed position with respect to the laser using a coupling system.

Variables in Coupling System

Position of the Patient—The first element in coupling is to position the patient comfortably in a stable position in front of the delivery system. Early attempts to accomplish this with the patient in a seated position before a slit-lamp apparatus achieved less control, so that most systems now allow the patient to lie on a bed beneath the overhanging delivery system.

Observation of the Cornea—The surgeon should have visual control of the ablation process through an operating microscope to monitor its progress, preferably viewing coaxial with the laser beam path.

Aiming the Laser—Because the lasers used for PRK have wavelengths outside the visible spectrum, an auxiliary aiming laser (usually a helium-neon laser) that is coaxial to the ablating laser is required to align and aim the laser.

Stabilization of the Eye—Early attempts at excimer laser corneal surgery used manual stabilization of the eye and manually controlled micromanipulators to aim the beam. This can be adequate for therapeutic purposes, such as ablating the bed of an excised pterygium, but the level of control is far from that required for refractive purposes.

Eye movements create two problems. The first is ablation of areas of the cornea outside the target zone, so that linear ablations become wide, V-shaped troughs and surface area ablations have more irregular margins and surfaces. The second problem concerns pulses that strike areas other than those intended; these aberrant pulses alter the calculated amount of tissue ablation and disrupt the desired new corneal profile.

Types of Coupling Systems

Contact Lens Mask—The eye can be stabilized during procedures that use a fixed aperture, such as a slit, by having the slits in a contact lens placed directly on the cornea. This approach has been taken by Seiler et al[65] and by the Meditech system. If the eye moves, the contact lens moves and the ablated area remains located beneath the opening in the mask. The contact lens mask is made of polymethymethacrylate, which is readily available to fit the patient's corneal curvature. The lenses are coated with a reflective layer foil, so that the material is not heated and the laser only passes through the slit. The size of slit shape perforations used by Seiler are 0.12 mm wide and 3 to 5 mm long. The laser beam, configured as a

straight linear slit is aligned to overlap the slit opening in the contact lens.

Fixation Rings—The eye can be stabilized by mechanical devices such as fixation rings. These can be suction rings, such as the Barraquer or Hanna ring used with keratomileusis and corneal trephination. The ring can be hand-held or mechanically attached to the delivery system. Compression rings, such as that designed by Thornton, can also be used either hand-held or mechanically secured.

Eye Tracking Systems—The most elegant type of coupling system has not yet been devised—an optical tracking system. Tracking systems available in the defense industry could be adapted, using computers to calculate the deviations between two serial images on the cornea. This deviation would be transformed to an electrical signal that could move a mirror or lens in the delivery system so that the laser beam would always hit the same area of the cornea. Alternatively, the tracker would inhibit firing of the laser until the eye was in an acceptable location.

ENVIRONMENT OVER AREA OF ABLATION

A homogeneous and perfectly shaped laser beam must still traverse the distance between the condensing lens of the delivery system and the surface of the cornea. Events here can disrupt the beam and make it less effective.

Tissue fragments are ejected from the surface before the next nanosecond pulse arrives but the cumulative effect of this debris falling back onto the surface of the cornea or accumulating in the trough of a linear ablation may absorb some of the laser energy, disrupting the exact calculations for the amount of tissue ablated or creating an irregular surface. This problem can be decreased in part by blowing or sucking gas across the surface of the cornea, so that the effluent is cleared and does not accumulate in the area of ablation.

Ultraviolet excimer laser light is absorbed to some degree by particulate matter in room air, and it is an advantage to remove this air and replace it with an inert gas such a nitrogen. However, blowing nitrogen gas across the surface will dehydrate and thin the cornea, disrupting the calculated tissue ablation.

Fluid on the corneal surface, whether from tears or irrigation, will also absorb the laser photons, so the surface must be kept dry during photoablation. This can be accomplished by using an eyelid speculum to prevent blinking by mechanical drying and by using grooves in a contact lens mask to wick away surface liquid.

Little information has been published concerning refinement of coupling systems, because researchers have concentrated on laser delivery systems and tissue interactions.

EXCIMER LASER INTERACTIONS WITH THE CORNEA

Ablative Photodecomposition

The atomic and molecular events that occur when a pulse of excimer laser light strikes the cornea and the effects of different wavelengths of excimer lasers on the cornea are discussed in the preceding sections. The essential feature of this process is low penetration depth of excimer laser photons, so that most of the energy is dissipated in the shallow volume of tissue near the surface and a few molecular layers can be removed with each pulse, the exact amount being determined by the pulse energy, the pulse frequency, the number of pulses, and the radiant exposure at the surface of the cornea.

Ablation of Epithelium and Stroma

The amount of tissue removed with each pulse also varies with the nature of the tissue itself. For example, with a single set of laser variables, a pulse will ablate more corneal epithelium than corneal stroma. In fact, even within the epithelium, the nuclei are more resistant to ablation than the cytoplasm. This fact has led some investigators to mechanically scrape off the epithelium prior to the ablation, so that the ablation can proceed more quickly and so that calculations do not have to take into account the effect of the epithelium. I discuss the ablation characteristics of the epithelium in more detail below.

Electron microscopic studies of the surfaces and edges of corneal tissues ablated at 193 nm emphasize three important observations. First, that the surface is generally smooth, but contains focal irregularities that result from homogeneities of the beam and surface particles on the tissue that are carried forward as "shadows" during the ablation process. As we demonstrate later, increasing the homogeneity of the beam and working at higher fluences can create a smoother surface. The second observation is the frequent appearance of a layer of condensed material on the surface, sometimes called a "pseudomembrane." Marshall and colleagues[22,56] have described this pseudomembrane in detail, observing that it consists of a dense exterior component 20 to 100 nm thick and a less dense interior portion 60 to 200 nm thick. The precise nature of this pseudomembrane is unknown, but Marshall and colleagues speculate that it may form from the recombination of organic double bonds uncoupled during the photoablation process. This tissue condensate exhibits properties similar to real membranes in that it wrinkles during critical-point drying procedures before scanning electron microscopy and transiently seals the exposed surface with a water repellent barrier. Holland and Marshall (personal written communication, 1987) have demonstrated that this condensed

tissue is less permeable to water than normal stroma and that it can decrease stromal swelling. It may also provide a smooth surface over which epithelial cells can migrate, with the usual layer of fibronectin appearing in front of them.

The third observation is the general lack of disruption of remaining tissue. Beneath the pseudomembrane, a layer of slightly condensed and disrupted tissue approximately 1 μ thick is present in some areas, but beyond that the tissue retains its normal ultrastructural configuration.

These three observations form the basis for the creation of a uniform smooth surface with micrometer accuracy that may allow PRK to become a clinical reality.

Thermal Effects

The cornea is a temperature-sensitive tissue and corneal collagen extracts denature at approximately 40°C.

As mentioned above, the time for heat diffusion in the cornea is on the order of 1 second, so heat accumulates when repetition rates higher than 1 Hz are used. In order to shorten the time required for surgical procedure, repetition rates of 5 to 20 Hz are used, so that the tissue temperature increases adjacent to the area of ablation. The gaseous mixture formed by the ablation process has a temperature of more than 1000°C, but most of this heat is dissipated as the fragments are ejected from the surface. The highest residual temperature is at the boundaries of the ablated tissue and it declines logarithmically as the distance from the edge decreases. Seiler has measured a maximal temperature rise in the corneal tissue of 80°C adjacent to the trough with a half value distance of 610 μm. Thus, the temperature at the edge of the ablation rises to approximately 42°C and at a distance of 610 μ it rises to approximately 38°C. On this basis, one would expect collagen denaturation, but the only evidence of thermal damage is the surface condensate (pseudomembrane) and slight disruption of tissue at a distance of 1 μ. On the other hand, this temperature rise acts only for 30 to 60 seconds; in such a short time denaturation does not occur at temperatures around 40°C.[70]

Mutagenesis Induced by Excimer Lasers

Ultraviolet light is absorbed by deoxyribonucleic acid (DNA) and therefore may have a mutagenic and carcinogenic effect on the rapidly multiplying corneal epithelium. The less active stromal fibroblasts are at less risk. It is well known that excimer laser radiation between 248 nm and 308 nm is mutagenic. The best experimental evidence shows that 193 nm radiation is not mutagenic. Skin fibroblasts irradiated in tissue culture

with subablative fluences showed no more anaplastic change than controls and significantly less than cells exposed to x-ray.[54] Unscheduled DNA synthesis is a measurement of DNA damage, and when this was measured in the cornea after 193 nm ablation, it was not different than that found with a diamond knife, both showing much less unscheduled synthesis than radiation with 248 nm excimer and an ultraviolet germicidal lamp.[71] Another experiment using photoreactivation with yeast cells revealed evidence of DNA damage in cells that are closer than 1 cm to the 193 nm excision.[72] These findings have not been verified in other test systems or in observations of rabbits, monkeys, and humans over a period of 2 years. Perhaps vertebrate cells have different repair mechanisms than yeast cells.

PATTERNS OF LASER CORNEAL SURGERY AND OPTICAL CALCULATIONS

Four different types of laser cornea surgery have been described: linear excisions, either radial to correct myopia or transverse to correct astigmatism (Fig 11); keratomileusis (surface area ablation) to correct myopia, hyperopia, and astigmatism (Fig 11); circular trephination for corneal transplantation; and superficial keratectomy for the removal of corneal scars and the smoothing of an irregular corneal surface. I discuss here the first three.

Radial Linear Keratectomy for Myopia

When Trokel et al[32] married the excimer laser to corneal surgery in 1983, their first thought was to use the laser as a light scalpel—a substitute for the diamond knife in the performance of radial keratotomy for myopia. Puliafito and co-workers[24] compared a 193 nm laser with slits of different

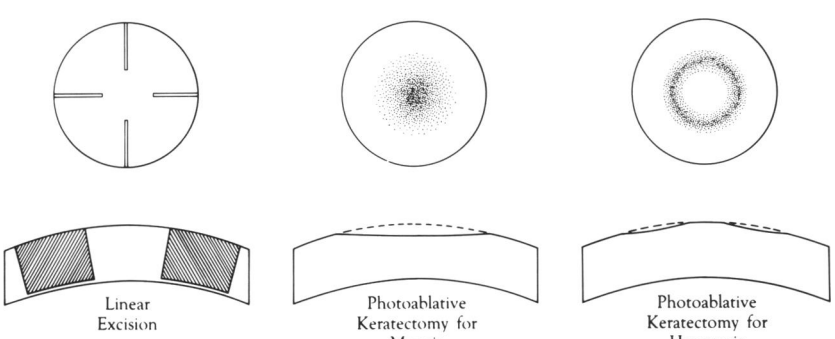

FIGURE 11
Two basic types of laser PRK: linear excisions for myopia and astigmatism and keratomileusis (surface area ablation) for myopia, hyperopia, and potential astigmatism.

widths to diamond knife incisions. They showed comparability between the two, the major difference being the electro-dense condensate along the surface of the laser wound. Marshall and co-workers[8,23] demonstrated the superiority of cuts made by the 193 nm excimer laser when compared to diamond and steel knives, because the edges were so much smoother.

Cotliar and colleagues[73] demonstrated a curvilinear correlation between the total laser output, the depth of excision and the change in refractive power of the cornea in human eye bank eyes.

Stern and colleagues[74] have described a femtosecond optical ranging technique for measuring the depth of a corneal excision made with an excimer laser during the ablation process. The resolution limits were estimated to be 5 to 10 μm. Such a technique would be useful in attempting to control the exact level of a cut, a factor extremely important in determining the outcome of linear keratectomy surgery.

Tenner and colleagues[58] used an ArF 193 nm laser to make eight linear radial excisions 50% to 67% of the corneal thickness with a 5 mm clear zone in three living human eyes. The mask used in the study had slits, each 70 μm wide and 3.5 mm long. One hundred eighty to 200 pulses per excision were used, requiring 5 to 7 minutes under peribulbar anesthesia. In two of the patients aged 72 and 73 years, a mean change of 1.25 to 1.85 diopters (D) in central average keratometric reading occurred at 6 months, the small change reflecting their relatively shallow linear excisions.

Transverse Linear Keratectomy for Astigmatism

Seiler et al[65] has carried out experiments with transverse linear keratectomies in both rabbits and humans that have demonstrated a number of new observations.

The authors used a 193 nm excimer laser configured as an unstable resonator, with a radiant exposure of 160 to 180 mJ/cm^2 at the corneal surface, a repetition rate of 20 to 30 Hz, and 150 to 200 pulses. Experiments in rabbit eyes and enucleated human eyes demonstrated that the relationship between excision depth and the number of pulses is linear with a correlation coefficient of 99.9. In human corneas of different hydrations, it could be disclosed that the ablation rate was dependent on the water content. In addition, the ablation rate in Bowman's layer is more than two times smaller than in the stroma. The ablation rates in human corneas were remarkably consistent, as long as the corneal thickness was between 550 and 600 μm. The configuration of the linear keratectomy was uniform with vertical edges and a depth that varied only ± 4%, as measured in serial histologic sections across the cuts.

Seiler and colleagues[65] also examined the effect of different shapes of linear excisions—straight, concave and convex—in enucleated human eye

bank eyes under controlled conditions. He demonstrated that the curved excision with the convex side facing toward the center of the cornea achieved approximately 60% more effect than straight or concave excisions when the depth ranged from 70% to 80%.

Most importantly, Seiler has treated 10 eyes of 10 patients with straight linear transverse excisions. All eyes were blind or intended for enucleation and the procedure was done under informed consent. The contact lens mask was secured to the surface of the eye and two perforations 4.5 mm long, 0.15 mm wide, and 6 mm apart allowed passage of the laser beam. Grooves in the posterior surface of the contact mask drew fluid away from the area of ablation, preventing tear fluid from entering the excisions and blocking the laser pulses. The globe was fixated manually with a Thornton compression fixation ring. The irradiation time lasted 30 to 50 seconds.

Slit-lamp microscopy immediately after surgery disclosed stromal edema surrounding the excision sites. The edema disappeared within several days as re-epithelialization occurred. Over 1 to 2 years the wound demonstrated persistence of a moderately wide, clear epithelial plug between the slightly opaque edges of the excision, more prominent than that seen after keratotomy with a diamond knife.

The amount of flattening in the previously steep vertical meridian was proportionate to the excision depth as measured by digital imaging of slit-lamp photographs. Having demonstrated that the excision depth is proportionate to the number of pulses, Seiler computed the incision depth for each case. There was a curvilinear relationship between the incision depth and the magnitude of astigmatic change, the amount of change increasing markedly as the incisions got deeper than 80%. Incisions from 50% to 85% depth generally accomplished 1.5 to 2.5 diopters of change in astigmatism, but incisions from 85% to 95% depth accomplished 3 to 4 D change. This observation could be modeled using biomechanical principles so that the amount of astigmatism change could be predicted for given transverse linear excisions.

An unexpected finding was the pattern of steepening in the meridian parallel to the linear excision. In general, with a diamond knife creating a straight transverse incision, the amount of flattening perpendicular to the incision is approximately equal to the amount of steepening in the meridian parallel to the incision. This is the expected finding, based on experience with astigmatic keratotomy using a diamond knife.[75] However, with the laser keratectomy in humans, there was always more steepening in the meridian parallel to the excision, sometimes with values two to three times the amount of flattening 90° away. The explanation for this is not

apparent. It may result from the fact that the laser excises a trough that is many times wider than the incision created by a diamond knife.

On the basis of this experience, Seiler has proceeded to use this system for the correction of naturally occurring astigmatism and of astigmatism after penetrating keratoplasty in sighted eyes, the published results of which are pending (Seiler T: Personal verbal communication. American Academy of Ophthalmology. Las Vegas, Nevada, November 1988).

Laser Keratomileusis (Surface Area Ablation)

The qualities of the wounds made by the excimer laser quickly suggested to Marshall et al[8] the concept of using the laser to carve the surface of the cornea into a new anterior radius of curvature and alter its optical power—laser keratomileusis. The major advantage over linear keratectomy was the ability to achieve a direct optical correction, rather than depending on the indirect effects of paracentral and peripheral cuts to change the shape of the central cornea. Also, the role of the stromal wound healing would be minimized and a stable refraction might be achieved more quickly.[8,66,67,76] The major disadvantage was the one that accompanies all lamellar refractive keratoplasty, surgery occurred across the visual axis, and any surgical error or problem with healing that created scarring or irregular astigmatism would degrade visual acuity.

The optical calculations for acute change are simple enough—though used for the manufacture of contact lenses.[55] Munnerlyn and colleagues[55] performed these calculations assuming that the posterior surface of the cornea remains fixed and the anterior surface of the cornea is modified, so that the true index of the refraction of the cornea of 1.376 must be used, not the keratometric index of 1.3375. Calculations of the amount of tissue that needs to be removed can be approximated by the formula:

$$\text{Thickness of tissue removed } (\mu m) = \frac{\text{Refractive change (D)}}{3} \times \left(\text{Diameter of ablated zone (mm)}\right)^2$$

Fig 12 plots the relationship of these three variables.[55] Unfortunately, epithelial and stromal wound healing may disrupt the results of these ideal optical calculations, as discussed in the next section.

The initial studies by Marshall and co-workers[23] demonstrated the ability to make a very smooth wound bed, and this became the major challenge, as laboratory and clinical experience demonstrated less opacification with smoother beds. Thus, technical improvements made the beam more homogeneous, delivery systems able to ablate a small area with minimal surface irregularity, and the configuration of the ablated

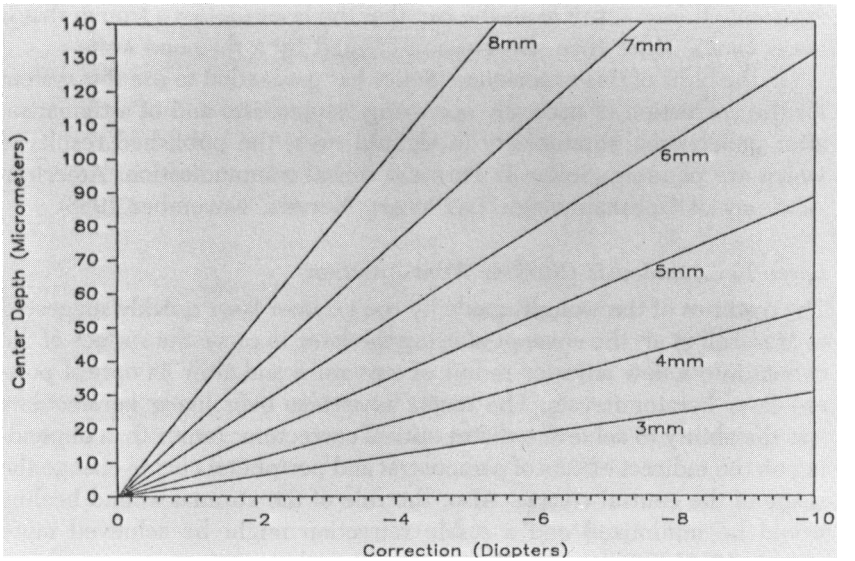

FIGURE 12
Plot of the center depth of tissue removed against the myopic correction achieved for ablation zones of 3 to 6 mm in diameter. (From Munnerlyn CR, Kooms SJ, Marshall J: Photorefractive keratectomy: A technique for laser refractive surgery. *J Cataract Refract Surg* 1988; 14:46-52.)[55]

area to have smoother edges—all of which may enhance wound healing without opacification.[8,67]

Two major challenges face laser keratomileusis: excision of a disc of tissue (including excision of Bowman's layer) without anterior stromal scarring and creation of a predictable stable refractive change. As of early 1989, the published literature lags behind verbal presentations in accurately representing the state of progress on these two objectives. However, all published studies and verbal presentations have given a variety of conflicting results, most reports demonstrating some degree of subepithelial scarring and some epithelial hyperplasia in the ablated zone, but other reports demonstrating clear corneas with a close-to-predicted change in refractions.

Marshall et al[8] and Kerr-Muir et al[76] demonstrated the ability to make punched out circular cylindrical excisions that had a reasonably smooth surface, especially when compared to conventional surgical excisions. They also demonstrated in rabbits and primates that epithelial healing occurred rapidly, completely, and apparently without difficulty. The authors have reported clinical and pathologic findings on 12 monkeys with up to 24 months of follow-up.[56] Immediately after epithelialization, the

anterior cornea was clear. At 1 to 6 months after surgery, most corneas showed a faint subepithelial haze, but the four corneas followed to 8 months and the two corneas followed to 24 months after laser keratomileusis showed grossly clear corneas, although some subepithelial haze was apparent on slit-lamp examination. McDonald and co-workers[67] have shown good epithelial wound healing but mild subepithelial scarring. In a series of unpublished presentations, McDonald and co-workers have presented increasingly improved results with laser keratomileusis in monkeys, early results showing subepithelial scarring, but most recent results showing essentially clear corneas with very faint subepithelial haze in the ablated zone, a result of improved management of the laser beam in the laser cavity and delivery system.[77] I report results in our laboratory in rabbits and monkeys in a later section of this thesis.

Experience in humans is also showing improved results. An early report from Aron-Rosa and co-workers[78] reported the results in a single living human cornea, which showed subepithelial opacification by 14 days after ablation and histologically showed no inflammatory cells but a moderate subepithelial fibrosis. L'Esperance and colleagues[79] have reported in three human eyes that corneas remain clear within 1 week or 2 weeks after initial laser keratomileusis. In a follow-up study of 11 blind human eyes, the authors observed normal re-epithelialization but the persistence of mild to moderate subepithelial haze within the first few months after treatment.[60] McDonald and colleagues have verbally reported on an expanding series of myopic laser keratomileusis performed on blind or partially sighted human eyes, observing uncomplicated re-epithelialization and "clear" corneas in the area of ablation. (McDonald M: Verbal communication. Contact Lens Association of Ophthalmologists. New Orleans, Louisiana, January 1989.)

One of the underlying difficulties in assessing the clinical results of laser keratomileusis is the absence of an instrument to objectively measure corneal opacification. What may be a clear cornea to one observer may be a somewhat hazy cornea to another, depending on one's visual and subjective assessment of subepithelial light scattering. This emphasizes a necessity of having independent well-trained observers without a vested interest in the project as monitors for any study of excimer laser keratomileusis.

To date, there are no published detailed reports of refractive change in either monkeys or humans after excimer laser keratomileusis. L'Esperance and colleagues[60] qualitatively reported changes in refraction, with refractive outcomes ranging from no change to 40% regression. McDonald and colleagues have presented a series of monkeys in which the laser

keratomileusis was calculated to give 3 and 6 D of myopic correction, but the total myopic correction achieved was similar in both groups as judged by retinoscopy. (McDonald M: Lans Distinguished Refractive Surgery Lecture. International Society of Refractive Keratoplasty. Las Vegas, Nevada, January 1989.) More recently, however, in a series of partially sighted human eyes, McDonald and colleagues have reported refractive results similar to those calculated, with some eyes remaining stable and others showing some regression.

These early published and verbal presentations emphasize the variability of results at this stage of development of laser keratomileusis and form a background for further studies.

Circular Trephination

One of the major challenges in penetrating keratoplasty is the creation of a perfectly round donor and host with uniformly-shaped edges, on the premise that uniform wounds will decrease the amount of astigmatism after the sutures are removed.[80] The ability of lasers to cut a perfectly round circle with perfectly vertical edges could be an advantage in corneal transplantation, especially if tissue adhesives could be used to close the wound without distorting the tissue.

Using an axicon lens system as described above, Loertscher and colleagues[43,44] have used an infrared laser to create circular trephination wounds.

An axicon is a conical shaped lens used to produce a circular annulus of focused laser energy. The axicon is placed between a spherical condensing lens and focal point. The beam is focused into a circle instead of a spot. In the optical system devised by Loertscher et al,[43] the diameter of the annulus could be varied from 5 to 7 mm by altering the position of the axicon along the longitudinal beam axis. At the focal plane of the annulus, the width varied from 100 to 150 μ over 340°, and narrowed to 50 μ for 20° at the 5 o'clock position. Using a HF laser in the axicon lens optical delivery system, rapid noncontact trephination of the cornea was performed. The HF laser was run at a fixed repetition rate of 10 Hz and delivered an average rating exposure to the cornea of 2 mJ/cm^2. Seventy-five to 85 pulses were required to penetrate the cornea. Due to nonuniformities in both beam homogeneity and corneal thickness, it is not possible to trephine the cornea full thickness for 360°. Instead, corneal perforation occurs at one point corresponding to the thinnest area of cornea or the highest rated exposure. Immediately following perforation the wound fills with aqueous impairing further trephination.

Serdarevic et al[57] have used the rotating slit delivery system described later in this thesis to create circular full thickness trephination wounds in

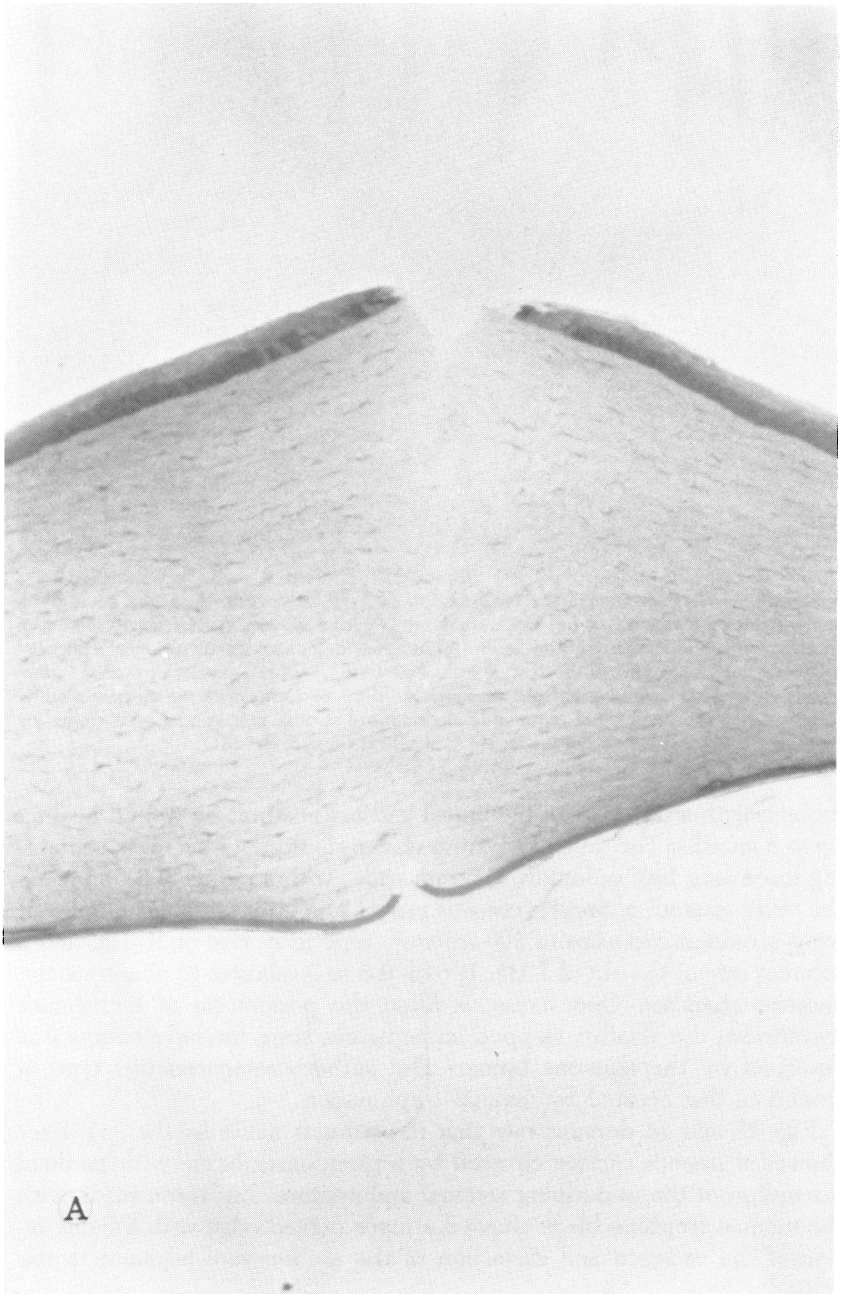
A

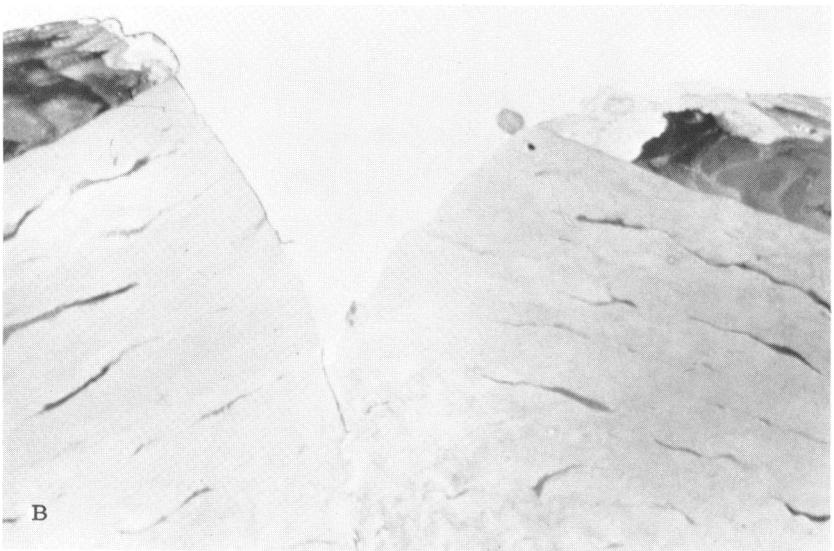

FIGURE 13
Full thickness ArF excimer laser trephination of a rabbit cornea. A: Light micrograph demonstrates appearance of full thickness laser trephine wound. B: Histologic section of anterior cornea immediately after laser trephination demonstrates bisection of epithelial cells, and anterior gaping of the stroma (toluidine blue, ×500). C: Posterior cornea immediately after laser trephination shows severed edges of Descemet's membrane slightly retracted and maintenance of reasonable alignment of stromal collagen lamellae (toluidine blue, ×500). (Courtesy of Olivia Serdarevic, MD).

rabbits, with a description of clinical and histopathologic wound healing up to 3 months. The delivery system was configured with a mask containing three arcs 100° in length, 0.5 mm wide, with a radius of 3.5 mm. As the mask rotated, a circular cut was made. The laser variables employed were a radiant exposure of 200 mJ/cm^2, repetition rate of 10 Hz, and a rotation rate of the slit of 1 Hz. It took 0.5 to 3 minutes to penetrate the anterior chamber. Once aqueous filled the perforation of Descemet's membrane, the ablation stopped immediately, since the laser energy was absorbed by the aqueous humor. The authors compared this type of wound to that created by manual trephination.

Figs 13 and 14 demonstrate that the wounds made by the ArF laser showed a smooth surface covered by a pseudomembrane with minimal disruption of the underlying stromal architecture, but those made with the manual trephine blade showed a more ragged edge with fragmentation of the collagen and distortion of the architecture adjacent to the wound.

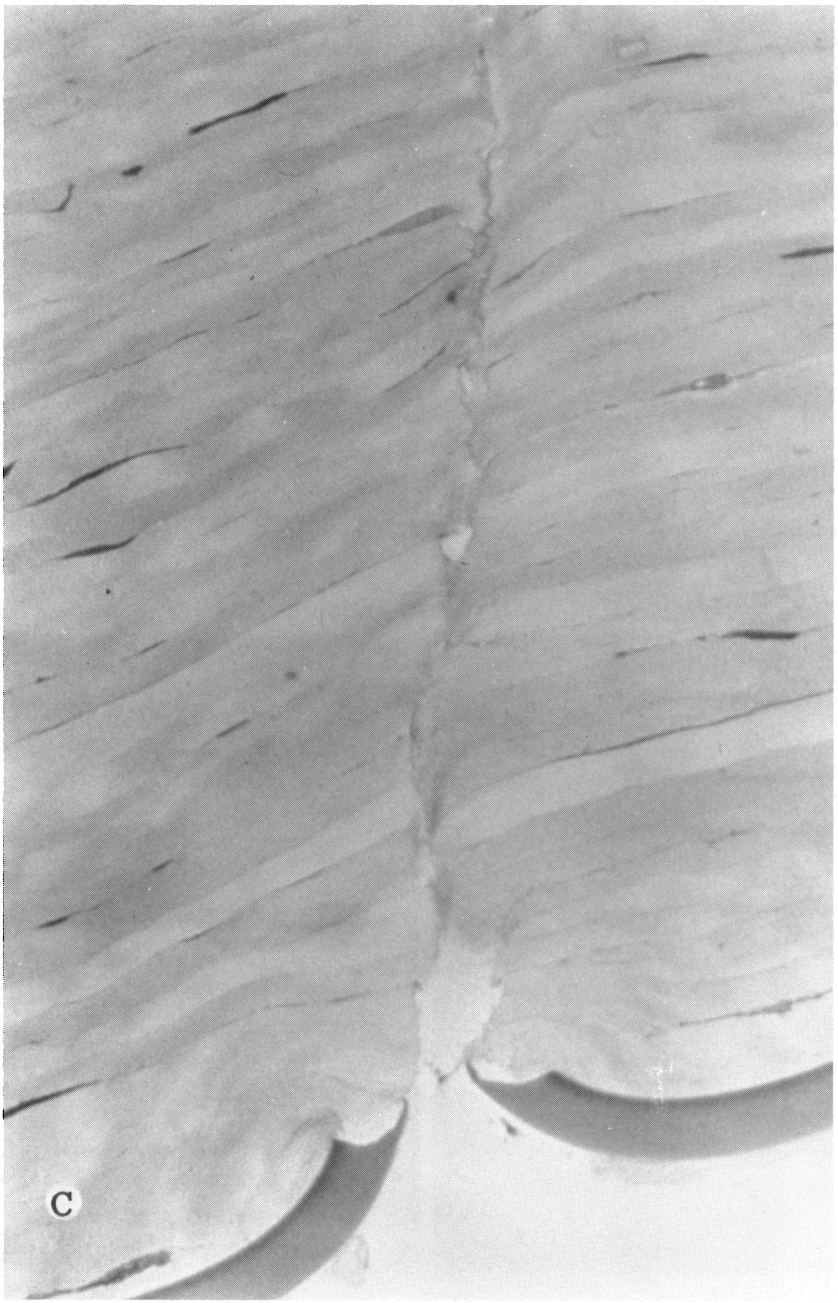
C

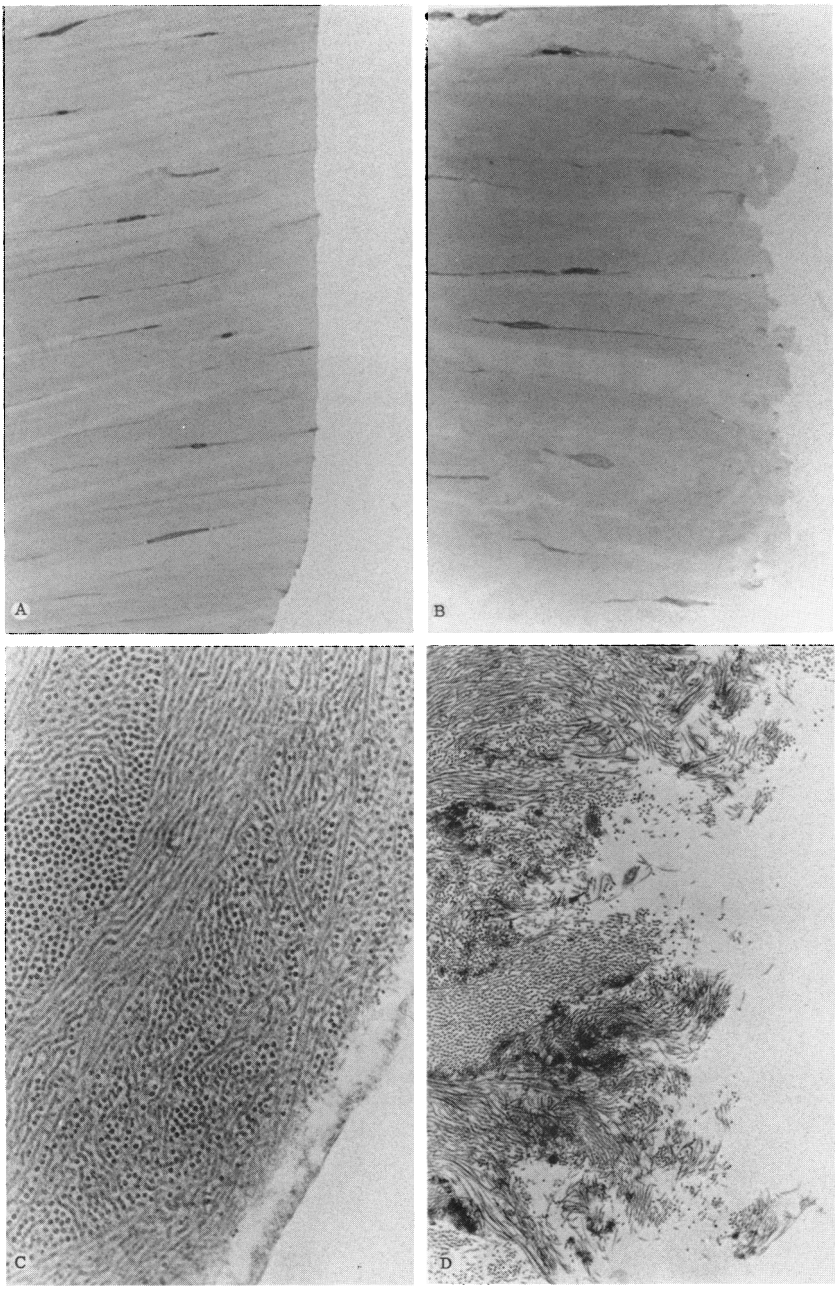
A
B
C
D

FIGURE 14
Comparison of trephine wound made by ArF excimer laser and manual circular razor blade of the corneal wound in rabbit cornea. A: After laser trephination, the edge of the corneal wound is smooth and regular with minimal disruption. B: After manual trephination, the edge of the corneal wound is ragged and disrupted (toluidine blue, ×500). C: After excimer laser trephination, the surface of the wound is covered by a slightly detached pseudomembrane and the underlying collagenous stroma is minimally disrupted (×14,000). D: Transmission electron micrograph after manual trephination shows fragmented wound margin (×4000). (Courtesy of Olivia Serdarevic, MD).

Parel and colleagues (personal verbal communication, December 1988) have used shadowgraphs to compared the edge contour of circular trephinations made with manual trephines, the Hanna suction trephine, and HF and ArF lasers in human eye bank eyes under controlled conditions. In general, the manual trephines produced the most distorted contours, the HF the next most uniform, and the ArF and Hanna suction trephines the most uniform contours.

Whether laser corneal trephines for penetrating keratoplasty will prove superior enough to manual methods to warrant the increased expense and complexity remains to be seen.

EFFECTS OF CORNEAL WOUND HEALING ON PHOTOREFRACTIVE KERATECTOMY

In this section, I discuss the general effect of corneal wound healing on all types of laser corneal surgery.

EPITHELIAL WOUND HEALING

Epithelial Regeneration and Adhesion

Two aspects of PRK seem to facilitate normal epithelial regeneration and adhesion, the presence of the surface condensate (pseudomembrane) and the generally smooth surface itself. Both of these factors create a more optimal surface for epithelial sliding. This is in contrast to the rougher stromal surface created by manual or mechanical instruments. Studies of wounds made by laser keratectomy indicate normal epithelialization without difficulty in man and experimental animals.[8,67,78,81] The epithelial basement membrane is produced and hemidesmosomal and attachment complexes laid down in an orderly manner similar to that seen after a gentle scrape injury of the epithelium.[82,83] The rate of wound healing seems normal although it has not been quantified. Recurrent epithelial erosions and persistent punctate epithelial keratopathy have not been reported.

Epithelial Mitosis and Hyperplasia

More problematic is the thickness of the healed epithelium. In linear keratectomy, the epithelial plug that fills the initial corneal defect is particularly large, because current techniques create wider linear excisions than the incision gaps produced with a diamond knife. The epithelium fills in these defects and remains present for months to years, as described by Seiler et al.[65] Indeed, if the gap in the linear excision is wide enough, the cornea may interpret it as a stromal defect and create a permanent facet of epithelium, rather than interpreting it as a wound that is to be closed by stromal scar formation. Colloquially stated, if the width of the wound is greater than the "fibroblast jumping distance," the wound will remain filled indefinitely with the epithelial plug, which may create refractive instability and decrease the tensile strength of the cornea.

In laser keratomileusis, the healing epithelium determines the final surface contour of the cornea and therefore the final contour of the refracting tear-air interface. If the epithelium covers the ablated area smoothly and mitosis produces a normal five-layered tissue with a smooth surface, then there can be reasonable computation of a predictable optical outcome. The cells will also fill in the surface irregularity created by the laser beam, reducing irregular astigmatism. However, if the epithelium becomes hyperplastic and tries to fill in the ablated defect by creating a tissue 10 to 20 cells thick, then some of the optical effect from the stromal ablation will be neutralized.

This phenomenon of epithelial facet formation within a stromal defect has been well described since the time of Vogt. The thickened epithelium can be seen on slit-lamp microscopy with a narrow beam, particularly if fluorescein is instilled in the tear film, as a clear zone between the tear film and the relucency of Bowman's layer or subepithelial scarring. Steinert and colleagues[84] have described this phenomenon after myopic epikeratoplasty in a patient who achieved approximately 20 D of correction initially, but who then developed epithelial hyperplasia within the central flatter zone of the cornea, reversing the refractive change by some 10 to 15 D. When the thickened epithelium was scraped off and the graft allowed to re-epithelialize, the 20 D refractive effect was restored.

Thus, the ability of the epithelium to fill in surface irregularities of the cornea has both desirable and undesirable effects for laser keratomileusis. The desirable effect is that the epithelium can fill in small surface irregularities created during the process of laser ablation, absorbing these irregularities in the basal cell and wing cell layers, so that the superficial squamous cells form a smoother surface, much like poured asphalt on a gravel highway bed will create a smoother driving surface. Clearly, the

undesirable aspect of this is that the epithelial hyperplasia is not controllable clinically, and if the epithelium fills in the newly created contours necessary to produce the refractive change, refractive instability and reduction of effect will be the result. This is why the concept of using the laser to create a Fresnel prism on the stromal surface to enhance the optical effect is unsound, since the epithelium will smooth over the small steps.

The variables that determine the extent of epithelial hyperplasia remain undefined, but the diameter of the ablation and the contour of the surface may be important. A 3 mm diameter punched-out area with vertical edges is more likely to be filled in by a hyperplastic epithelium that will smooth over the entire defect than a 7 mm diameter ablated area with smooth sloping edges. The effect of the smoothness of the surface on hyperplasia of the epithelium is unknown. We can only speculate about the mechanical role of the eyelid and the metabolic role of the tear film in regulating epithelial thickness. No drugs are available to modulate the thickness of the epithelium.

BOWMAN'S LAYER AND SUBEPITHELIAL FIBROPLASIA

Once the acellular Bowman's layer is ablated it does not regenerate, and the underlying stroma must heal, either closing a linear excision or responding beneath the surface of the healing epithelium after keratomileusis. The minimal disruption of underlying tissues induced by the laser may alter the normal pattern of wound healing seen after conventional corneal surgery. It is not known whether the molecular messages that convert keratocytes to fibroblasts and that stimulate the migration of leukocytes into a wound will operate the same way after laser surgery as after mechanical surgery. There are three theoretical possibilities: (1) no stromal wound healing occurs at all, and the epithelium simply resurfaces the ablated bed; (2) subepithelial stromal wound healing occurs, but with the production of an extracellular matrix that is highly organized, similar to that of undamaged corneal stroma, creating good optical conditions with only physiological amounts of light scattering; and (3) subepithelial fibrosis and scarring occur, as seen after mechanical superficial keratectomies.

Stromal regeneration, fibroplasia and scar formation that occur in the ablated bed may have two effects on the outcome: opacification and reduction of optical effect. Two factors are important in the stromal tissue response: the regularity of the regenerated tissue and the volume of regenerated tissue. The regularity will determine the amount of light scattering which will influence the clinically detectable amount of opaci-

fication and the quality of the optical image. The volume of tissue—even if it were regenerated in a perfectly normal lamellar configuration—can fill in the ablated area, reducing the optical effect.

Studies in rabbits by Tuft and colleagues[81] have shown that after a 3.5 mm diameter, disc-shaped ablation 75 μm deep, the bed labeled with dichlorotriazinil aminofluorescein contains a thick layer of new collagen beneath the epithelium 1 or 2 months after epithelial wound healing.

Histopathologic studies in primates show some subepithelial fibroplasia or "stromal regeneration." What seems to be distinctive is the absence of leukocytes and the presence of a reasonably organized collagenous tissue in that area, as opposed to the commonly seen thicker subepithelial cicatricial fibrosis of disorganized extracellular matrix. Whether this type of response is compatible with clear, stable tissue in humans is currently unknown.

ENDOTHELIAL AND DESCEMET'S MEMBRANE DAMAGE

Marshall and colleagues[22] have shown that when the excimer incisions reach within 40 μm of Descemet's membrane, there is endothelial cell loss beneath the incision. Puliafito and colleagues[24] have demonstrated that when the excisions are of 90% depth, ridges occur between the endothelial cells, a phenomenon that also occurs with the diamond knife. Presumedly, shock waves and recoil forces are creating this endothelial damage.

Both our group (see below) and Burstein and colleagues (personal communications) have demonstrated in Descemet's membrane of rabbits a layer of electron dense, slightly banded material that appears subadjacent to the endothelium within 1 or 2 weeks after surface area ablation and moves anteriorly over a period of 1 to 6 months.

SUTURED LASER WOUNDS

Using the laser for a circular corneal trephination during corneal transplantation or possibly for other full-thickness corneal wounds raises the question as to whether or not wound healing is different when these very smooth wounds are sutured together as contrasted to the healing when conventional mechanical wounds are sutured. Barraquer and colleagues[85] reported no difference in bursting strength or histologic appearance of circular corneal wounds in rabbits made in these two methods.

RESULTS OF LASER CORNEAL SURGERY LABORATORY RESEARCH PROGRAM

I describe here the results achieved in our collaborative research program that attempts to solve the problems reviewed in the preceding sections

with the goal of creating a clinically useful system for corneal laser surgery.

The program involves laser physicists and technicians, laboratory researchers and clinicians. The material presented here is oriented toward an ophthalmic audience. Therefore, I have avoided including the physics, mathematics, engineering, and manufacturing information concerning the laser and the delivery system. To include this in more than a generally descriptive manner would at least double the length of the manuscript and would not be intelligible to most ophthalmologists.

ARGON FLUORIDE EXCIMER LASER

The laser used in this research is the Lambda Physik EMG 103 equipped with an Intelligent Laser Control System that facilitates operation by automatically evaluating the gas reservoir in the laser, mixing the laser gas with the correct concentration of halogen fluorine, rare gas (argon) and the buffer gas (helium). With a ratio of fluorine to argon to helium of 6:14:68 l, we achieved emission of a 193 nm wavelength. Pre-programmed menus developed by Lambda Physik contain all the information necessary to allow personnel who are not especially trained in laser technology to operate the laser. The control system measures the pulse energy as the beam emerges from the laser and this signal is used to drive the feedback loop in order to stabilize the pulse energy at a preset level, independent of the gas contamination that normally leads to decreasing output power. Power stabilization is achieved by regulation of the high voltage level needed to charge the storage capacitors of the laser and by controlling the concentration of impurities in the laser gas. This is accomplished by exchanging contaminated gas with fresh gas while the laser is operating or, at the instruction of the operator, stopping the process and refilling the chamber. These two methods of controlling the quality of the gases in the resonating cavity enable the laser to run without interruption for long periods of time.

Two problems confronted us immediately in using this laser. The first was inadequate power output and the second was an inhomogeneous distribution of energy within the beam.

Pulse Energy

Pulse energy was measured with a joulemeter (GenTec) as the laser beam left the cavity. The initial pulse energy was 120 mJ, too low for our experimental use. In addition, the beam energy profile was inhomogeneous both transversely and longitudinally. We negated these problems with a few modifications of the laser.

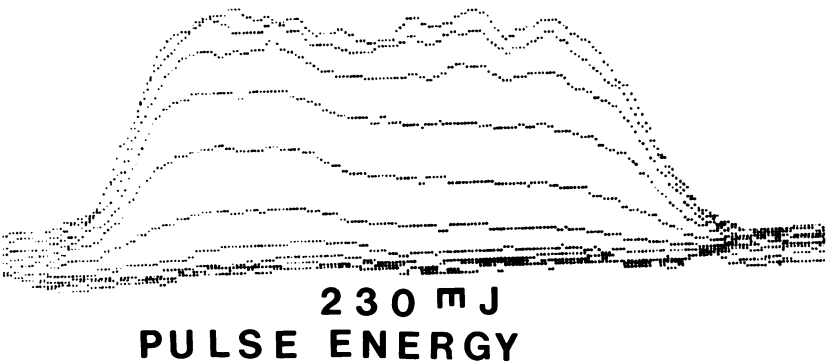

A

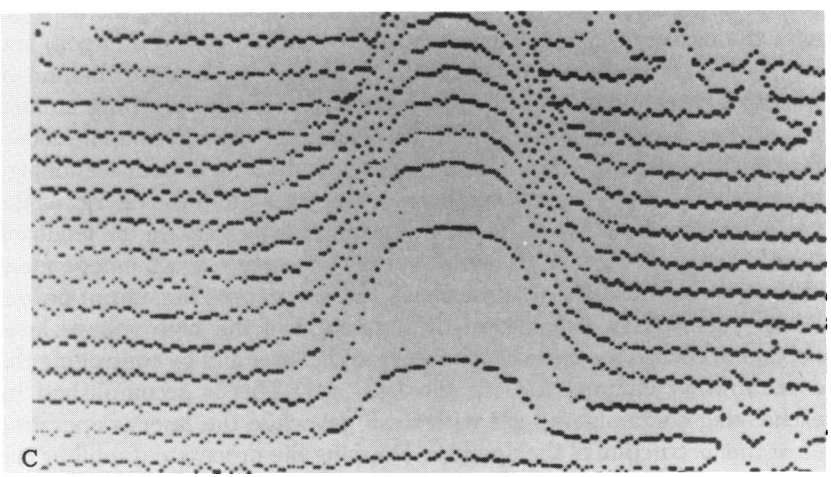

We converted the configuration of the resonator cavity from unstable to stable optics. This was done by replacing the partially reflective mirror at the exit end of the resonating cavity, substituting a uniform mirror to create a stable configuration in place of the mirror with a central fully reflecting surface as used in an unstable configuration. The technical details of this modification are beyond the scope of this thesis.

A helium-neon laser was installed at the fully reflective end of the cavity and was used to optimize the alignment of the mirrors to facilitate maximum beam uniformity. These adjustments gave a pulse energy of PTO 245 mJ as the beam emerged from the cavity, with a pulse to pulse variation of ± 4% and a ± 1% intensity variation over the plateau area within each pulse.

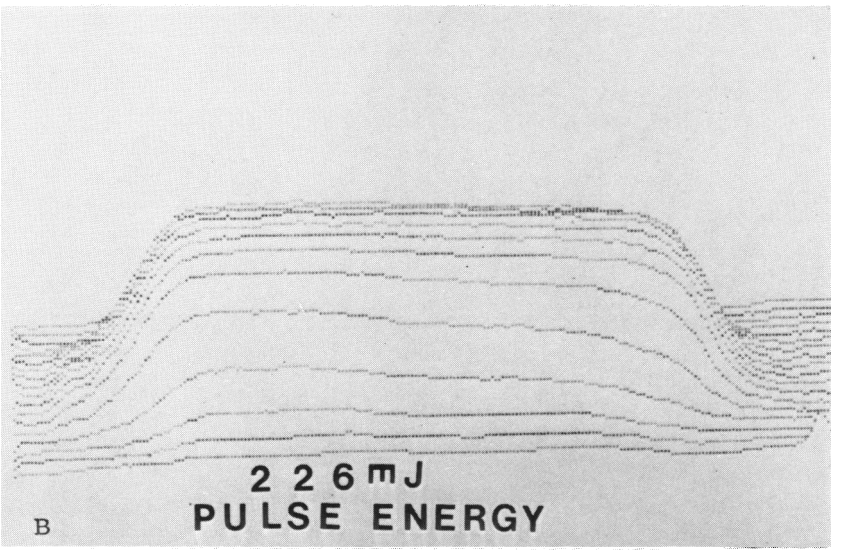

FIGURE 15

Configuration of one pulse of 193 nm ArF excimer laser beam as it emerges from the resonating cavity as imaged on a fluorescent screen. Details of method of imaging are explained in the text. A: With a pulse energy of 230 mJ, the beam profile shows longitudinal irregularity with hot spots (higher points on the profile) and cooler spots (lower points on the profile), as well as a sloping configuration on either end. B: After adjustment of the laser resonating cavity as described in text, the beam profile at the same pulse energy is more uniform, showing a flattened top, although the edges still have a sloping configuration. C: Another view of the beam configuration after improved homogeneity shows a relatively uniform configuration across the width of the beam, with slight sloping of the sides. Inserting a mask in the beam path can capture the uniform center of the beam as depicted in B and C, eliminating the sloping margins and creating a beam of uniform energy distribution which will create a smoother surface on the cornea after ablation with each pulse.

Homogeneity of Laser Beam

There are few commercially available instruments to measure the energy distribution in the excimer laser beam. However, this is an extremely important variable because the contour of the beam is imprinted on the tissue and the more irregular the beam, the more irregular the surface of the ablated cornea. Therefore, we developed a method of measuring beam homogeneity by imaging the beam on a fluorescent screen. The fluorescence emitted from this screen was proportional to the ultraviolet energy and was imaged with a television camera and frame grabber, fed into a computer programmed with software to print out a graphic cross section and three-dimensional image of the beam configuration.

Before making the adjustments described above, the beam profile was irregular, showing 5% to 10% variability from one side to another (Fig 15A). After the adjustments, firing at the same pulse energy, the homoge-

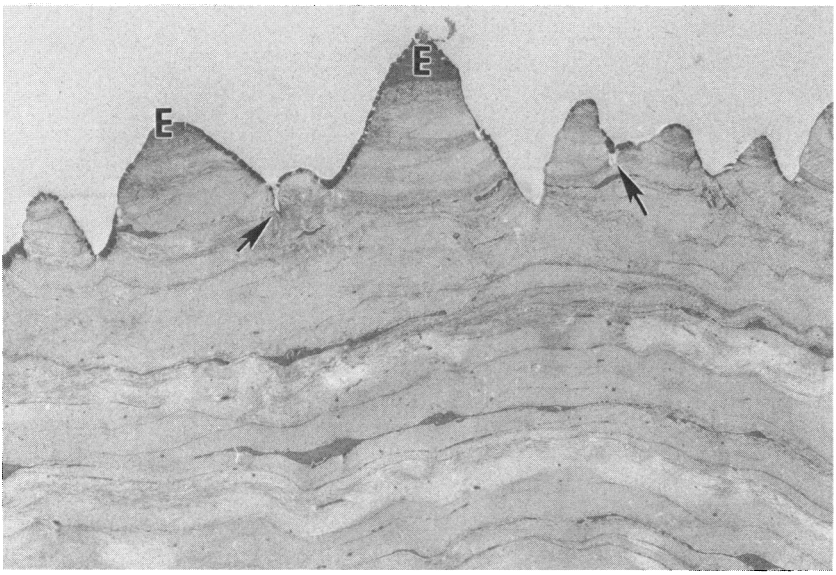

FIGURE 16
This is a transmission electron micrograph of a rabbit cornea ablated with 193 nm ultraviolet radiation using a circular mask and an inhomogeneous beam using a fluence of 200 mJ/cm^2 and a repetition rate of 20 Hz. E indicates residual parts of epithelial cells. *Arrows* indicate small focal troughs in the tissue (×2970). (Courtesy K Hanna, MD and Y Pouliquen, MD)

neity of the beam was greatly increased (Fig 15B and C). In general, the beam shape was wider and showed a flatter plateau in the center.

MOVING SLIT DELIVERY SYSTEM

Rationale for Moving Slit

The moving slit conception of Hanna and colleagues is designed to create maximum flexibility and minimal tissue damage. Preliminary reports using a rotating slit have been published[57,59,61,86] and are briefly reviewed herein. Unpublished material concerning the design and use of a translating slit configuration with results in rabbit and monkey eyes is presented here.

A modifiable slit mask that moves can create all types of corneal ablations, including straight radial, straight and curved transverse, myopic keratomileusis, hyperopic keratomileusis, astigmatic reprofiling, circular trephination, and surface lamellar keratectomy. The configuration of the slit can be customized for each type of surgery and, theoretically, for each individual eye. Such a system is more flexible than, for example, a

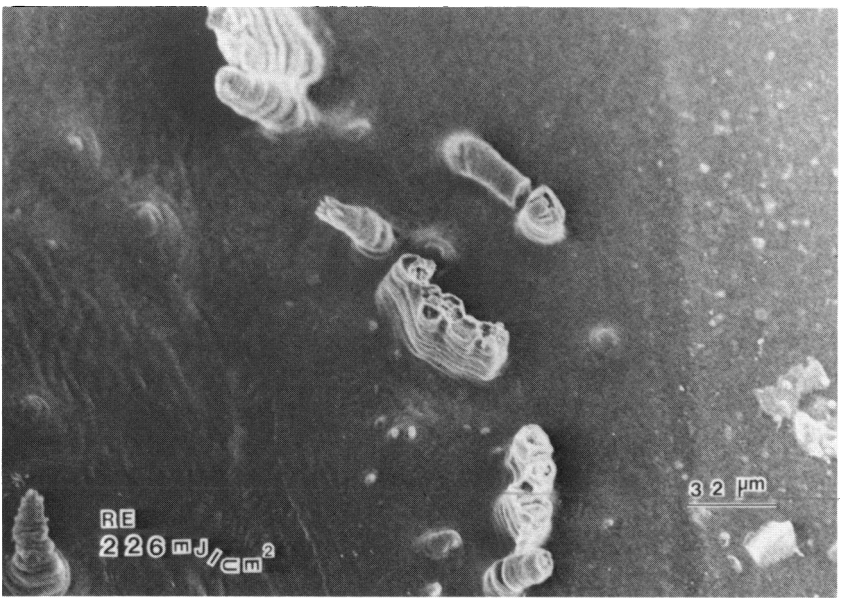

FIGURE 17
Scanning electron micrograph of rabbit cornea with surface area ablation at 193 nm, fluence of 226 mJ/cm², repetition rate of 20 Hz, and an ablation depth of approximately 50 μ. Numerous focal elevations are apparent, resembling the appearance of a chain of Pacific islands protruding up from the floor of the sea. These protrusions are the manifestation of inhomogeneities in the laser beam, being areas where the energy density is less and thus less tissue is removed. (Fantes FE, Waring GO: Effect of excimer laser radiant exposure on uniformity of ablated corneal surface. *Lasers Surg Med,* in press.)[87]

constricting diaphragm, which has the ability only to create a myopic correction.

Another advantage of the moving slit is that the imprint of the beam on the cornea is moved many times over the surface. Therefore, surface irregularities due to inhomogeneities of the beam will tend to cancel each other out, creating a relatively smoother surface. This is in contrast to a system in which the same beam profile impinges onto the same area of the cornea with each successive pulse—a circumstance that will exaggerate inhomogeneities and can create marked focal elevations in the surface that resemble a phallus-like obelisk or a flat-top mesa (Figs 16 and 17).[87] However, this advantage also creates a drawback, in that the image of the slit is projected onto the cornea with each pulse, creating an edge for each slit. The fact that the slits move tend to smooth over the edge-effect, but the final ablation in any given location will leave a faint imprint of the slit itself, creating mild surface irregularity. This can be seen against the red fundus reflection immediately at the conclusion of surgery.

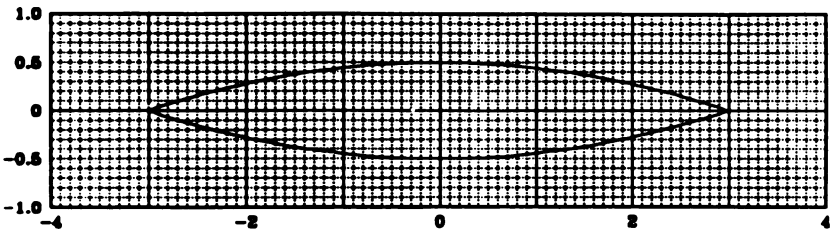

A

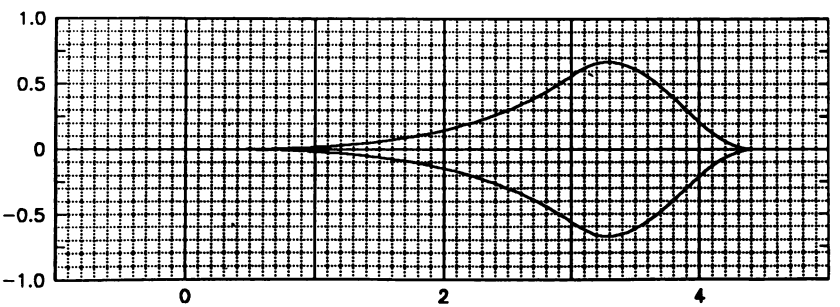

B

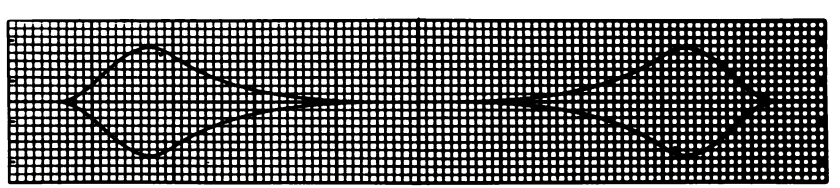

C

FIGURE 18

Drawing of configuration of slits. A: Slit for a laser myopic keratomileusis can be rotated around the center point (00) or translated across the corneal surface. Units indicate only relative size. B: Slit for hyperopic laser keratomileusis can be rotated around the center point (00). Units indicate only relative size. C: Slit for hyperopic laser keratomileusis can be translated across the cornea in different meridians. (Hanna KD, Chastang JC, Asfar L, et al: Scanning slit delivery system. *J Cataract Refract Surg* 1989; 15:390-396.)[86]

The movement of the slit must be computer-controlled for accurate placement and location of the successive pulses. For example, using a rotating slit, the center of rotation must be accurately aligned and precisely maintained, to avoid overlapping of the slits with the creation of a central divot and to avoid missing the center of rotation so that a focal central elevation results. This central alignment problem is eliminated by the use of a translating slit that sweeps across the cornea. The location of each slit must be precisely designated to create the desired surface profile or linear cut. A computer control system ensures this.

Calculation of Shape of Slit

The shape of the slit is mathematically determined to create an exact ablation profile (Fig 18).[86] To correct myopia, the slit is wider in the middle so that more tissue is removed from the central and paracentral cornea. To correct hyperopia, the slit is wider close to its outer end, to remove more tissue from the midperipheral area. The location of the slit is varied, so that more tissue is removed from the steep meridian of the cornea. To make linear excisions, a rectangular slit is used.

The radius of curvature of the anterior corneal surface is modified (Fig 19) at its intersection "0" with the visual axis OZ from an initial value r_o to a new value r with $r > r_a$. The model assumes that the cornea is parabolic, with an initial radius of curvature r_o. Measuring z from the intersection of the visual axis with cornea ($z > 0$ inwards) and denoting by h the perpendicular distance from the visual axis to the point considered, the parabolic model gives the following equation for the surface shape:

$$z = \frac{h^2}{2r_o}$$

After ablation, the same equation applies to the new corneal surface, and the ablation profile for a circular disc of radius R is given by:

$$A(h) = \frac{1}{2}\left(\frac{1}{r_o} - \frac{1}{r}\right)(R^2 - h^2), \text{ when } h \leq R \qquad (1)$$

$$= 0, \text{ when } h > R$$

where A(h) is the ablation profile. The form of this ablation takes its maximal value at the center (where $h = 0$), which is on the visual axis, and its minimal value (0) at the periphery of the carved zone (where $h = R$). R is chosen such that the ablated area contains the optical zone and the wing (about 0.6 mm), eg, $R = 3.75$ mm. There is another limit to R, which

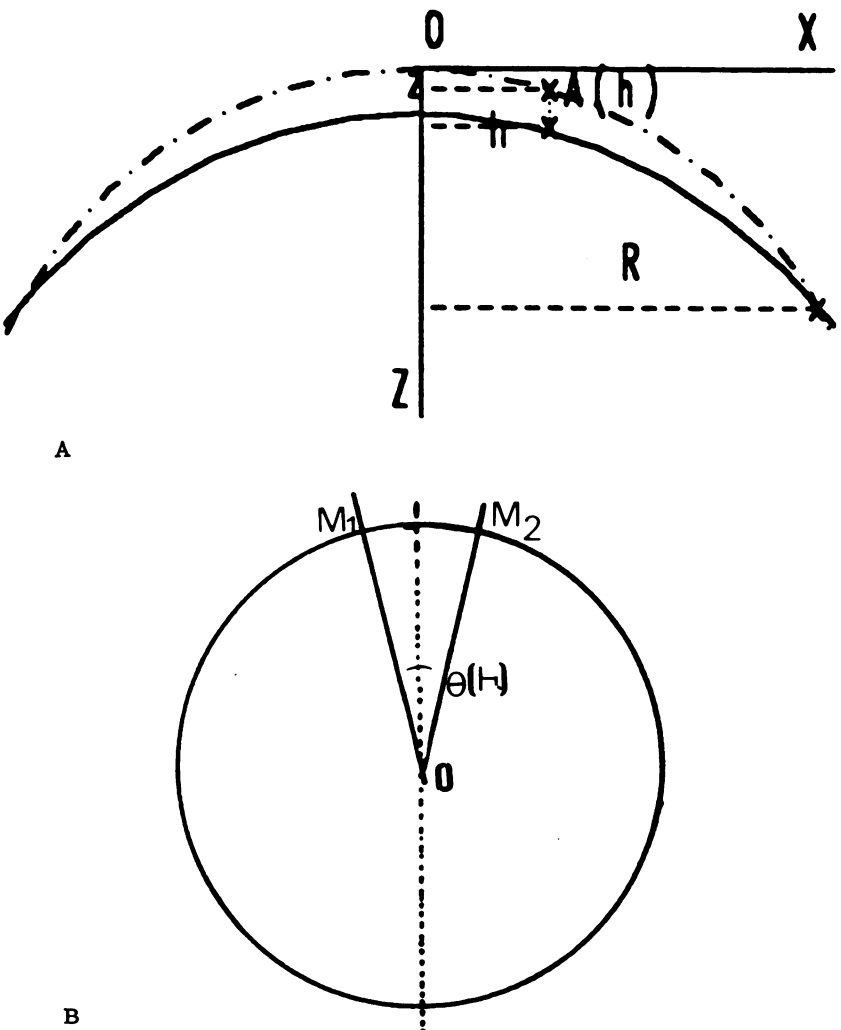

FIGURE 19
A: Reduction of the parabolic profile of the cornea during myopic keratomileusis with a rotating slit beam. B: Surface view of calculations or shape of slit for laser myopic keratomileusis. Explanation of symbols is in the text. (Courtesy KD Hanna, MD)

comes from the maximum allowable thickness for the ablation at the central zone. It is estimated that more than 0.2 mm ablation for myopia may lead to unexpected changes of the corneal shape due to mechanical factors. Thus, the value of R is limited by the following expression:

$$R = \min \left(R_{max} \quad \frac{2A_{max}}{\frac{1}{r_0} - \frac{1}{r}} \right)$$

which gives R = 3.1 mm, for the extreme case where A_{max} = .02 mm and r = 12 mm, r_o = 9 mm and R_{max} = 3.75 mm in laser myopic keratomileusis.

To calculate the slit shape, let h be the radius of a circle which intersects the slit at the points M_1 and M_2. Let θ(h) be the angle subtended from 0 of radius h by the arc M_1M_2. The function θ(h) defines the shape of the slit. If one assumes that the ablation at a given point is proportional to the number of pulses received at the point if the fluence is constant, one can write the ablation profile A(h) as a function of: the number of slit rotations N, the slit length R (mm), the repetition rate F(Hz), the average depth of ablation per laser pulse a(e) (mm), the fluence e, and the angular speed of the slit (Rad/second):

$$A(h,N) = N\ F\ a(e)\ \frac{\theta(h)}{\Omega} \tag{2}$$

From equations (1) and (2), one derives the following expression for the slit shape function:

$$\theta(h) = S(R^2 - h^2) \tag{3}$$

Where S is a factor which determines the slit surface. S is given by

$$S = \frac{\frac{\Omega}{2N\ F\ a(e)} \left(\frac{1}{r_0} - \frac{1}{r} \right)}{R^2 S << 2\Pi} \tag{4}$$

We have used the value S = 0.023.

This rotating slit principle could also be used to correct myopic or hyperopic astigmatism. From equation (4), one sees that if the laser repetition rate F varies with angular position $_a$ of the slit, one could obtain parabolic ablation profiles which vary with the meridians and thus correct

myopic astigmatism. The equation below defines the ratio of the laser repetition rate for two perpendicular meridians where $_a$ is the angular position of the first meridian and r_a, $r_a - \frac{x}{2}$ are the initial curvatures at the center on these meridians:

$$\frac{F_a}{F_{a-\frac{x}{2}}} = \frac{\left(\frac{1}{r_a} - \frac{1}{r}\right)}{\left(\frac{1}{r_{a-\frac{x}{2}}} - \frac{1}{r}\right)} \tag{5}$$

This process requires, in order to produce equal ablation at the center for myopic keratomileusis, an extra pass with a triangular slit that produces uniform ablation and thus does not change curvature. We are developing computer programs to control the laser pulse rate and to coordinate the angular position of the slit. The same astigmatic ablation profile could be obtained varying the slit rotation speed with its angular position.

From equation (2), one can also derive $\theta(h)$ functions for different ablation profiles to treat hypermetropia.

To avoid thermal effects of the cornea adjacent to the area ablated, we combined a high repetition rate and a high angular speed of the slit. In this case, the angular speed Ω of the slit is a function of the laser repetition rate F so that for consecutive pulses, images of the slit do not overlap. The result is similar to that obtained by two more separate slits rotating at very low speed ω. Let k be the desired number of consecutive disjoint slit images, the relation between Ω, ω and the laser repetition rate F is:

$$\Omega = \frac{1}{k}(2\pi F + \omega). \tag{6}$$

Note that the value of k is limited by the following relation:

$$\max k\,\theta(h) = k\,S\,R^2 \leqslant 2\pi$$

Otherwise, the consecutive slit image will overlap at the rotation center in a myopic ablation or at the periphery in a hypermetropic ablation.

Optical Elements in the Delivery System

As mentioned previously, there is a loss of energy as the laser beam passes through the optical element of the delivery system, depending on the absorption of the beam. In addition, the more irregular the surface and

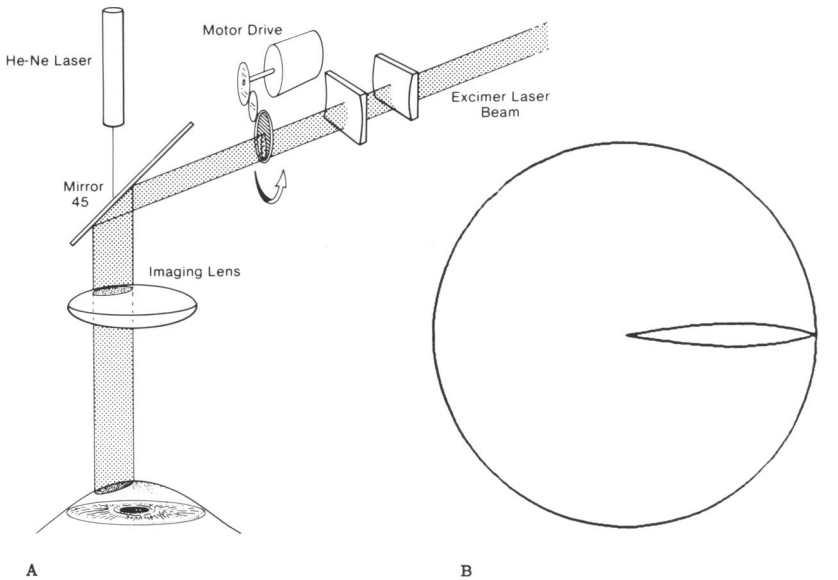

FIGURE 20

Rotating slit delivery system. A: Diagram of system demonstrates excimer laser beam made square with two cylindrical lenses and projected through the rotating slit driven by a small motor. A mirror reflected the beam toward the cornea where it was imaged by a lens onto the corneal surface. A helium-neon laser was used to position the beam on the cornea. As the slit imaged rotated around the center of the cornea, photoablation was carried out. B: Drawing of slit profile used for myopic keratomileusis.

optics of the element, the less homogeneous the beam becomes. To obviate these problems, we have reduced the number of optical components where possible and have coated the lenses and prisms with antireflective coatings and mirrors with high reflectivity coatings. This involves the deposition of 30 to 40 layers of coatings in the proper sequence—an engineering art.

Three different moving slit delivery systems have been designed and further refinements continue.

Rotating Slit Delivery System

The first delivery system utilized fixed optical elements and a rotating slit mask (Fig 20).[59] The beam emerged from the laser in an elongated rectangular cross section and was made square with an anamorphic telescope that had a magnification of one in the horizontal plane and approximately 2.3 in the vertical plane. This square beam illuminated a rotating disc that contained a single radial slit extending out from the center in the

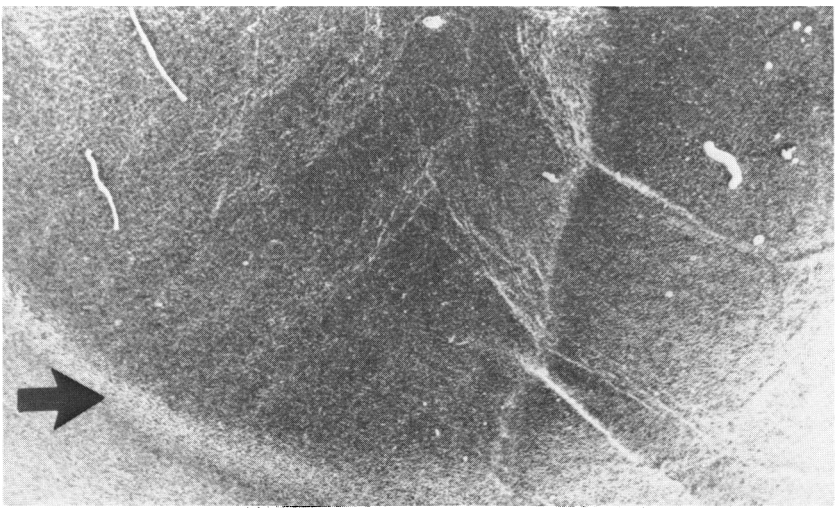

FIGURE 21
Scanning electron micrograph of human eye bank cornea with full thickness ablation using a rotating slit profile for myopic correction shows edge of cut epithelium (*upper arrow*), sloping surface, and central perforation in Descemet's membrane (*lower arrow*) (×20). (From Hanna K, Chastang JC, Pouliquen Y, et al: Excimer laser keratectomy for myopia with a rotating slit delivery system. *Arch Ophthalmol* 1988; 106:245-250. With permission of the American Medical Association.)

shape of a feather (widest at the middle). The ablation takes its maximal value at the center on the visual axis, and its minimal value (0) at the periphery of the carved zone. The chosen radius of this zone was 3.75 mm.

A motor rotated the disc at a rate of 0.033 Hz. A 45° mirror directed the beam toward the cornea and a spherical lens imaged the slit onto the cornea, the length of this image measuring 3.75 mm long, with an area of 2.25 mm^2. This created a circular ablation area 7.5 mm in diameter as verified on photographic film. An auxiliary helium-neon laser was used for centering; an operating microscope allowed magnified viewing.

One advantage of using a converging optic in the objective lens is the ability to change the radiant exposure (fluence) on the surface of the cornea by simply moving the focal point of the lens closer to the corner (with greater radiant exposure) or further away from the cornea (with less radiant exposure).

The rotating slit delivery system had two major drawbacks. The first was the difficulty in aligning the slit centrally, so that overlap created a marked central depression and left a central elevation. The second problem was utilizing the laser beam properly. As the slit rotated, the entire disc in which the slit was located was irradiated by the laser, so that only a

small percentage of the indicent light exited through the slit aperture. In addition, the laser beam was used from its center toward its peripheral part, propagating inhomogeneities that were present across the radius of the profile.

Even with these limitations, a reasonable myopic keratomileusis could be obtained in eye bank eyes and, as described in a subsequent section, a reasonably smooth surface could be obtained (Figs 21 and 22).[59]

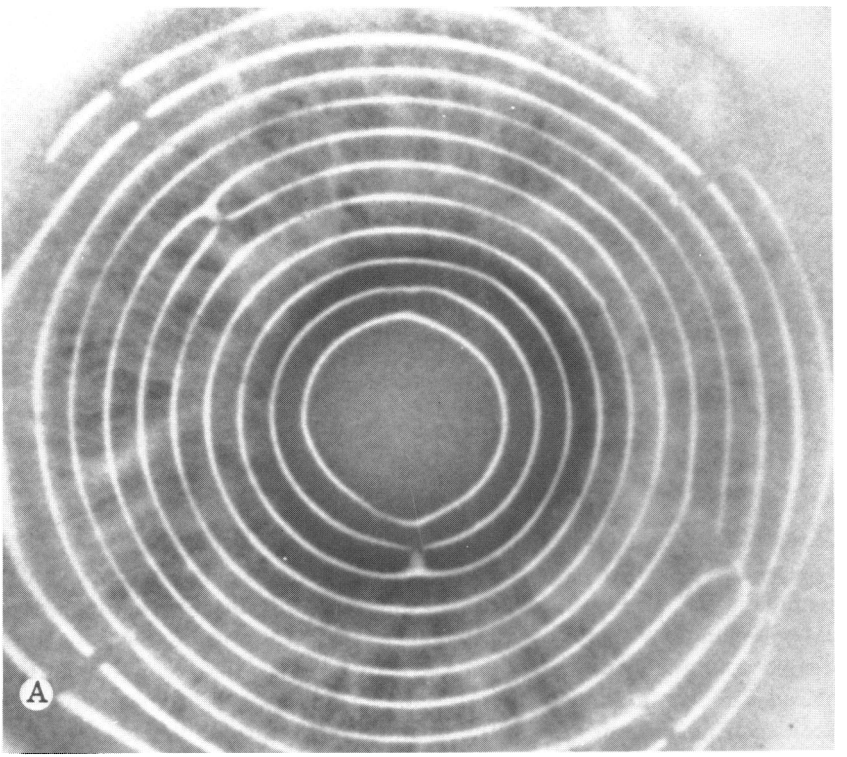

FIGURE 22

Keratographs of cornea before and after myopic keratomileusis with rotating slit. A: Before ablation, central mires are reasonably regular and round. B: Quantitative image analysis of the keratograph before ablation gives a surface power of the cornea with an average central reading of 42.90 D and a normal, gradual decrease in refractive power toward the peripheral cornea. C: Keratograph after surface ablation shows larger diameter circle centrally because of a flatter cornea. Irregularity in rings 1 to 3 inferiorly is a surface artifact. D: Quantitative image analysis after ablation demonstrates a central power of 37.85 D with a gradual steepening of the paracentral rings and then flattening in the peripheral rings. These keratographs demonstrate the ability of a rotating slit delivery system to create a myopic keratomileusis profile and are not meant to quantify the exact effect in this eye bank model. (From Hanna K, Chastang JC, Pouliquen Y, et al: Excimer laser keratectomy for myopia with a rotating slit delivery system. *Arch Ophthalmol* 1988; 106:245-250. With permission of the American Medical Association.)

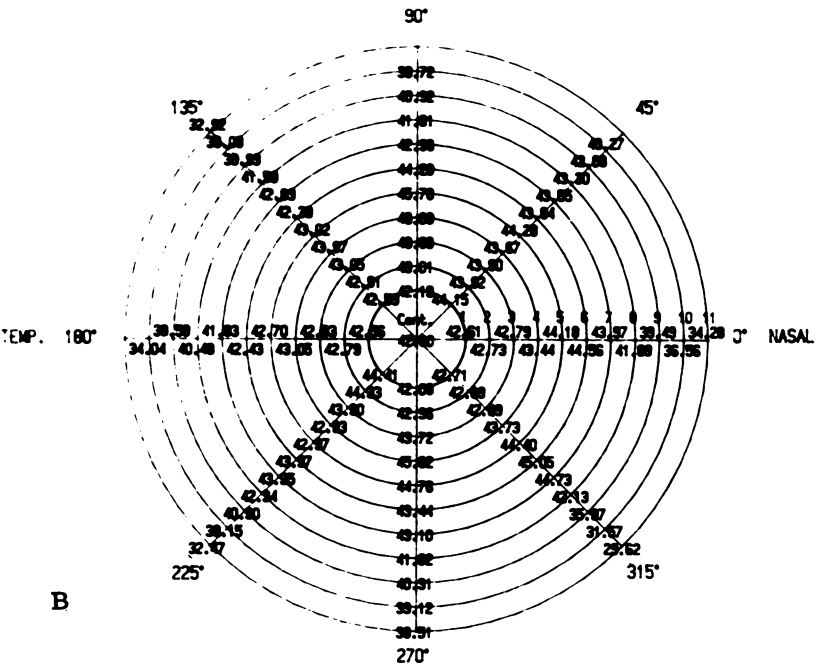

Rotating Dove Prism Delivery System

To improve the rotating slit image concept, a second delivery system was designed in which the slit mask was placed close to the emerging laser beam (Fig 23). The beam itself, as it emerges from the resonating cavity has a rectangular shape of approximately 5 × 20 mm, a generally slit-shaped configuration. The slit mask with its calculated configuration is placed directly in front of the laser beam, allowing the more homogeneous central plateau area of the beam intensity profile to pass directly through. The best fit of the mask shape to the beam geometry provides a 50% transmission through the mask, selecting the most homogeneous part of the beam. The slit image is then expanded with a lens, and passed through a rotating Dove prism, driven by a motor. This rotates the slit image through a subsequent lens that focuses the image, which is relayed by a 45% mirror onto the surface of the cornea. A helium-neon laser is used to allow the operator to locate the beam on the cornea.

This delivery system is compact with a distance of 1.5 m from the laser cavity to the cornea, in order to minimize absorption losses in the air. The phoroptical elements are coded, and the system is capable of providing up to 500 mJ/cm^2 radiant exposure at the cornea.

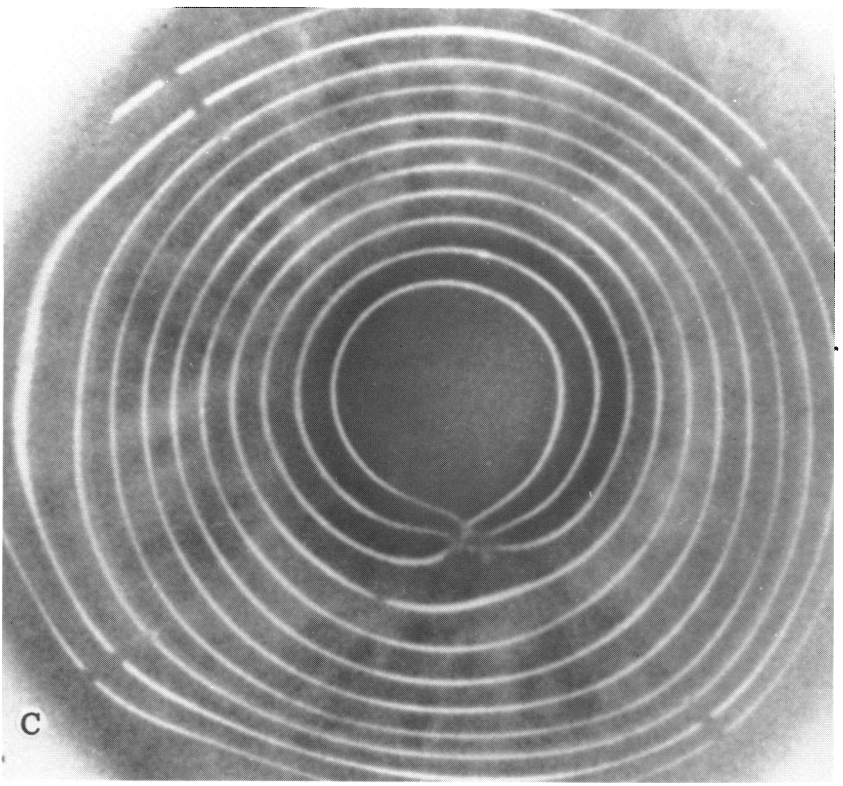

The rotating prism delivery system increases the efficiency, but still suffers from the fundamental problem of centering the moving slit image on the cornea. Because of this drawback, a translating slit delivery system was developed.

COMPUTER-CONTROLLED TRANSLATING SLIT DELIVERY SYSTEM

This delivery system is designed for maximum stability and versatility in an experimental setting, where modulation of many different variables is necessary (Fig 24). For clinical use, the system would have to be modified. Nevertheless, this laboratory model realizes the goal of programmable robot laser for refractive corneal surgery (Fig 25).[86]

Design of system: The laser beam passes through the delivery system, undergoing five right angle folds. The configuration has the following constraints:

1. The laser was separated from the delivery system to remain easily accessible for adjustments, maintenance, and repair.

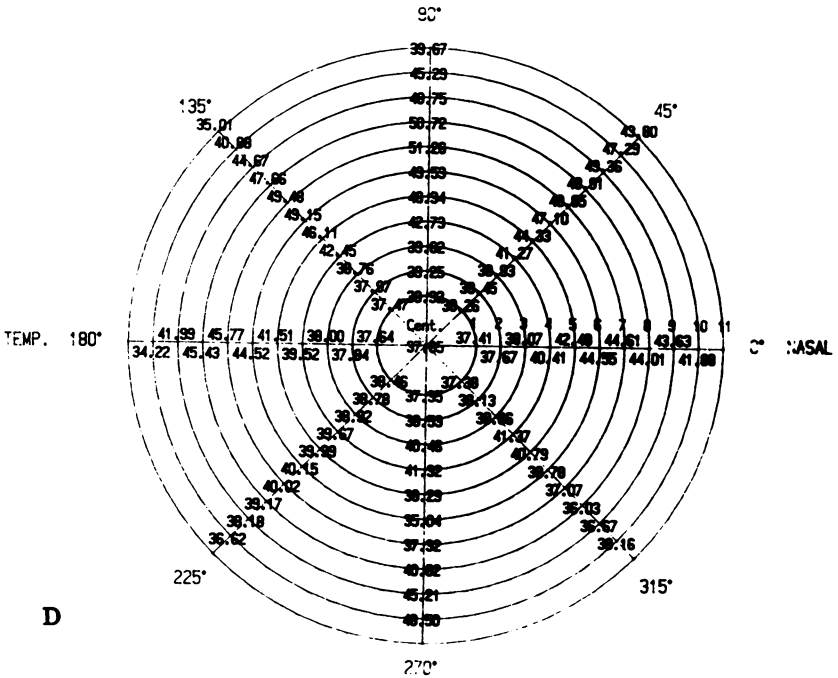

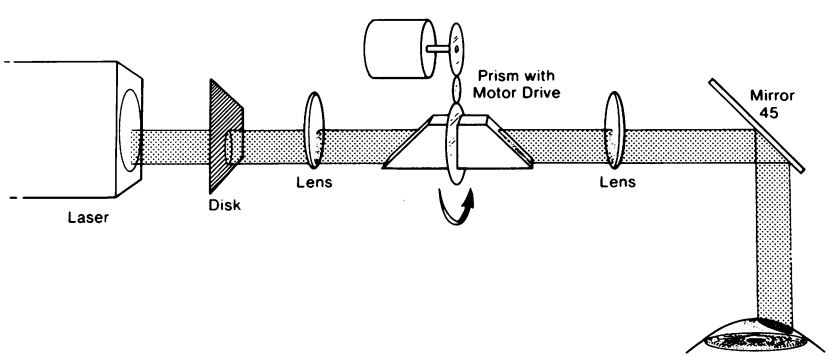

FIGURE 23

Diagram of rotating of slit delivery system demonstrates that the disk containing the slit mask is oriented close to the laser and that the rotation of the slit image is accomplished with a motor driven rotating of prism. Not illustrated is the helium-neon laser to identify the beam on the cornea and the binocular operating microscope to observe the procedure.

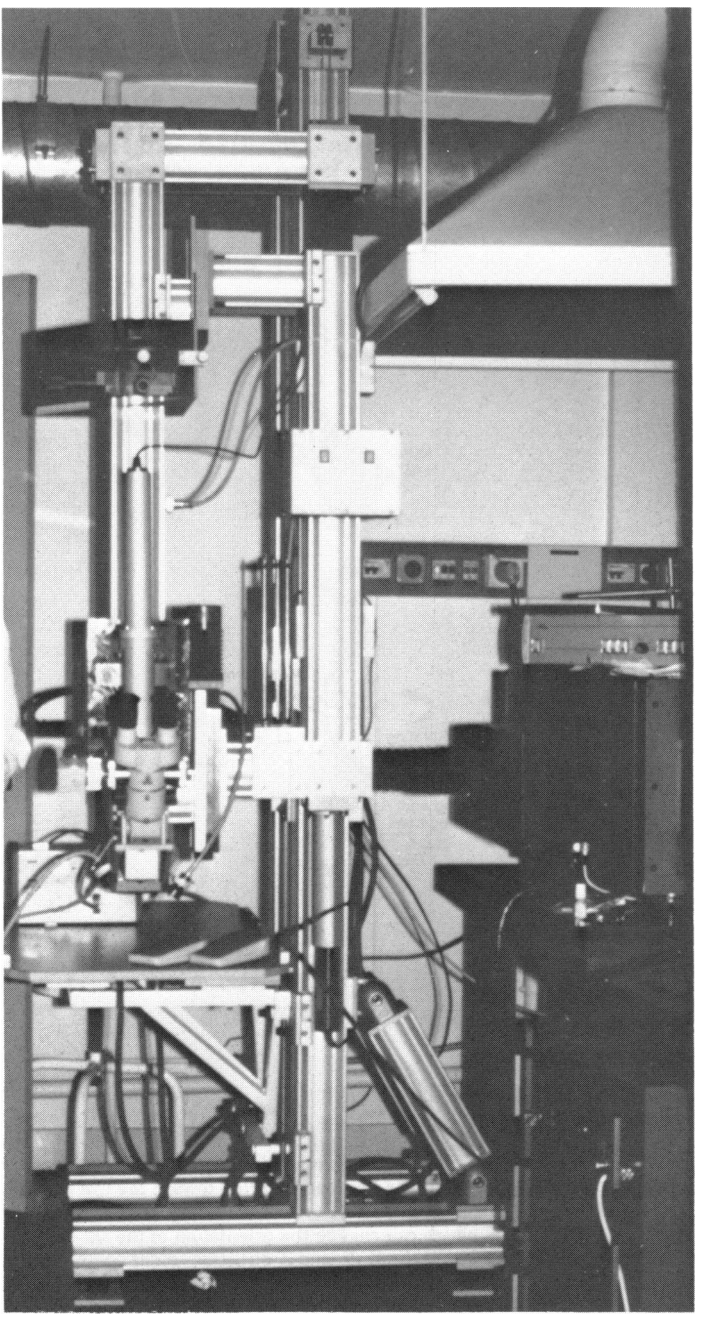

FIGURE 24

Experimental laboratory model of computer-controlled translating slit delivery system. Laser is located at right of picture. Laser beam traverses the inverted-U-shaped column, emerging over the table. The height of the delivery system and the height of the table are both adjusted by motors. Three helium-neon lasers assist in the alignment and viewing. The slit mask is housed in the black box on the upper left-hand corner. The computer-controlled, motorized dove prism and spherical lens are located in the enclosure behind the binocular microscope.

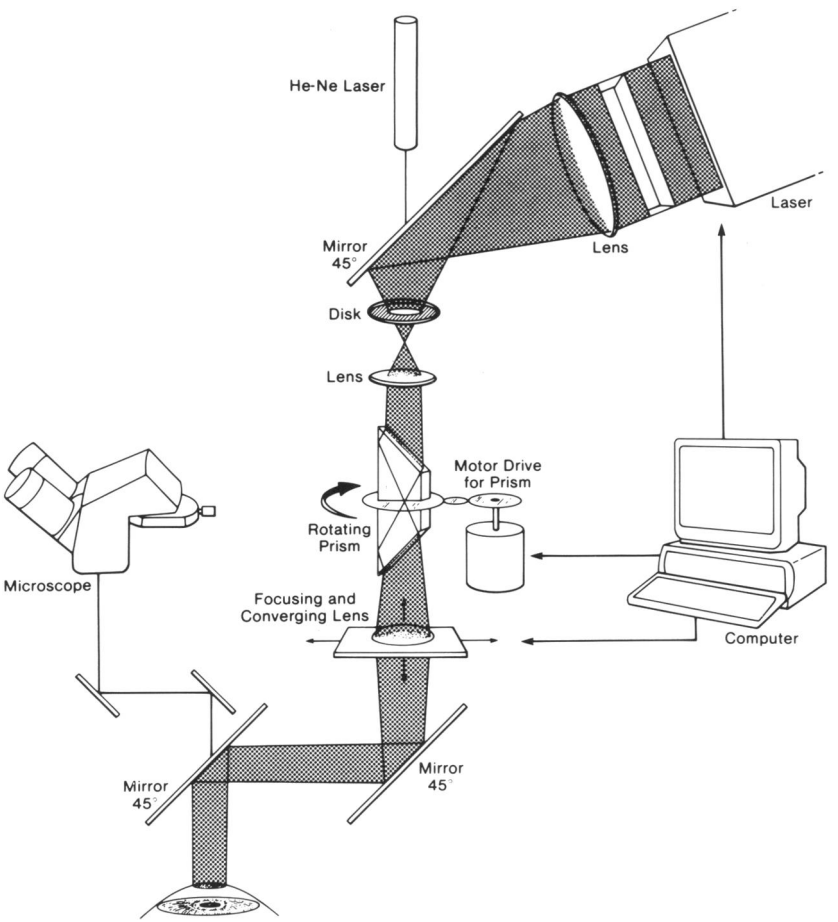

FIGURE 25

Drawing of the major components of the computer-controlled, translating slit delivery system. The laser beam is expanded by a lens and diverted toward the eye through a series of mirrors. It passes through the calibrated slit mask, and the image of the slit is passed through a rotating dove prism which can change the orientation of the slit under computer control. The objective lens moves in the X, Y, and Z direction under computer control and moves the slit image over the surface of the cornea. Details are presented in the text. (Hanna CD, Chastang JC, Asfar L, et al: Scanning slit delivery system. *J Cataract Refract Surg* 1989; 15:390-396.)[86]

2. The space surrounding the patient's head was totally free of obstacles to allow the surgeon and assistants access to the surgical site of the eye.

3. The laser beam had to be delivered directly to the cornea along a vertical direction parallel with the visual axis to allow linear corneal excisions (radial keratotomy, transverse keratectomies).

4. The laboratory space and commercial availability of mechanical and optical components influenced the design.

5. The system can move with respect to the eye in X, Y, and Z directions.

The delivery system is suspended over a motorized operating table that moves in the X-Y coordinates. The first vertical portion of the delivery system is also motorized to provide motion along the Z coordinate.

The laser beam is deflected by five mirrors, each a multiple dielectric type, specially tuned to reflect 193 nm radiation at a 45° incident angle with high reflectability.

The rectangular laser beam emerges horizontally from the laser and strikes the first mirror which reflects the beam vertically to strike the second mirror deflecting the beam horizontally through the first spherical lens, which reduces the cross-section of the beam, increases its energy density, and focuses the beam in the plane of the slit mask. The converging beam strikes the third mirror and passes vertically through the slit mask. At the plane of the slit, the beam is blocked except for a small portion that goes through the opening of the slit mask, which is mounted on a horizontal micrometric X-Y stage that can be moved to place the slit aperture in the most homogeneous portion of the beam. The position of the slit itself is fixed during operation. Each individual slit mask has its own set of characteristics, particularly with regard to the diffraction pattern at the edge of the slit, and therefore, the code for each slit mask is individually entered into the computer, which adjusts for the exact length, width, edge configuration and mathematical shape factor of that individual mask.

The diverging beam passes through a second spherical lens that brings the beam parallel as it enters the dove prism, which permits rotation of the image. A motor rotates the dove prism under the control of computer algorithms that determine the meridian along which the slit image intersects the surface of the cornea.

The parallel laser beam emerges from the dove prism and passes through the third and final spherical lens that images the slit onto the cornea. The position of this lens is controlled by two motors, one moving in the X axis and the other in the Y axis, so that the image of the slit can be translated across the surface of the cornea in any direction, when com-

bined with the rotation of the dove prism. The position of the moving spherical lens is also controlled by computer programs.

The vertical beam is then deflected by two more mirrors to bring it in vertical alignment with the viewing path of the surgical microscope attached to the delivery system.

Alignment of System

Three helium-neon lasers are used to align the delivery system. One of the lasers is used to align the optical path of the delivery system and the other is used by the surgeon to define the focal plane of the slit image beam on the cornea. This helium-neon laser passes through a three aperture diaphragm and a focusing lens, so that when the laser beam is out of focus, three separate red triangular patches appear on the surface of the cornea and when the laser is in focus, these three patches converge as a single small red dot. A third helium-laser is used to align the mirrors in the excimer laser resonating cavity.

The entire optical column of the delivery system is connected to an external port that allows flooding of the column with positive pressure nitrogen gas that keeps dust and dirt contamination away from the optical components and improves the transmission of the ultraviolet radiation through the system.

Maintenance of System

For ease of inspection, maintenance, and repair, each optical component can be assessed individually. Each mirror and lens is mounted in a separate removable housing that not only allows easy replacement, but also allows variable orientation by adjustment of small set screws. The operating microscope is mounted as an integral part of the delivery system for stability and coaxial alignment.

Operation of System

The operator enters the following information into the computer terminal: (1) surgeon's identification number, (2) the preoperative central radius of curvature or dioptric power of the cornea, (3) the preoperative power and axis of the corneal cylinder, (4) the spherical and cylindrical dioptric correction desired, (5) the number of the slit mask aperture used, (6) the desired depth of ablation for each pulse (generally on the order of 0.50 μ), (7) the number of pulses allowed in the same location before the slit moves (1 to 20), (8) the amount of displacement between the location of two successive pulses, which will specify the overlap between the pulses (generally on the order of 98% overlap), (9) the number of passes to be made by the translating slit (2 passes a 90° and 180°, 4 passes at 0°, 45°,

90°, and 135°, etc, up to 10 passes), and (10) the repetition rate (5 to 10 Hz). With this information, the computer calculates the amount of tissue to be ablated from the center of the cornea and the final radius of curvature in both the steep and the flat meridians and then selects the pulse energy and radiant exposure for the procedure.

At this point, the computer presents on the screen a graphic simulation of the surgery in terms of the number of pulses, the location of each pulse, the direction of each translocational movement, and the overall result of the surgery. The surgeon can approve the results as presented in this model or modify the data entered to change the result. The eye is then stabilized and centered beneath the helium-neon laser beam which shows three different spots to superimpose for proper focus. The laser is activated and the procedure is carried out as programmed, with no further intervention from the operator.

The location of each laser pulse passing through the slit mask is under the control of a computer program. The meridian along which the slit images will pass is determined by rotation of the dove prism. Once this meridian is selected, the translating spherical lens moves the slit image along this meridian to create a series of overlapping or adjacent slit images. The number of ablations along this meridian is defined by the computer program while the amount of overlap of each ablation is programmable by the surgeon. After a single translating pass along a meridian is completed, the dove prism rotates the beam to a new meridian, and another series of ablations is made by moving the translating lens. In general, four passes are made at 0°, 45°, 90°, and 135°, although the pattern is infinitely variable. Clearly, a single pass along one meridian will produce an astigmatic correction and multiple meridians must be abated in order to produce a symmetrical correction (Fig 26).

Projected Improvements in System

Planned additions for the system include a device to measure the beam profile as it emerges from the system with a feedback through the computer programs in order to ensure uniform pulse energy and optimal homogeneity of the beam. A device to image the corneal surface and the

FIGURE 26

Computer graphic simulation of laser myopic keratomileusis by a translating slit image. *Dark circle* represents the cornea and *light circle* in the center represents the pupil. The *dotted line* represents the meridian of greatest corneal curvature. A: The translating slit image first demarcates both ends of the limit of the first pass and then in a successive slightly overlapping series of pulses, and slit image is moved translationally across that meridian. B: The slit image is then rotated, and a second ablation carried out in that meridian. Any number of directions up to ten may be selected. The final profile is that of a myopic keratomileusis with the cornea flatter in the center than in the paracentral area.

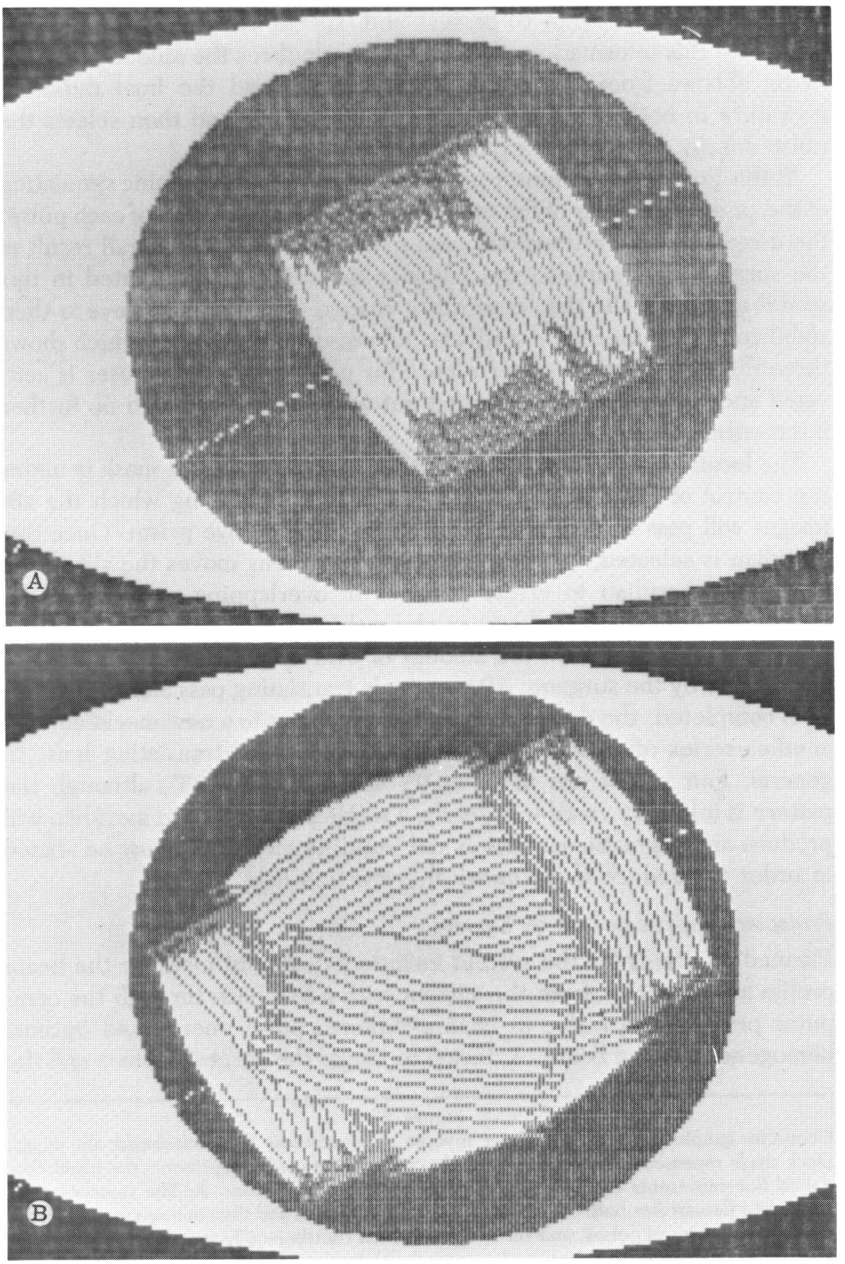
A
B

surrounding limbus will be integrated into the system to control eye stability and measurement of curvature changes. Finally, biomechanical computer models based on nonlinear, viscoelastic, anisotropic assumptions will increase the preoperative simulation of the outcome of surgery.[88-90]

Laser Myopic Keratomileusis

The slit mask selected for myopic correction is symmetrical in two perpendicular directions and fusiform in shape, with two parabolic edges.

The length of the slit defines the diameter of the ablated zone; the shape of the ablated zone is determined by the number of passes of the slit. The first pass along a meridian creates an ablation pattern that is comprised of three different regions. In the central region, the ablation is deepest and perfectly astigmatic; at either end of the meridian the thickness of the ablation decreases from the maximum value to 0. The length of the pass is mathematically defined in both the central and peripheral regions.

The dove prism is then rotated 90° so that the slit image now makes a second pass under the same conditions but perpendicular to the meridian of the first pass. These two perpendicular ablations produce a perfectly rotationally symmetric paraboloid lens within the square intersecting area. This paraboloid represents an excellent approximation of the corneal shape and the ablation is the same along the two orthogonal meridians as well as along the meridians at 45°. However, some small distortion appears in the peripheral areas (Fig 27A).[86]

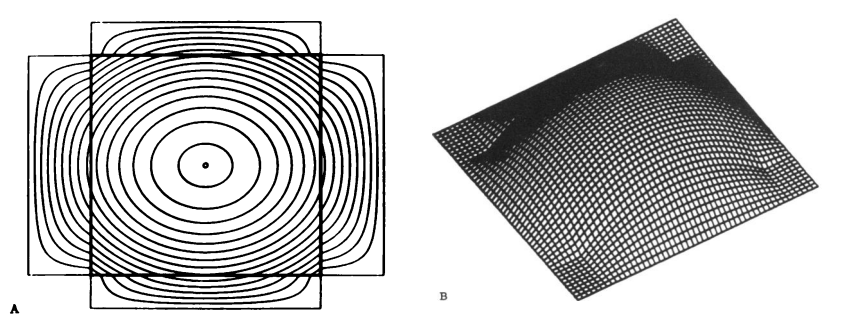

FIGURE 27

Computer simulations of the contours of the surface created by an excimer laser during the correction of compound myopic astigmatism. A: Simulation of two sweeps of the translating slit demonstrate the creation of an oval ablated zone with irregular edges, for the correction of the astigmatism. The contour lines show the topography to be flatter in the center than at the periphery of the ablated area. B: A three-dimensional contour diagram of the ablated tissue, using the same information contained in A. (Hanna KD, Chastang JC, Asfar L, et al: Scanning slit delivery system. *J Cataract Refract Surg* 1989; 15:390-396.)[86]

If the dove prism is now rotated 45° and a third pass made and then the prism is rotated 90° so that a fourth pass is made perpendicular to the third pass, the total of four passes will yield an ablated zone whose contour differs little from a circle. This is because the peripheral distortions are decreased by the additional passes (Fig 27B).

Laser Hyperopic Keratomileusis

The hyperopic slit has the shape of an hourglass with two parabolic edges diverging from each other. This allows a minimal ablation in the central portion of the slit image and a maximal ablation near the extremities. Two orthogonal passes with the slit will create four gutters, with a maximal ablation appearing at the four corners where the gutters intersect. To smooth this slightly irregular configuration, as many as 16 passes may be needed to create a more uniform circular contour. However, the hyperopic slit could be used by the rotation function of the prism and a more uniform contour will be obtained.

Correction of Compound Myopic Astigmatism

To correct an astigmatic refractive error, the number of pulses along the steeper meridian is greater than the number of pulses along the flatter meridian (Fig 28), thus ablating more tissue in the steeper than the flatter meridian and achieving a uniform radius of anterior corneal curvature throughout.

Radial or Transverse Linear Excisions

The slit mask for radial and transverse cuts has a length and width that corresponds to the desired size of the excised trough. The length and width of the slit are controlled by three sliding plates whose configuration is set manually. For radial excisions, the slit image is rotated by the dove prism. The size of the optical clear zone is programmed into the computer in advance, and the translating spherical lens is moved automatically to create this optical zone by moving the slit image away from the center toward the periphery. The actual length of each slit can be adjusted mechanically. The arcuate or transverse linear cuts are also located on the cornea by combined movement of the dove prism and the translating spherical lens.

SUCTION CONE COUPLING AND SURFACE CONDITIONING

To stabilize the eye during surgery and to couple it to the delivery system, we modified the basic suction ring from the Hanna suction corneal trephine (Fig 29). The suction cone consists of two parallel walls that form two concentric rings, the outer 15.5 mm in diameter and the inner 11.1

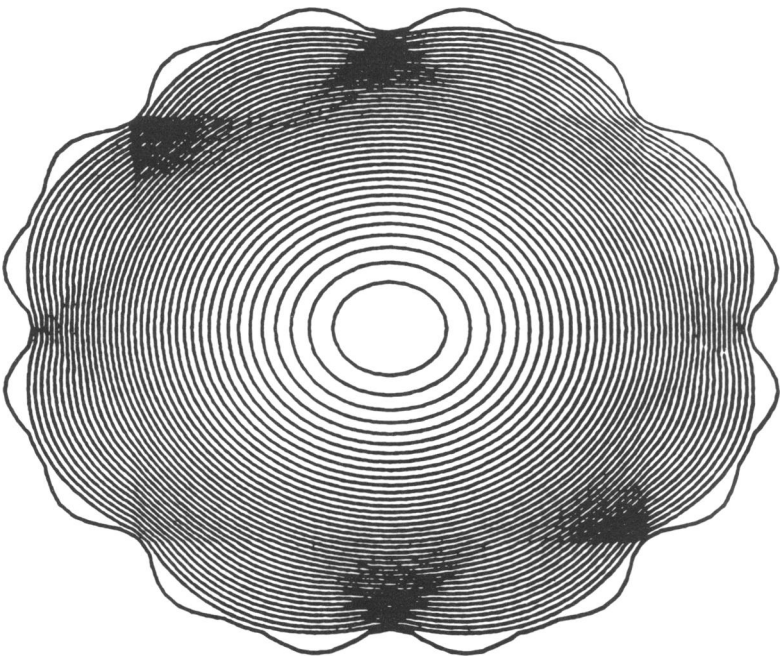

FIGURE 28
Computer simulation of the topography of a completed excimer laser keratomileusis for the correction of compound myopic astigmatism after four passes of the translating slit shows elliptical contour lines and a reasonably regular border, with the cornea flatter in the center.

mm. This creates an 82 mm^2 suction surface between the two. The edges of the suction ring fit the curvature of the conjunctival limbus. A cannula emerging from the space between the hollow walls can be connected by tubing to a spring-activated syringe or suction pump, securing the cone to the eye. The open end of the cornea can be mechanically secured to the end of the delivery system, stabilizing the eye in front of the emerging laser beam.

To condition the environment over the cornea during ablation, in-flow and out-flow ports are established on either side of the cone, with multiple openings inside the cone. The air within the cone is replaced with humidified nitrogen blown in through the in-flow cannula and then aspirated through the out-flow cannula. This decreased the absorption of the laser beam by air-born particles, removes the effluent of ablated tissue from over the surface of the cornea, and creates a uniform humidified environment to prevent thinning of the cornea from evaporation or thickening of the cornea from irrigating fluids.

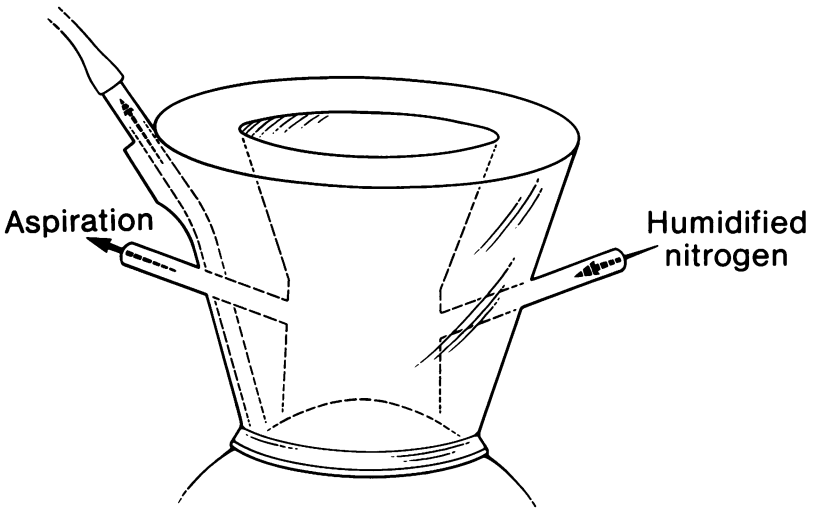

FIGURE 29
Drawing of suction cone coupling and surface conditioning system. Suction cone adheres to conjunctival limbus and can be connected mechanically to the end of the delivery system. The ablated debris and air are aspirated from the surface of the cornea and humidified nitrogen can be blown across the surface as well.

CALIBRATION OF RADIANT EXPOSURE (FLUENCE)

Ablation Curve in Rabbits

To determine the ablation curve for the depth of ablation at different radiant exposures, we performed a series of experiments in live rabbits.

Methods: Seven white rabbits were anesthetized by intramuscular ketamine. The lids were held open with a wire Barraquer lid speculum and the surface of the cornea gently dried. Corneal thickness was measured with a Storz ultrasonic pachometer using the velocity of sound in the cornea of 1640 n/sec. The epithelium was left intact. With the laser aimed at the area of the cornea where the thickness was measured and using a repetition rate of 23 Hz, the laser was fired until the cornea was perforated. The moment of perforation was easy to see through the operating microscope because of the gush of aqueous that quenched the laser beam. Rabbit tearing during the procedure was controlled with cellulose sponges so that the fluid on the surface would not interfere with the calibration of the ablation. If fluid did seep onto the area of ablation, that experiment was abandoned and begun in a different area. We used the following

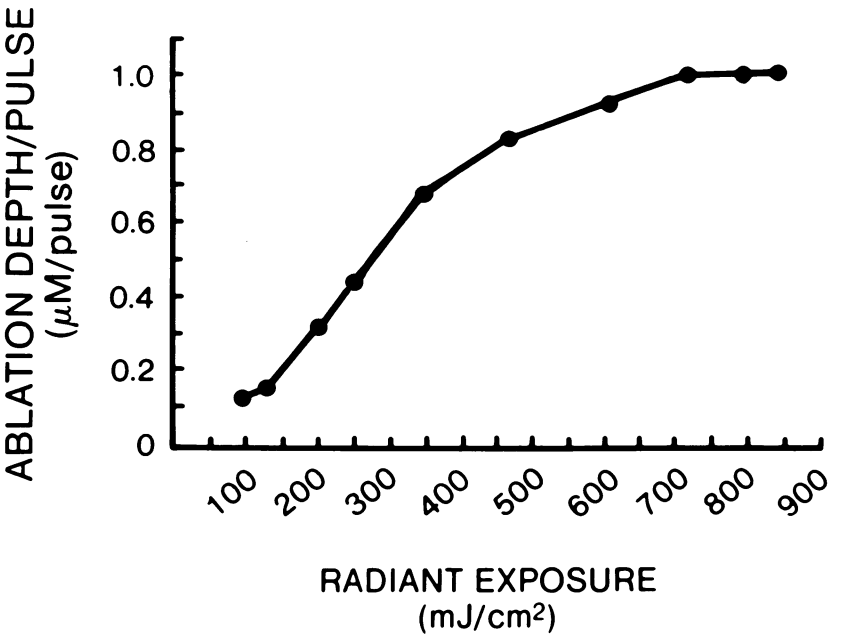

FIGURE 30
Ablation curve for 193 nm excimer laser ablation of the cornea in living rabbits with the epithelium intact. The ablation threshold could not be determined in this system, but there was a gradual increase in the ablation depth per pulse with increasing radiant exposure up to approximately 700 mJ/cm², where a plateau occurred.

radiant exposures: 100, 130, 205, 472, 608, 702, and 841 mJ/cm² in two different eyes each and the results were averaged for each fluence. The number of pulses needed to achieve perforation were counted and the ablation depth per pulse was computed by dividing the corneal thickness by the number of pulses. The ablation depth per pulse was plotted against the radiant exposure values (Fig 30).

Results: The threshold for ablation could not be accurately determined in this system, because it was difficult to decrease the pulse power of the laser to the resumed threshold value of approximately 50 mJ/cm². This is not important for our experiments, however, because we are seeking to characterize the entire curve and particularly to find the plateau. The ablation depth per pulse increased with increasing radiant exposure up to a value of approximately 700 mJ/cm². This is in general agreement with the values of Puliafito et al[49] of 600 mJ/cm² and lower than the values of Aron-Rosa and colleagues[64] of 120 to 1000 mJ/cm².

LASER MYOPIC KERATOMILEUSIS IN HUMAN EYE BANK EYES

Methods

Using the rotating slit delivery system with the myopic slit profile mask, four human eye bank eyes were fixated beneath the delivery system in a modified volume eye holder that controlled the intraocular pressure.[59] The radiant exposure was approximately 160 to 200 mJ/cm^2 at the cornea, the pulse energy 4.5 mJ, the repetition rate 20 Hz, and the rotation rate of the slit approximately 1 Hz. In two eyes, a surface area ablation 6 mm in diameter of approximately 150 μ deep was accomplished over 7 minutes. Centered keratographs were taken with the Nidek photokeratoscope immediately before and after the ablation with the intraocular pressure constant. A third eye was exposed to the laser for 30 minutes until the central cornea perforated.

The fourth cornea was used to imitate conventional myopic keratomileusis by using the Barraquer suction ring and microkeratome to remove a disc of anterior cornea 8.5 mm in diameter and 0.48 mm thick. (The swollen cornea was 0.72 mm thick at the center.) The removed disc was placed epithelial side down. The central part of the stromal surface was ablated in a myopic profile, creating a lenticule that could be sewn back onto the cornea.

Clinical Observations

As the laser beam passed over the cornea, a vapor of ejected fragments rose from the surface after each successive pulse. The ablation of each layer of the cornea had a different appearance. As the epithelium was removed, a superficial, frosted, blurred zone appeared. The rate of ablation of the epithelium was slower than that of the subjacent stroma. At Bowman's layer, the cornea became clearer. As the anterior stroma was encountered, the hazy surface recurred, blurring iris detail. When examined with the slit lamp microscope, a thick, superficial haze was apparent, and the cornea beneath it remained clear. Slit lamp microscope examination demonstrated that the central ablated area was flatter than before, had a smooth surface, and was demarcated by a well-defined border. These findings were confined by quantitative keratographs (Fig 22).

Tissue Preparation: At the conclusion of the ablation, buffered 2.5% glutaraldehyde was flooded over the surface of the cornea. The corneoscleral shell was excised and the ablated area bisected with a razor blade.

For scanning electron microscopy the tissue was immersed in 2% cold glutaraldehyde for at least 1 hour and then washed with three changes of

buffer for 1 hour. It was post-fixed in osmium tetroxide for 1 hour and then rinsed with several changes of distilled water and dehydrated in grade concentrations of acetone, each for 20 minutes. The 100% acetone bath was changed three times for a total of 60 minutes. The tissue was placed in a CO_2 critical-point drying apparatus and the acetone replaced under pressure by liquid CO_2. The apparatus was warmed above the critical point of CO_2, 31.3°C, to convert the liquid CO_2 to the gas. The specimen was then mounted on an aluminum pin with silver paint, shadowed with carbon followed by gold in a Denton evaporator. Tissues were examined with a ISI DS130 scanning electron microscope and photographed.

Fixation for transmission electron microscopy was similar, except smaller slices of the tissue were taken and after passing through osmium tetroxide, were dehydrated through a descending series of ethyl alcohol dilutions. The tissue was cleaned in 100% propylene oxide, infiltrated with Epon 812 plastic, embedded and incubated for 72 hours at 60°C. Care was taken during the embedding to preserve the orientation of the tissue. Thick sections of the block were cut at 0.5 to 1.5 μm with a glass knife on an ultramicrotome and were stained with 1% toluidine blue in 0.5% borax for light photomicroscopy. The blocks were then oriented for thin sections which were cut with a diamond knife on an ultramicrotome, stained with alcoholic uranil acetate followed by Reynold's lead citrate. They were examined under the transmission electron microscope.

Light and Transmission Microscopic Observations

Scanning electron micrographs of the ablated corneal epithelium presented a striking appearance, resembling a smooth beach strewn with stones, because the nuclei of the epithelial cells resisted ablation more than the cytoplasm and remained as round protuberances (Fig 31). Light micrographs and transmission electron micrographs demonstrated a smoothly sloping wall to the ablation, with the epithelial cells smoothly tapering onto the surface of the gradually thinning Bowman's layer and a slightly corrugated stromal surface—all covered with surface condensate (pseudomembrane) (Fig 32). Scanning electron microscopy of the ablated Bowman's layer showed a diffusely bumpy appearance, that could have been a result of the "shadows" cast by the more slowly ablated epithelial nuclei or from inhomogeneities in the beam.

The cornea that was ablated to perforation demonstrated edges of Descemet's membrane and corneal epithelium. The anterior banded and posterior nonbanded layers of Descemet's membrane were apparent. The disc that was removed with the microkeratome and ablated across the

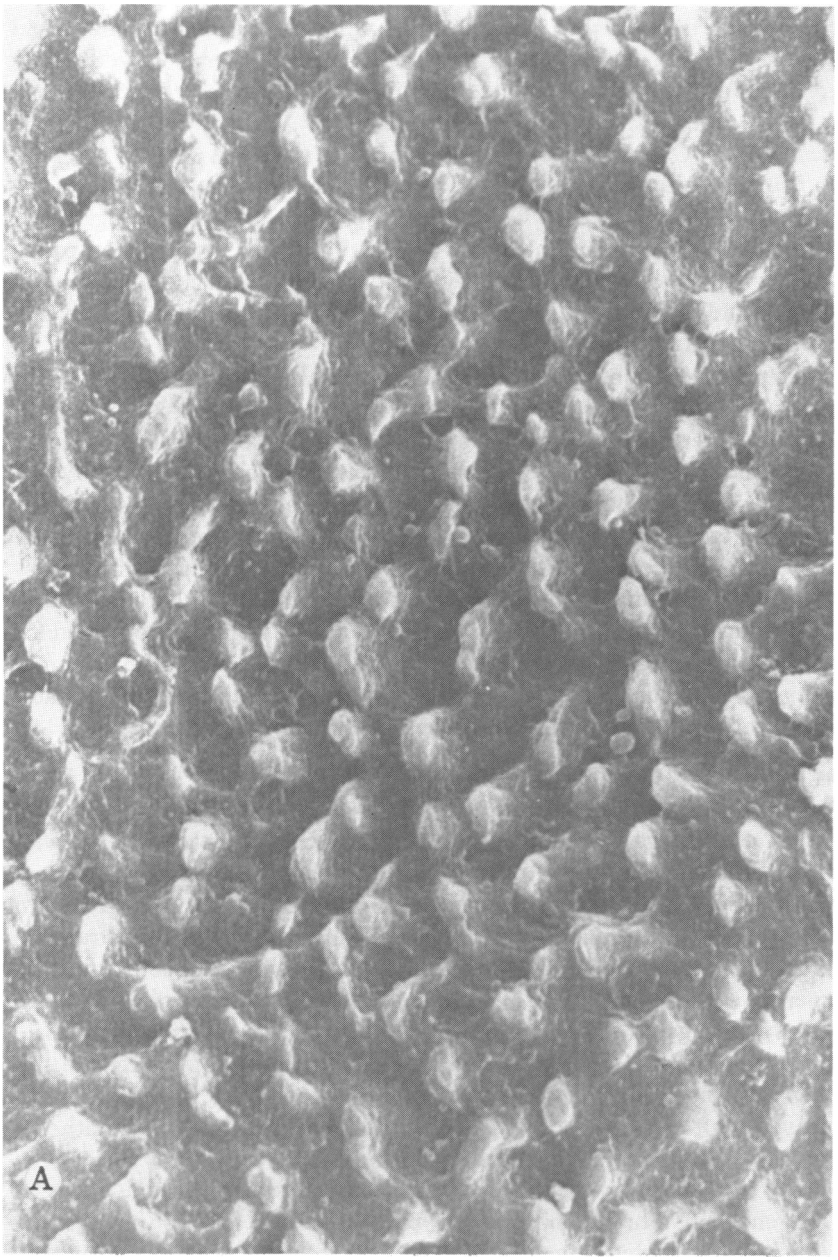
A

FIGURE 31
Scanning electron micrographs of ablated corneal epithelium in a human eye bank eye. A: Photograph at junction of a more sparsely spaced polygonal cells (*above*) and more compact basal cells (*below*) demonstrate nuclei protruding from the surface of the surrounding cytoplasm (×500). B: Higher power view demonstrates a single nucleus with sloping ablated margins rising above the cytoplasm (×20,000). (Courtesy G Renard and K Hanna, MD)

stromal surface with the excimer laser demonstrated a smooth surface with minimal disruption of the stromal lamellar architecture.

SHORT-TERM EPITHELIAL HEALING (AFTER SCRAPE INJURY AND LASER ABLATION)

Methods

Using two New Zealand white rabbits, one eye each had a central epithelial debridement in a diameter of 7.5 mm with a blunt spatula. The other eye had a central ablation with the laser using the rotating slit delivery

FIGURE 32
Ablated surface of cornea in human eye bank eye. A: Light (*above*) and transmission electron (*below*) microscopy at the margin of the ablated epithelium demonstrate the tapering margin of the basal epithelial cells (EP), the smooth surface of the gradually thinning Bowman's membrane (BM), overlying the corneal stroma (S) (above: hematoxylin-PAS, ×130; below: ×2180). B: Transmission electron micrograph of the ablated stroma demonstrates a surface condensate (pseudomembrane) slightly separated from the surface with minimal disruption of the underlying stromal architecture (×4150). (Hanna KD, Chastang JC, Pouliquen Y, et al: Excimer laser keratectomy for myopia with a rotating slit delivery system. *Arch Ophthalmol* 1988; 106:245-250.)[59]

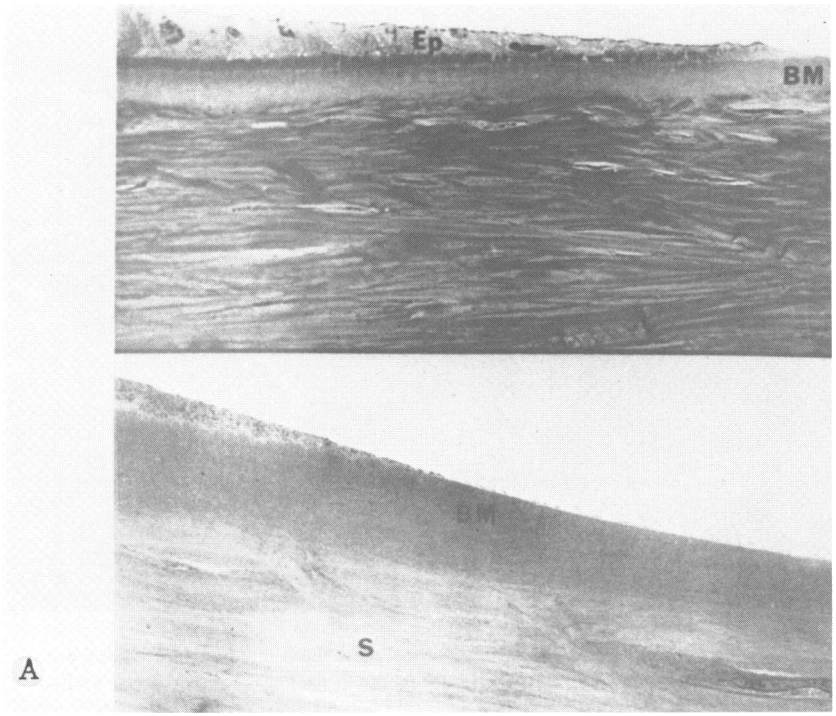
Ep
BM
BM
S
A

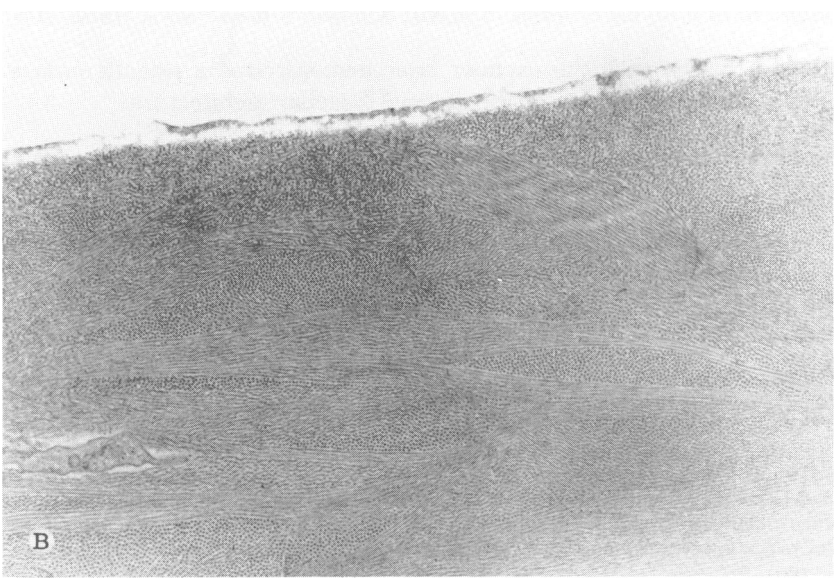
B

system, fluence at the surface of the cornea of 200 mJ/cm^2, repetition rate of 20 Hz, ablation for approximately 150 seconds to a depth of approximately 30 μm. The laser ablation removed both the epithelium and the anterior stroma.

The corneas were allowed to heal spontaneously without medication for 3 weeks, at which time slit-lamp microscope examination revealed a smooth glistening epithelium with a very faint haze and mild surface irregularity in the anterior stroma in the cornea with the laser ablation. This simple comparison demonstrated the capability of the rabbit corneal epithelium to heal normally after laser keratomileusis.

Histologic and transmission electron microscopic comparison of a normal central area, the area of mechanical epithelial scraping, and other areas of laser ablation showed no recognizable differences in the epithelium, basement membrane—hemidesmosome complexes, and anterior stroma (Fig 33).

HEALING OF RABBIT CORNEA AFTER ANTERIOR LASER KERATOMILEUSIS

Methods

A Lambda Physik EMG 201 ArF excimer laser produced 193 nm ultraviolet radiation using stable optics in the resonating cavity and the rotating slit delivery system described above (Fig 23) with a radial slit whose shape was defined mathematically for the correction of myopia. Pulse energy was 180 mJ; repetition rate was 16 Hz; radiant exposure at the corneal surface was 220 mJ/cm^2, as measured by a joulemeter. The homogeneity of the laser beam was evaluated on photographic paper and showed small focal inhomogeneities.

Seventeen New Zealand white rabbits were anesthetized with an intravenous pentobarbital injection in appropriate doses of approximately 25 to 30 mJ/kg.[60] The rabbits were positioned on a table beneath the laser. Topical 0.5% proparacaine was instilled and the eyelids were held open with a wire speculum. Corneal thickness was measured using a Cooper Vision ultrasonic pachometer with a speed of sound set at 1640 m/sec. The thickness varied between 290 and 340 μm in all rabbits. The corneal epithelium was removed from the central 80% of the cornea by scraping. The globe was stabilized with a pneumatic Barraquer suction ring fixated to the conjunctival limbus with moderate suction (approximately 200 mm Hg) supplied by a vacuum pump. The ring was held manually throughout the procedure.

The ablated area was 7.5 mm in diameter. We used 2000 to 2050 pulses over approximately 2 minutes to ablate a depth of 60 μm in the center of the cornea, the depth gradually becoming shallower toward the edge of

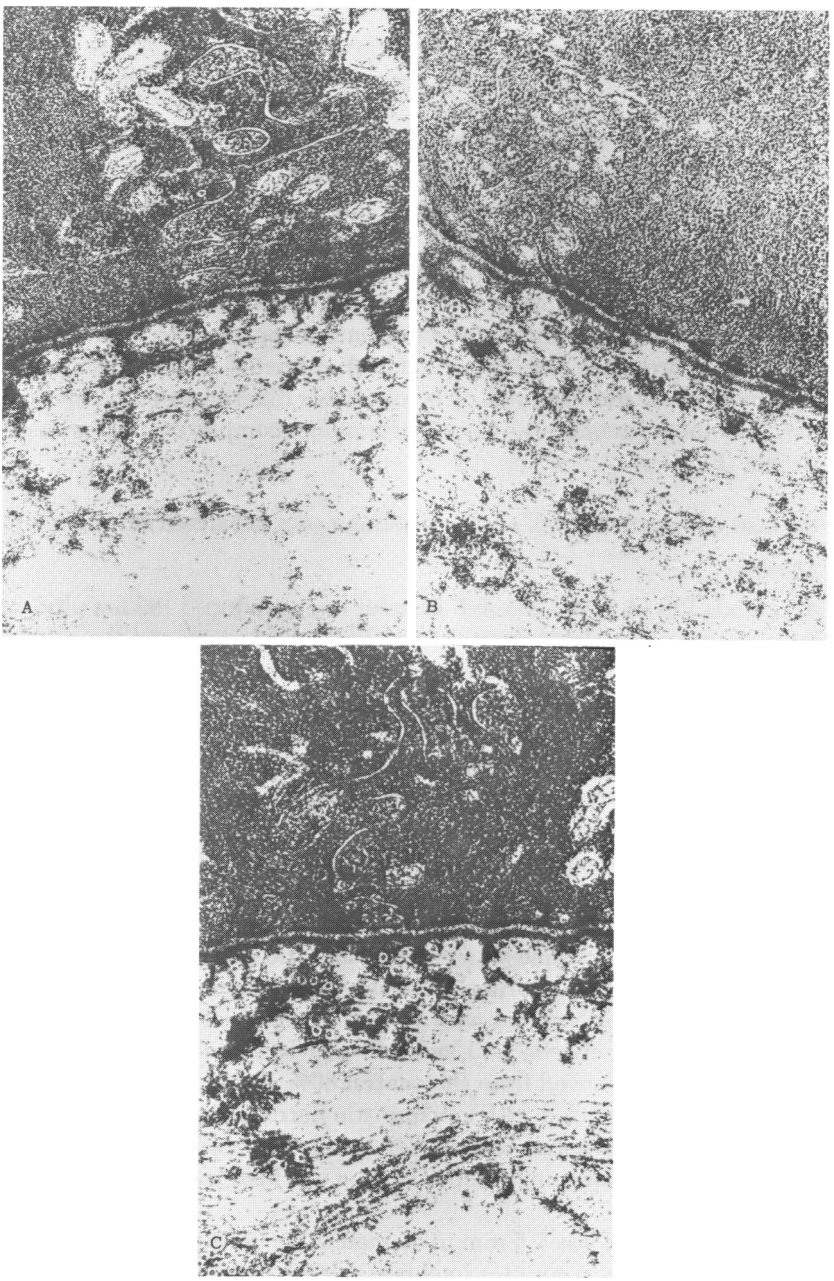
A
B
C

the ablated area, which flattened the radius of curvature of the cornea to correct myopia. Surgery was unsuccessful in two rabbits that moved during the procedure and they were omitted from the series. Both eyes of each rabbit were ablated in succession. At the conclusion of the laser treatment gentamicin drops were instilled and the eyelids were sutured closed with a single 8-0 Vicryl suture that remained intact for approximately 24 hours and then dissolved spontaneously.

The rabbits were sacrificed at postoperative days 0, 3, 7, 14, 21, and 100 with an overdose of sodium pentobarbital. The corneas were removed and prepared for histology and electron microscopy as described above.

Four eyes of two rabbits received a mechanical epithelial abrasion only, serving as controls and were sacrificed 3 weeks after surgery. Thirteen rabbits (26 eyes) were followed and examined with a slit-lamp microscope by an independent ophthalmologist who did not do the surgery, at days 3, 7, 14, 21, 50, and 100. A clear cornea was defined as one devoid of stromal haze in which the central ablated area was as clear as the peripheral untreated area.

Clinical Observations

During the laser ablation, the ablated corneal surface became frosty but no areas of opacification of the tissue beneath the surface were observed. The superficial haze disappeared when the eye was washed by balanced salt solution. Mild surface irregularities appeared in the central 2 mm of the ablated area where the rotating slit failed to overlap exactly. After the epithelium healed, the subepithelial haziness gradually decreased over approximately 3 weeks without changes in the stroma. During these 3 weeks, seven of the rabbits were sacrificed. Of the remaining six rabbits, four eyes of three rabbits remained clear and eight eyes of five rabbits had some degree of central spotty subepithelial haze. This was a faint, lightly ground-glass haze that occupied only the subepithelial stroma, and in four eyes could be appreciated only on very careful slit-lamp examination. The haziness decreased gradually over 3 months but never disappeared completely.

FIGURE 33

Comparison of healing at 3 weeks in rabbit's eyes of mechanical epithelial removal, laser ablation, and normal control cornea, using transmission electron microscopy. A: Area of normal epithelium outside the ablated zone demonstrates basal epithelial cell with intact hemidesmosomal-basement membrane complexes and normal distribution of amorphous material among the anterior stromal collagen fibrils (×40,000). B: Area of scrape injury shows similar findings to normal zone (×40,000). C: Area of laser ablation shows findings similar to normal cornea and zone of mechanical epithelial removal. The comparison demonstrates the ability of the rabbit corneal epithelium to heal normally after laser keratomileusis (×40,000). (Courtesy KD Hanna, MD and Y Pouliquen, MD)

Pathology of Epithelium and Stroma in Clear Ablated Corneas

Figs 34 to 36 present the light microscopic and ultrastructural findings that are representative of this series. Prior to ablation, the control corneas showed normal ultrastructure (Fig 34A). Immediately after keratomileusis (Fig 34B and C), the ablated stromal surface appeared generally smooth with some focal irregularities at the center. Residual fibrocytes in the plane of the ablation was consistent with that of a myopic correction.

FIGURE 34

Histopathology and ultrastructure of healing of excimer laser myopic keratomileusis in rabbits from baseline to 3.5 months. A: Transmission electron micrograph of normal rabbit basal cornea epithelium and anterior stroma shown for comparison with the photographs in the healing series. The basal epithelial cells contained numerous hemidesmosomes. A lamina lucida is present between the epithelial cell membrane and the lamina densa of the basement membrane. The zone immediate subjacent to the basement membrane showed poor organization of the collagen fibrils and was peppered with islands of amorphous extracellular matrix. This area is roughly comparable to Bowman's layer in humans. An interweaving lamellar structure began to define itself just beneath this area, and became a well demarcated series of orthogonal lamellae posterior to the area in this figure (×10,000). B: Light microscopy of acutely ablated surface shows residual keratocyte nuclei as dark areas and a thin pseudomembrane. The underlying stromal architecture is normal (hematoxylin-PAS, ×200). C: Acutely ablated stromal surface showed slightly detached pseudomembrane and slight edema and disorganization of underlying anterior stroma (×4000). D: Three days after ablation, the surface was epithelialized with a partially differentiated, seven-layer thick epithelium with multiple mitotic figures in the basal layers. Beneath the epithelium was an acellular zone that was slightly edematous. Keratocytes bordering this zone showed some activation, resembling fibroblasts. No leukocytes were present (hematoxylin-PAS, ×250). E: Three days after ablation, sparse and spotty epithelial basement membrane synthesis had begun overlying the slightly edematous and acellular subepithelial stroma (×15,000). F: Three days after ablation, high power transmission electron micrograph demonstrates discontinuous, poorly defined epithelial basement membrane (*arrow*) with the early appearance hemidesmosome precursors (×45,000). G: By 7 days, the epithelium appeared better differentiated and the subepithelial zone was being repopulated by keratocytes, with the return of a generally lamellar structure. No leukocytes were present (hematoxylin-PAS, ×200). H: Seven days after ablation, the basal epithelial cells were filling in the surface irregularities created by the laser. A thin epithelial basement membrane was present continuously, but hemidesmosomes were still developing and were not uniformly distributed (×15,000). I: Twenty-one days after ablation, the epithelium had become hyperplastic, being approximately 12 layers thick. It had smoothed over some of the surface stromal irregularities created by the laser. The subepithelial stroma had been repopulated by active keratocytes (hematoxylin-PAS, ×250). J: Twenty-one days after ablation, a uniform epithelial basement membrane was present along with well formed hemidesmosomal complexes and anchoring fibrils. The normal appearance of amorphous material beneath the basement membrane has also reappeared (×40,000). K: Approximately 100 days after ablation, the epithelium was slightly thickened, formed a smooth surface, and had filled in the surface stromal irregularities. There was no active fibrosis in the subepithelial stroma (hematoxylin-PAS, ×200). L: Approximately 100 days after ablation, the lamellar structure of the anterior stroma was well preserved, with no signs of subepithelial fibrosis. The appearance resembled that of a normal rabbit epithelium (×2000). M: At 100 days after ablation, some areas of duplication of the epithelial basement membrane were present, but the general architecture of the stroma immediately subjacent to the epithelium appeared normal (×40,000). (Courtesy KD Hanna, MD and Y Pouliquen, MD)

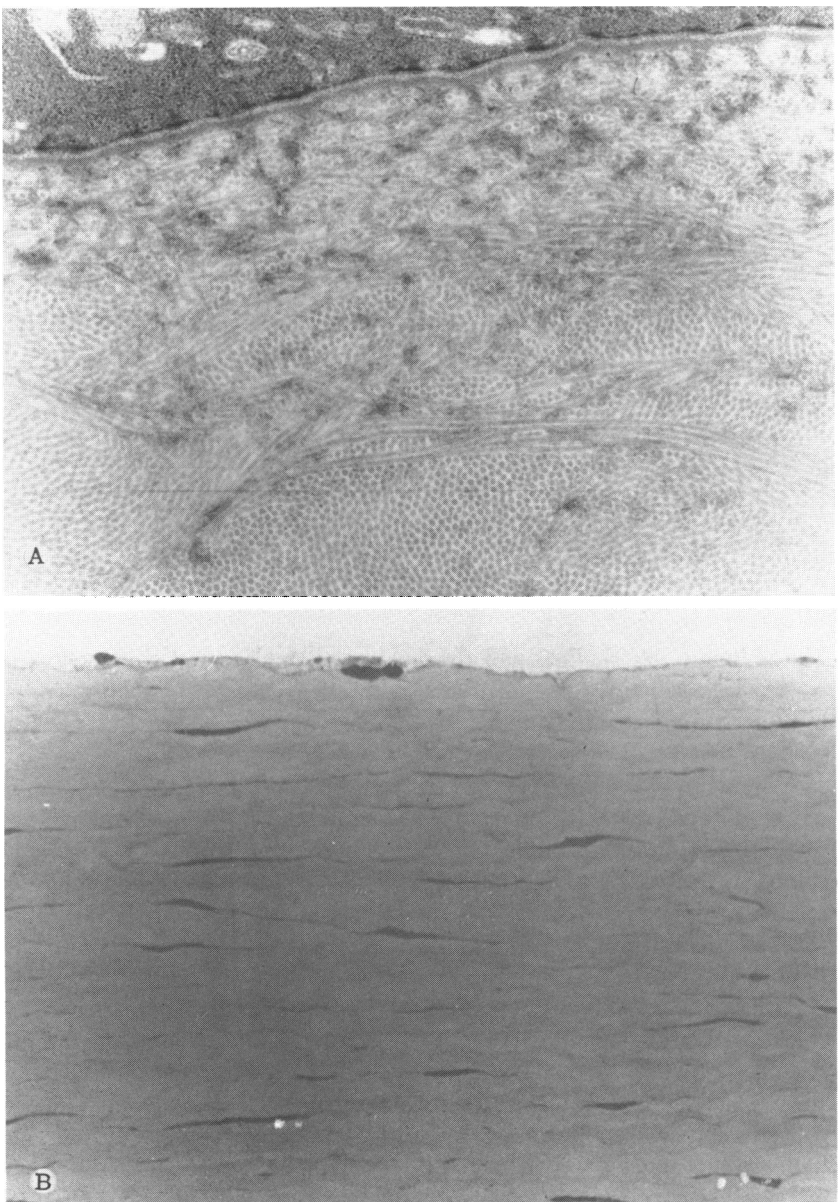
A
B

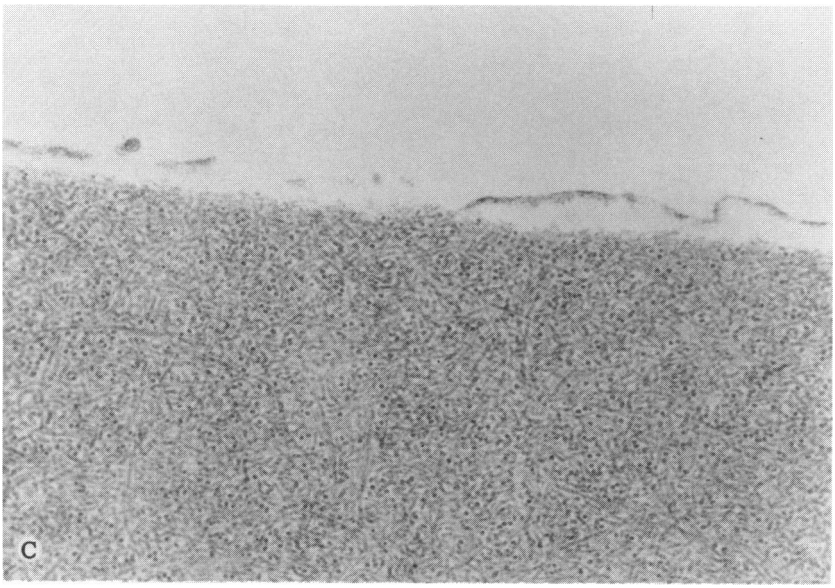

The ablation was shallow and the measured thickness of the remaining cornea was 300 μm, the same as the thickness of the scraped corneas, indicating some stromal edema. The underlying stromal architecture was not disturbed and the lamellar pattern was easily detectable. A condensate of tissue was present on the surface of some sections, consisting of electron-dense material 0.05 μm thick. Beneath this there was a 0.25 μm microgranular zone of slightly disrupted collagen fibrils and ground substance. Immediately underneath this zone, a 4 μm thick area of apparent edema was present. Beyond this the stroma appeared normal. The fibrocytes in the anterior 45 μm had vacuolated cytoplasm and ruptured cell membranes.

At day 3 (Fig 34D to F), epithelium had recovered the surface with a thickness of six to seven cells and some mitotic figures. The basal epithelial cells seemed to fill in the small surface defects, such that the epithelial surface had a generally smooth appearance. The anterior stroma beneath the ablation was acellular for a thickness of approximately 45 μm and beneath this zone, a few damaged keratocytes were present. Those present were abnormal with swollen vacuolated cytoplasm, marked indentation of the nucleus and some disruption of the cell wall. The posterior stroma appeared normal. Even though the general stromal architecture remained lamellar, there was a waviness and mild disorganization.


D

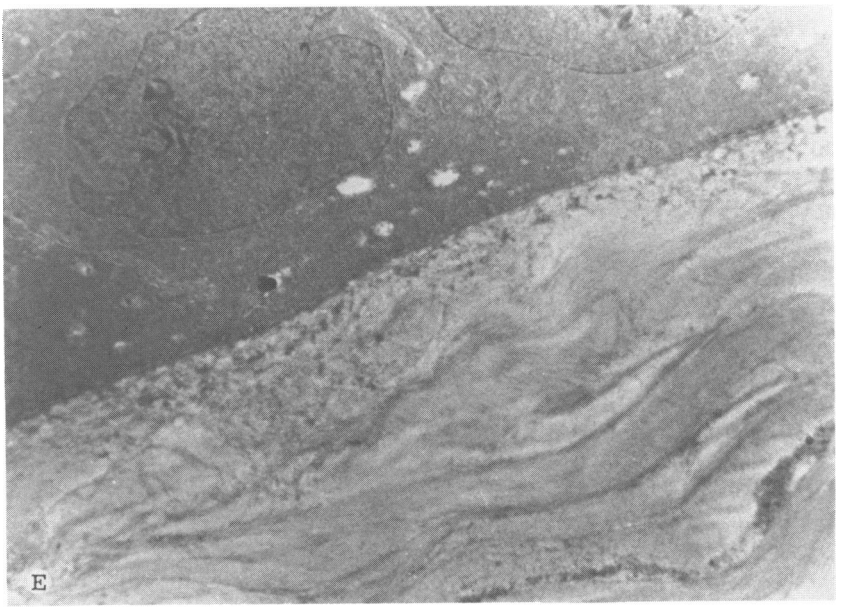
E

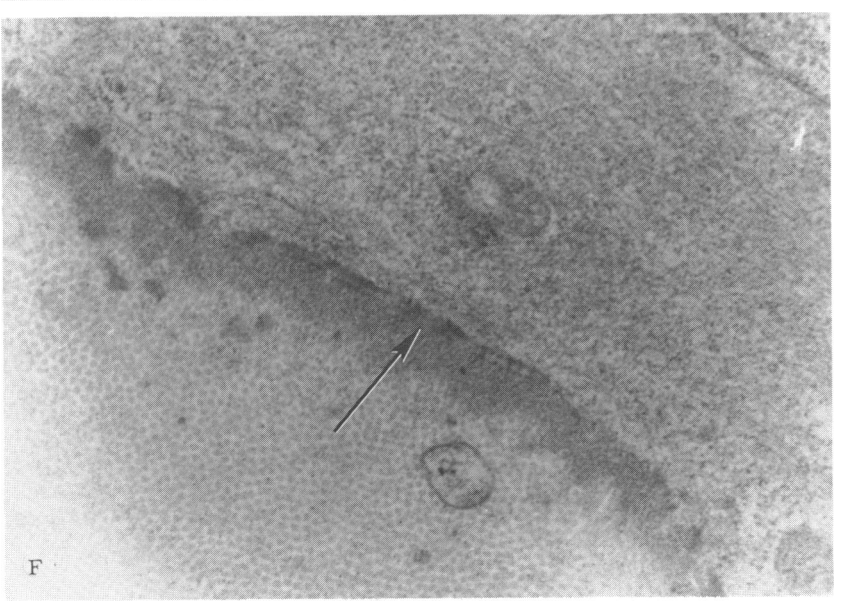
F

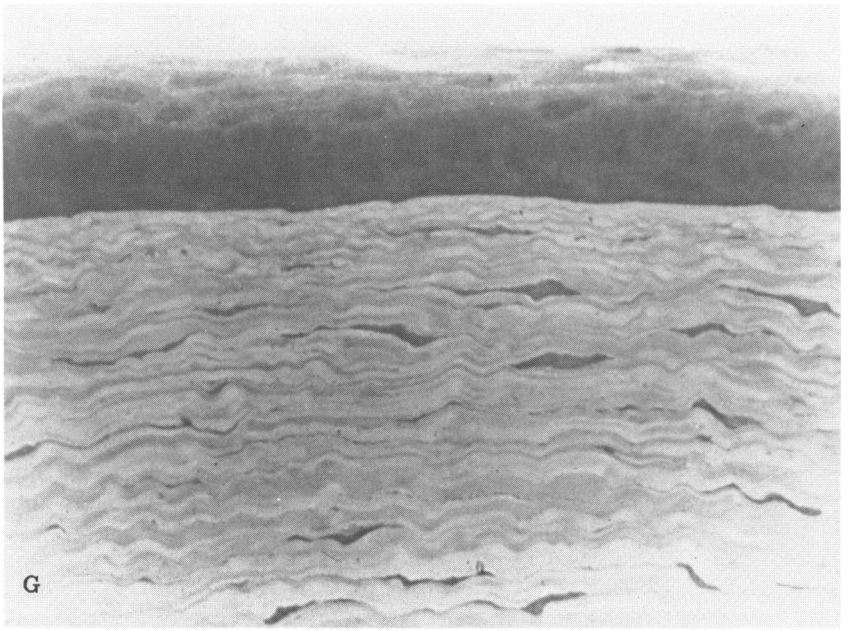

G

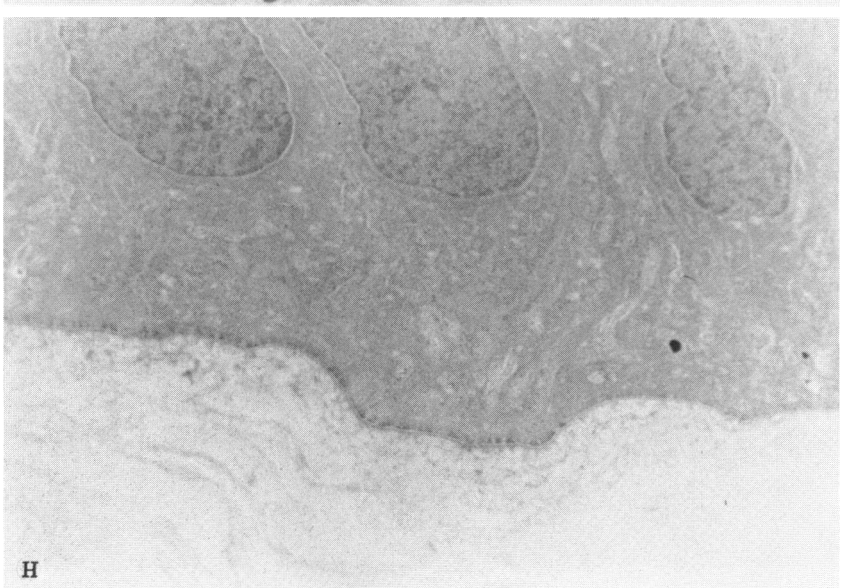

H

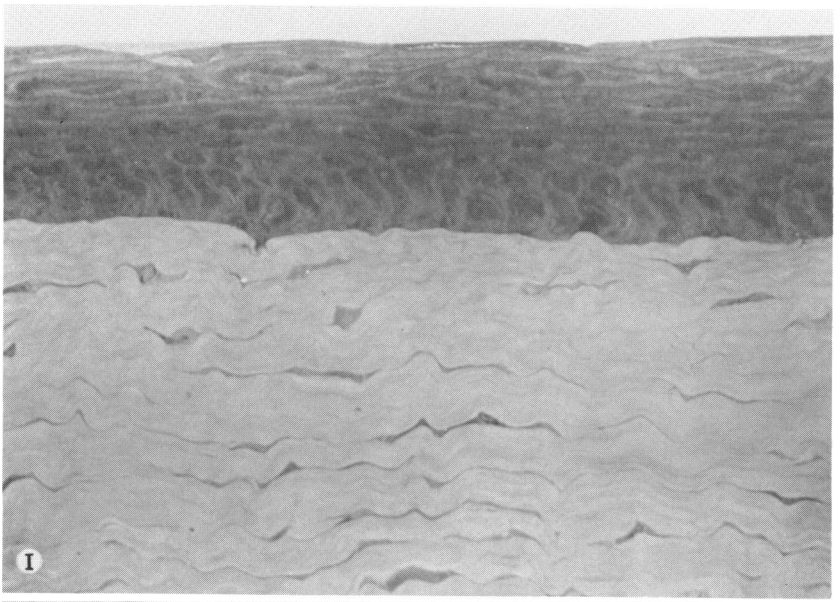
I

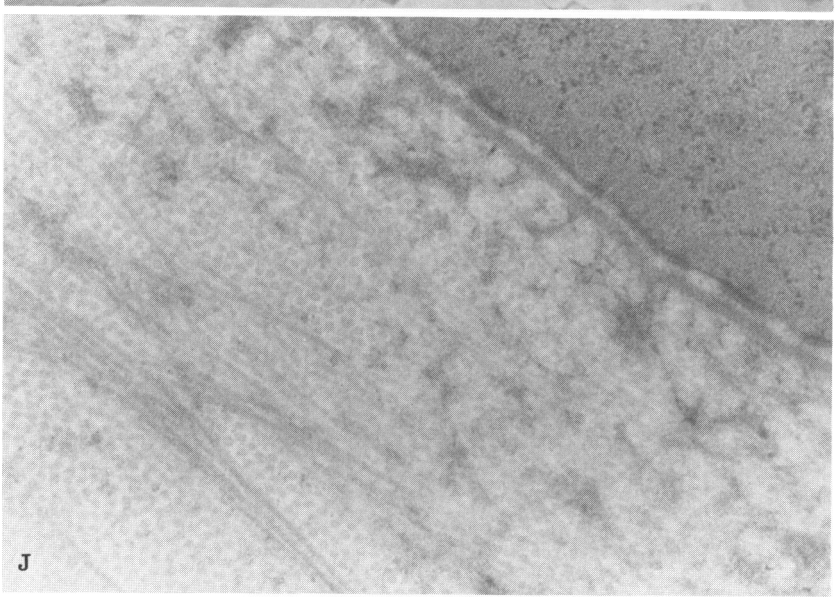
J

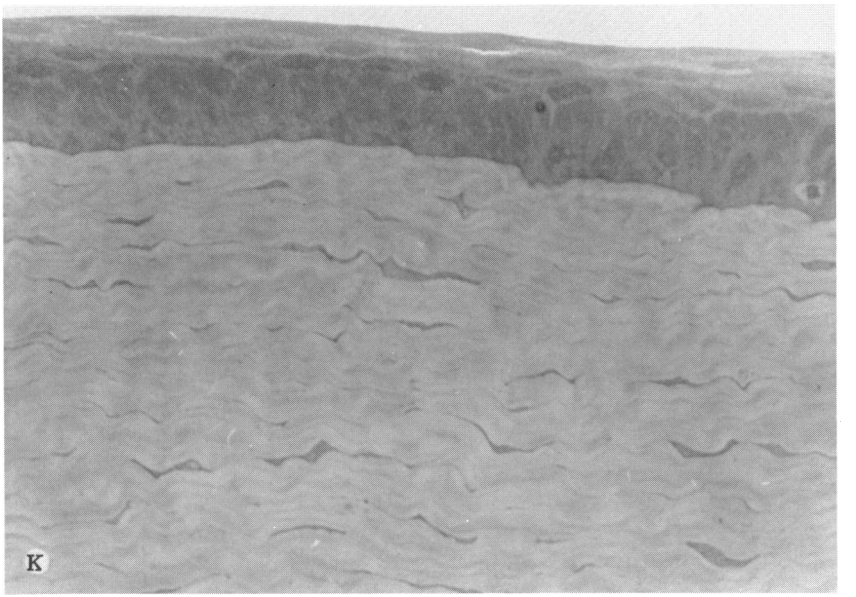

At day 7 (Fig 34G and H) the epithelium appeared slightly hyperplastic, 10 to 12 cells thick. The overall epithelial surface appeared smooth. The basal cells were taller with a regular plasma membrane. In areas where the ablated surface was irregular, the basement membrane was less distinct. Vertical fibrils extended from the basal lamina into the stroma, resembling anchoring fibrils. The immediate subepithelial stroma was acellular for approximately 10 μm. The remainder of the anterior stroma was repopulated with fibroblastic cells in increased numbers. The fibrocytes in this area showed marked cytoplasmic activity. In the posterior stroma, collagenous architecture was normal, but the keratocytes also showed increased cytoplasmic activity. The stromal lamellae were better organized but still exhibited waviness.

By day 21 (Fig 34I and J), the epithelium had resumed a normal thickness of six to seven cells (approximately 30 μm) consisting of a single layer of basal cells, two to three intermediate polygonal cells, and one to two superficial cells. The basal layer of the epithelium, the basement membrane, was normal. The hemidesmosomes and anchoring fibrils appeared normal. The fibroblasts were still increased in the subepithelial stroma. Dense amorphous deposits were spread throughout the anterior stroma, especially where the surface was irregular. There was minimal disruption of stromal architecture. Anterior and posterior fibrocytes continued to show increased cellular activity without pericellular secretion.


L

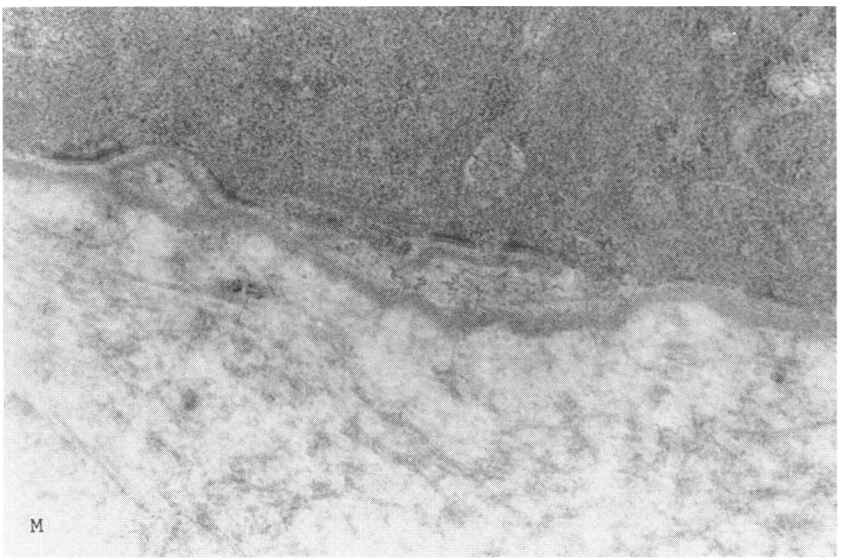

By day 100 (Fig 34K to M), the epithelial structure remained normal. The surface of the ablated stroma showed a few irregularities that were filled in by the basal cells. There was duplication of the basement membrane with subepithelial deposits of amorphous material. The anterior stromal architecture was more uniform and there was no sign of subepithelial fibrosis or scar formation. The fibrocytes were present in normal numbers, most with a normal, more elongated configuration; but in the subepithelial zone, some were contracted, suggesting continued wound healing.

Fig 35 presents a composite of these findings.

Pathology of Epithelium and Stroma in Clouded Corneas

In general, the cloudy corneas showed epithelial hyperplasia, a zone of subepithelial hypercellularity and fibrosis with occasional inflammatory cells, and minimal disruption of the anterior stroma beneath that zone (Fig 36A). In the first few weeks following ablation, the subepithelial zone demonstrated a loosely-knit area densely occupied by numerous fibroblasts and newly secreted extracellular matrix (Fig 36B). By 2 to 3 months after ablation, this area became more compact and less cellular, constituting a subepithelial scar of variable thickness from 0 to 10 to 12 μm.

Pathology of Endothelium and Descemet's Membrane

A striking finding was the appearance of a discontinuous layer of amorphous fibrillogranular material that migrated from the basal endothelial

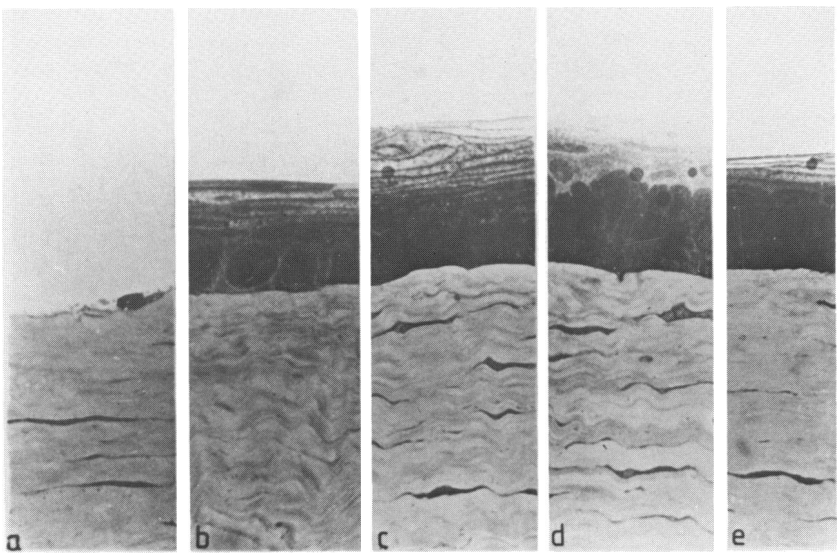

FIGURE 35

Light micrographs of the ablated surface of clear rabbit corneas. A: Day 0. The acutely ablated surface showed cellular debris. The anterior stroma demonstrated normal fibrocytes. B: Day 3. The surface was epithelialized with six to seven layers, the basal cells showing mitotic figures. The anterior stroma (approximately 45 μm) was acellular. C: Day 7. The epithelium was thickened with 10 to 12 differentiated layers. The subepithelial stroma was being repopulated by fibrocytes of normal appearance. D: Day 21. The epithelium was of normal thickness, with a tall basal layer. The intermediate and superficial layers were well differentiated. The subepithelial stroma has been repopulated by apparently normal fibrocytes. E: Day 100. The anterior stroma appeared normal with no sign of subepithelial fibrosis (hematoxylin-PAS, ×200). (Hanna KD, Pouliquen Y, Waring G, et al: Corneal stromal wound healing in rabbits after 193 nm excimer laser surface ablation. *Arch Ophthalmol* 1989; 107:895-901. With permission of the American Medical Association.)

plasma membrane anteriorly in Descemet's membrane. During the 3-months time of observation, Descemet's membrane was not observed to thicken. The thickness in ablated corneas remained 6.5 ± 1.1 μm, while in the four control corneas it was 6.6 ± 0.8 μm. It maintained a normal homogeneous configuration throughout.

FIGURE 36

Histopathology of anterior stromal scarring after excimer laser ablation of rabbit cornea. A: Four days after ablation, a lymphocyte (L) is interdigitated between the healing vacuolated epithelium (E) and the residual stroma that contains activated fibrocytes (F) (×13,400). B: At 21 days, epithelium is slightly hyperplastic with delayed maturation. A lymphocyte (*arrow*) lies between the epithelium and the underlying connective tissue. A layer of hypercellular, loosely organized scar tissue lies beneath the epithelium. The remaining stroma shows active keratocytes with a generally compact lamellar architecture (toluidine blue, ×200). (Courtesy KD Hanna, MD and Y Pouliquen, MD)

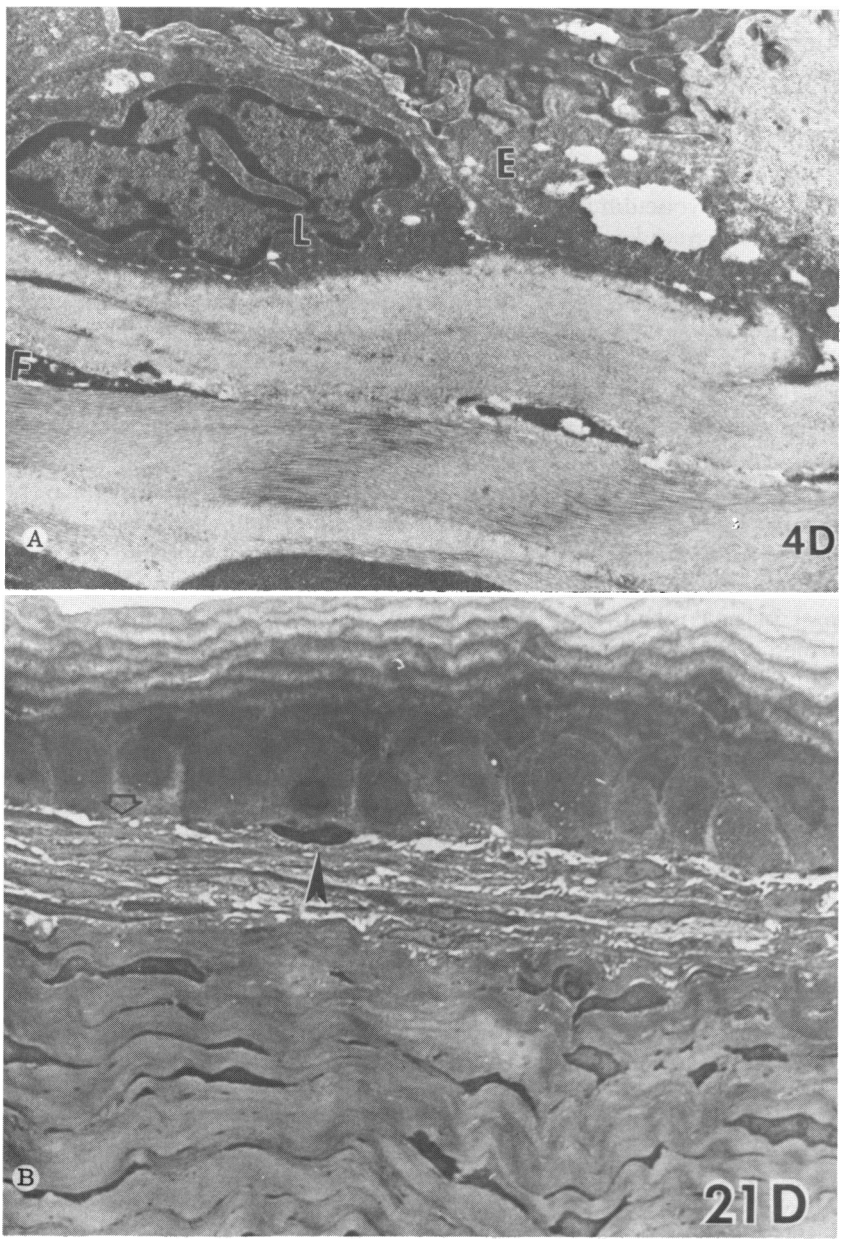
E
L
F
A
4D
B
21D

Immediately after ablation, the endothelial monolayer was intact and individual cells appeared normal, with gap junctions at the apices, intracellular spaces of normal width, a central nucleus, mitochondria with a normal oval shape, and a small amount of smooth endoplasmic reticulum (Fig 37A).

Six hours after ablation, some mitochondria were dilated and the endoplasmic reticulum was more visible, with focal dilations filled by dense microgranular substance. The Golgi apparatus was more prominent. The intracellular spaces had a normal width in the apical region, and the intercellular junctions were preserved. But in the basal region closer to Descemet's membrane, the intercellular spaces were dilated and contained a fibrillogranular substance that seemed to spill out over the basal surface of the cell adjacent to Descemet's membrane. The amorphous granular material appeared in the intercellular space and along the basal aspects of the endothelium.

By 3 days, these early changes were all exaggerated. The monolayer remained intact, but there was more swelling of mitochondria, marked dilation of the endoplasmic reticulum, and the accumulation of large amounts of fibrillogranular substance between the cells and along their basal plasma membrane. The material in Descemet's membrane had formed a spotty layer and was slightly separated from the endothelium (Fig 37B).

Between 4 and 100 days after ablation, the endothelial morphology gradually returned to normal, although the endoplasmic reticulum remained somewhat prominent and dilated. The discontinuous layer of amorphous material apparently migrated anteriorly in Descemet's membrane, being separated from the endothelium at 100 days by approximately 3 μ (Fig 37 C to E).

The migrating material had an amorphous, finely granular appearance without distinct structural elements, such as fibrillar collagen, 110 nm banded material or oxytalan fibrils. The material appeared in Descemet's

FIGURE 37

Ultrastructure of endothelium and Descemet's membrane after 193 nm excimer laser keratomileusis in the rabbit cornea. A: Immediately after ablation, Descemet's membrane and the corneal epithelium appear normal (×8000). B: Three days after ablation, small focal areas of an electron dense, amorphous, discontinuous material appeared at the anterior surface of the endothelium in Descemet's membrane (×16,000). C: Seven days after ablation, the amorphous material formed a discontinuous line across the entire posterior surface of Descemet's membrane in the area of ablation. It was absent in the area outside the ablation (×12,000). D: By 21 days after ablation, the amorphous material had migrated anteriorly (×12,000). E: By 100 days after ablation, the line of amorphous material was midway between the anterior and posterior surfaces of Descemet's membrane. The nature of this material is unknown, as discussed in the text (×12,000). (Courtesy KD Hanna, MD and Y Pouliquen, MD)


A

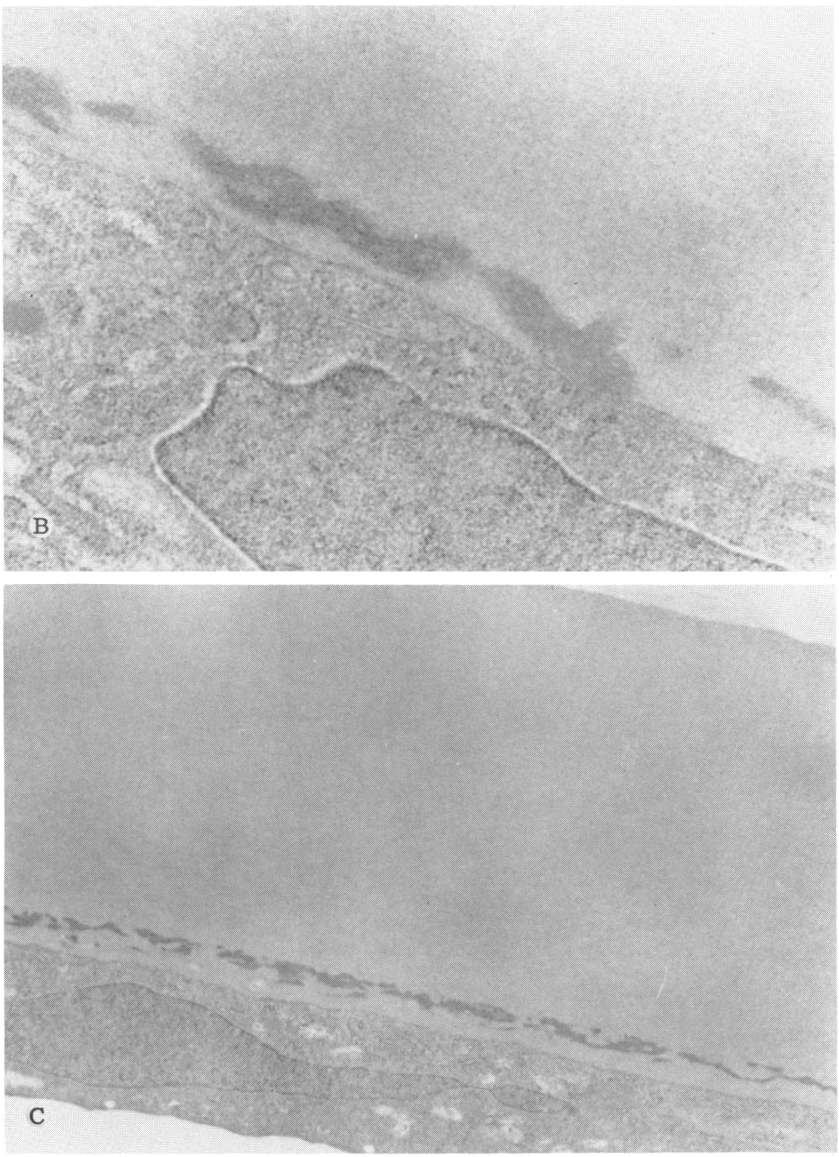
B
C

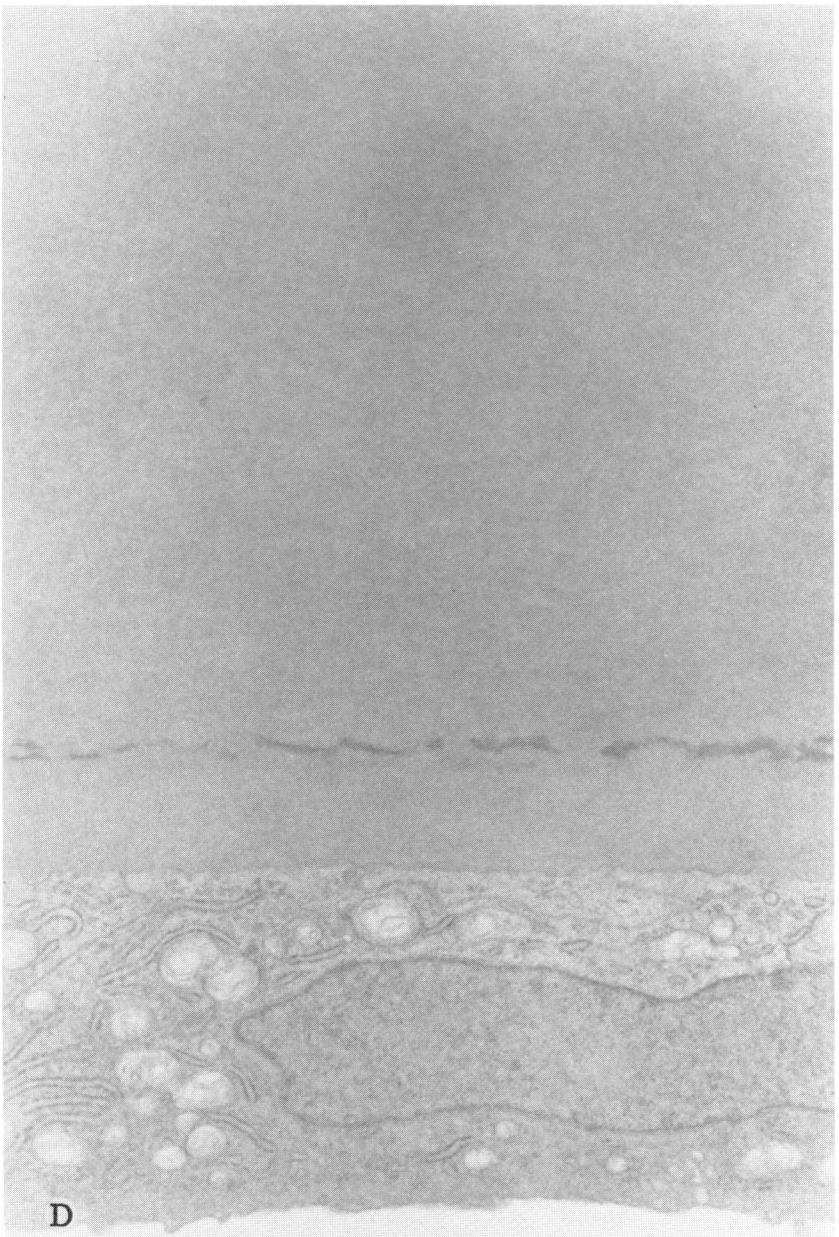
D

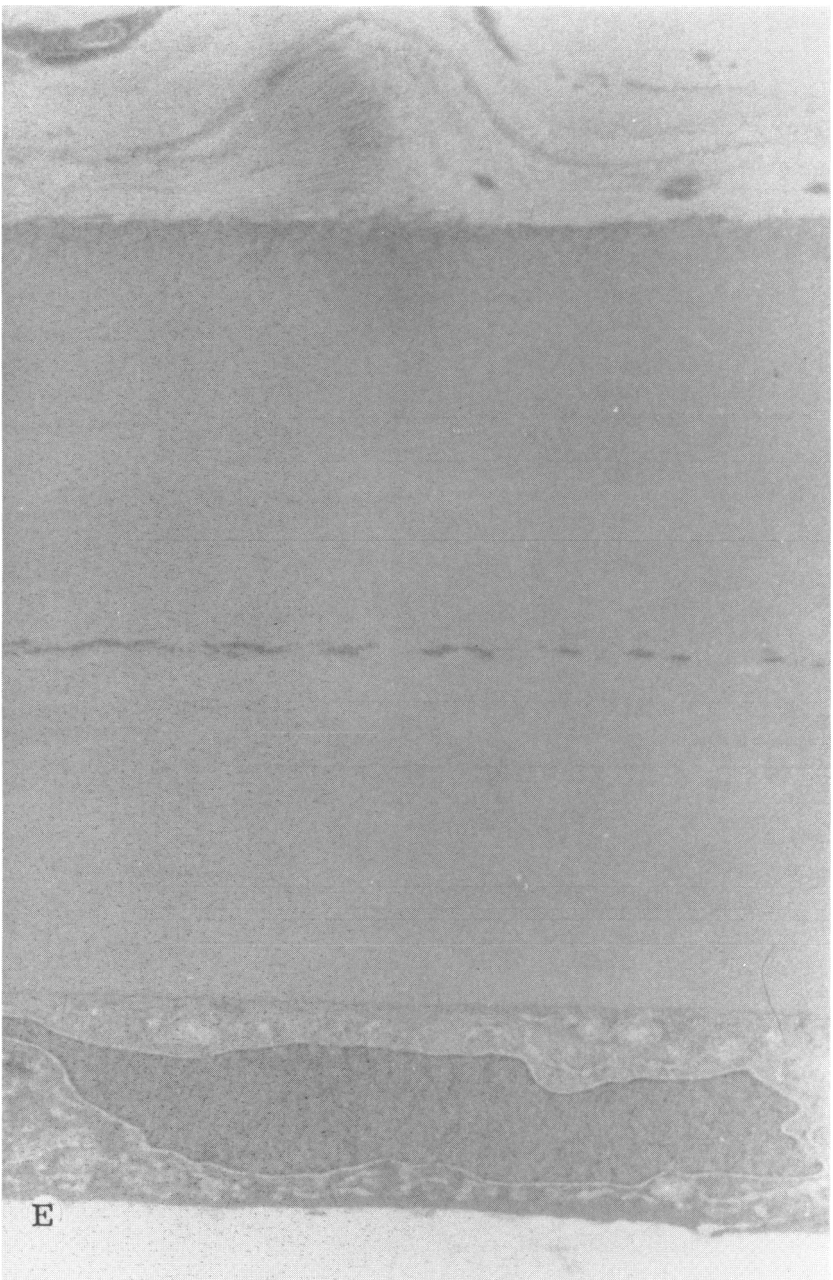
E

membrane only beneath the 7.5 mm diameter area of surface ablation. At the edge of this zone, the material became more spotty. One was present outside the area of ablation. Histochemical attempts to identify the nature of the material in Descemet's membrane were unrevealing. Thin sections stained with Mallory's alcian blue and periodic acid-Schiff (PAS) showed no specific reaction.

Examination at 1 and 21 days of the control corneas that had an epithelial scrape injury or a superficial manual keratectomy showed slight changes in endothelial cells: enlargement of the intercellular spaces, increased visibility of endoplasmic reticulum, and the appearance of a granular material both at the basal side of endothelial cells and in the intercellular spaces. At 21 days the granular material was seen only in the intercellular spaces; it had not migrated anteriorly in Descemet's membrane.

Interpretation of Findings

The rabbit experiments we report here document three major findings: (1) epithelial healing and adhesion over the ablated surface occur without difficulty; (2) subepithelial scarring occurs in some eyes but not others treated in the same manner; and (3) there is mild remote injury to deep stromal keratocytes and the endothelium.

In areas of anterior stromal irregularity (especially near the center of the cornea where the ablation was the least uniform), the basal cells filled in the small surface irregularities. However, because the surface was generally smooth with a gradual transition between the ablated and unablated zones, there were no gross irregularities or concave surfaces to be filled in by hyperplastic epithelium.

All corneas showed a reaction to the insult, both the epithelial scraping and excimer laser ablation. In the corneas that remained clear, the response was mild and consisted of a subepithelial acellular zone that gradually became repopulated by activated fibrocytes without the production of detectable extracellular matrix. However, when the response was more vigorous, a layer of subepithelial scar tissue did result.

An unexpected finding in this series of experiments were ultrastructural changes in the posterior keratocytes, endothelium, and Descemet's membrane. The fact that material appears in Descemet's membrane within a few hours of the insult suggests that it is a material discarded directly from the plasma membrane or cytoplasm of the endothelial cell, rather than a newly synthesized material. This might be dubbed "endothelial sweat." The fact that it is seen after both chemical[91] and laser insult suggests that this is a nonspecific response of the rabbit corneal endothelium.

The mechanism by which far ultraviolet radiation on the surface of the cornea transiently damages the endothelium with resultant extrusion of material into Descemet's membrane is unclear. However, the demonstration by Zabel and colleagues[92] of 100 atmospheres of pressure produced from the acoustic or shock waves creates an attractive hypothesis: that this pressure wave damages the endothelium. Another possible cause is fluorescent radiation from the anterior stroma that may be absorbed by or toxic to the endothelium. A third speculative possibility is that the ablation process at the surface produces free radicals or other toxic tissue products that may pass through the cornea and damage the endothelium (JM Parel, personal communication, May 1988).

Why the material migrates forward through Descemet's membrane is also unknown. Aqueous humor normally leaks between the corneal endothelial cells and passes along the gradient from the anterior chamber across Descemet's membrane and the stroma to the epithelium. Presumedly this constant flow of aqueous humor might carry the amorphous material with it gradually across Descemet's membrane. It is unlikely Descemet's membrane turns over fast enough to replace itself at the rate of approximately 1 μm per month.

Fortunately, these posterior corneal changes seem minimal, transitory, and without permanent result. The keratocytes showing no proclivity to secrete new extracellular matrix and return to a normal appearance by 100 days. The endothelial cells showed minimal transitory changes, with the production of a small amount of amorphous material into Descemet's membrane.

LASER MYOPIC KERATOMILEUSIS IN RHESUS MONKEY EYES

We utilized the translating slit delivery system (described above) to perform laser myopic keratomileusis in 15 rhesus monkeys. At the time of this writing, this primate research is still underway, allowing a report of the clinical findings through 9 months follow-up and of the histopathological, ultrastructural, and immunohistochemical findings in eyes with subepithelial opacification through approximately 3 months follow-up.[93] Table VII summarizes the clinical course.

Methods

A Lambda Physik EMG 103 ArF (193 nm) excimer laser was used, with the cavity configured as a stable resonator and the mirrors carefully aligned using a helium-neon laser. The translating slit delivery system described in detail previously was attached to the laser, and the conical suction ring coupling device (described above) was attached to the end of

TABLE VII: CLINICAL RESULTS OF ArF EXCIMER LASER MYOPIC KERATOMILEUSIS IN RHESUS MONKEYS

MONKEY NO.	DATE OF SURGERY	EYE AND MYOPIC CORRECTION PROGRAMMED (D)	EYES REOPERATED	DATE OF SACRIFICE	LENGTH OF FOLLOW-UP	DENSITY OF CORNEAL OPACITY AT SACRIFICE (0-3+)*
N694	4-5-88	OD −2		6-14-88	2.5 mo	OD 1.5
		OS −8				OS 1.4
RUY	4-6-88	OD −2		6-14-88	2.5 mo	OD 1.5
		OS −4				OS 1.5
966T	4-5-88	OD −2	OD 6-15-88	Alive		OD (2.0)
		OS −4	OS 6-15-88			OS (2.0)
N707	4-6-88	OD −8	OD 6-21-88	9-20-88	5.5 mo	OD 2.0
		OS −2	OS 6-21-88			OS 2.0
RQR	4-6-88	OD −2	OD 6-21-88	1-3-89	9 mo	OD 1.5
		OS −4				OS 1.0
563D	4-7-88	OD −2		7-6-88	3 mo	OD 0.0
		OS −4				OS 0.0
N735	4-7-88	OD −8		9-20-88	5.5 mo	OD 2.0
		OS −2				OS 1.5
N766	4-7-88	OD −4		Alive		OD (1.0)
		OS −8				OS (1.5)
634 D	4-11-88	OD −8	OD 6-21-88	1-3-89	9 mo	OD 0.5
		OS −4				OS 0.5
RRV	4-11-88	OD −4		Alive		OD (0.0)
		OS −8				OS (0.0)
641T	4-6-88	OD −4		Alive		OD (1.5)
		OS −2				OS (1.5)
RTA1	4-11-88	OD −8		Alive		OD (1.5)
		OS −4				OS (1.5)
531D	6-1-88	OD −8		1-13-89	7 mo	OD (0.5)
		OS −8				OS (0.0)
MC161	7-12-88	OD −4		7-19-88	1 wk	OD 0.0
		OS −4				OS 1.5
OBE	7-12-88	OD −8		7-12-88	Acute	OD N/A
		OS −8				OS N/A

*(0 = none, 1+ = mild, 2+ = moderate, 3+ = severe).
( ) indicates score on most recent examination.

the delivery system and secured to the conjunctival limbus with a mechanical vacuum pump. The pulse energy at the exit from the laser was 160 mJ. The radiant exposure at the surface of the cornea was 250 mJ/cm^2. A repetition rate of 5 Hz was used. A specified slit mask for myopic ablation was inserted into the delivery system and its number programmed into the computer. The optical zone ablated was 4 mm in diameter. Based on calibration studies with rhesus monkey eyes, an ablation rate of 0.5 μm per pulse was assumed. The IBM computer that controlled the delivery system was programmed to correct 2 D, 4 D, or 8 D of myopia. The computer algorithms then selected the maximum amount of overlap of the multiple slit images on the cornea (maximum of 98%), and the number of passes made across the ablated zone (4). The time needed for an ablation ranged from 1 to 3 minutes.

Thirty eyes of 15 adult rhesus monkeys were used. The animals were sedated by an intramuscular injection of ketamine and then anesthetized with an intravenous ketamine injection, the doses determined by the veterinarian in charge of the animals. Topical 0.5% proparacaine was instilled with the eyelid held open by a wire speculum and the corneal epithelium was removed by scraping with a scalpel blade over approximately an 8 mm diameter central zone. The ablation of each eye carried out in succession, followed by the instillation of gentamicin drops.

Clinical examinations were carried out by two observers on each occasion, each observer independently grading the clarity of the cornea using a Nikon slit-lamp microscope on the following scale: 0 = clear (no difference between ablated and unablated areas); 1+ = mild haze (did not obscure iris detail, not apparent on immediate examination); 2+ = moderate haze (apparent on immediate examination, slightly obscured iris detail); 3+ = marked (obscured iris detail).

Animals were euthanized with an intravenous overdose of phenobarbital according to the time schedule in Table VII. The corneoscleral shell was removed immediately, and each cornea was divided into three pieces with a razor blade, one piece being processed for light microscopy and another for electron microscopy as detailed previously. The third place was immediately frozen in liquid nitrogen for immunohistochemistry. The corneas re-epithelialized in 3 to 7 days. None exhibited a persistent epithelial defect or clinically apparent keratitis or microbial infection. There were no observed occurrences of epithelial breakdown or erosion once the epithelium healed.

Clinical Findings

Table VII summarizes the clinical findings in terms of the clarity of the cornea.

Corneas were epithelialized by 7 days. During the first 2 weeks, 63% of the corneas were clear. By 6 weeks, subepithelial scarring was apparent in 93% of the eyes (Fig 38). Some progressive clearing occurred over 6 months and two corneas cleared up completely. In general, the degree of opacity was worse in the shallower ablations. The opacity was located just beneath the epithelium, had a generally spotty-reticular appearance with feathered edges, and was usually fairly uniform, but varied in its diameter.

Histopathologic and Ultrastructural Observations

To date, we have examined selected corneas up to 2 to 3 months after surgery, concentrating on those with a subepithelial opacity.

Light Microscopy: The ablated surface was quite smooth, and as the epithelium healed, it exhibited a phase of hyperplasia with a thickness of 8 to 14 cells at 1 to 2 weeks, before returning to the normal thickness of

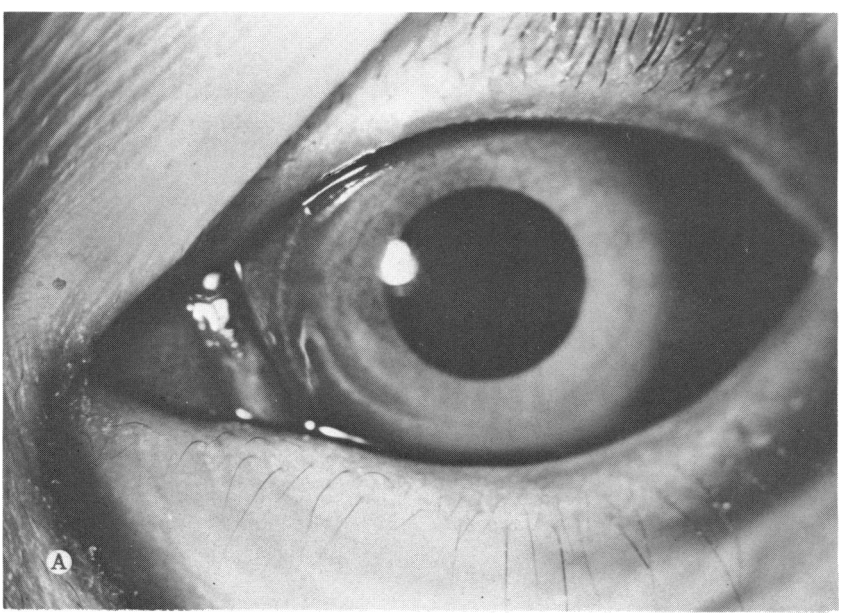

FIGURE 38

Clinical appearance of selected rhesus monkey corneas after excimer laser myopic keratomileusis. A: At 2 weeks, the cornea was completely clear. B: At approximately 3 months, the cornea showed a mild opacity just beneath the corneal light reflection. C: At approximately 3 months after ablation, the cornea showed a moderate opacity that covered approximately two-thirds of the pupil. D: At approximately 3 months after surgery after ablation, the cornea showed a marked opacity with a reticular appearance.

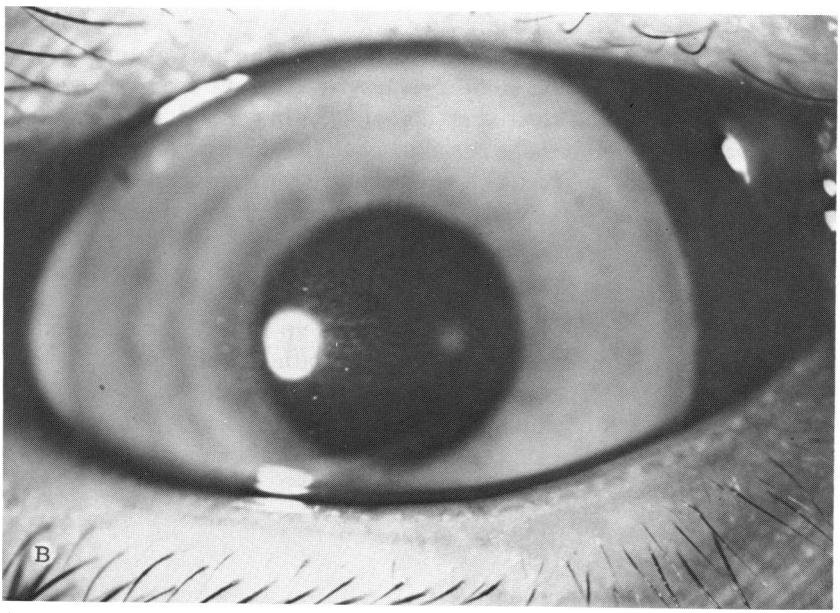
B

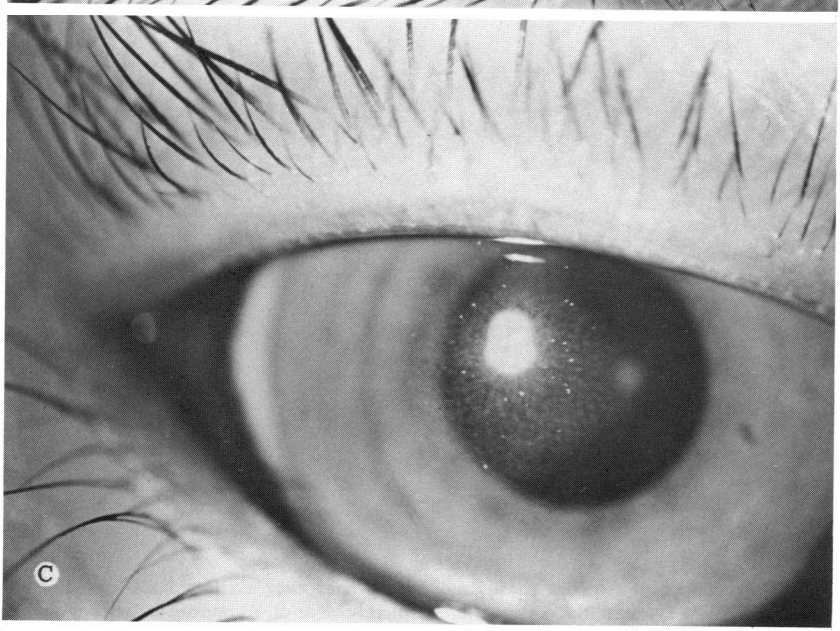
C

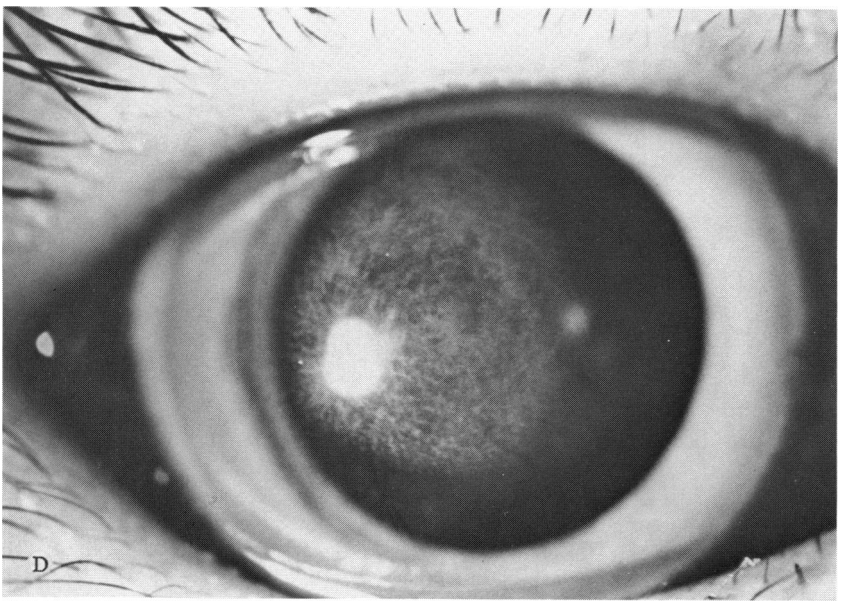

approximately 5 cells. However, abnormalities persisted in the epithelium up to 3 months, including vacuolization between the epithelium and the underlying ablated stroma, the presence of numerous dark cells, and some epithelial hyperplasia within the area of ablation (Fig 39).

The subepithelial stroma at 7 days showed decreased keratocytes, followed by a wave of fibroblasts occupying a thickness of 30 to 40 μ. The number of fibroblasts was large, but they generally remained oriented in a lamellar fashion and did not ball up into focal masses. Newly secreted collagenous tissue and extracellular matrix were apparent in the subepithelial zone (Fig 39B).

FIGURE 39

Light microscopy of excimer laser myopic keratomileusis in the rhesus monkey. A: At 7 days, the healed epithelium was hyperplastic, being approximately ten layers thick and consisting of cells with recognizable polarity. Vacuolated zone was present between the epithelium and the underlying stroma, which was hypocellular to a depth of approximately 40 μ (hematoxylin-PAS, ×200). B: At 2 months, the epithelium showed a generally smooth surface and a thickness of approximately five cells, although some zones of hyperplasia (right side of figure) were apparent. Numerous dark basal cells were present, interspersed with lighter basal cells. The vacuolated zone between the epithelium and stroma persisted. The underlying stroma was densely populated with active fibroblasts. Some newly secreted extracellular matrix was present in a generally lamellar array (hematoxylin-PAS, ×200).

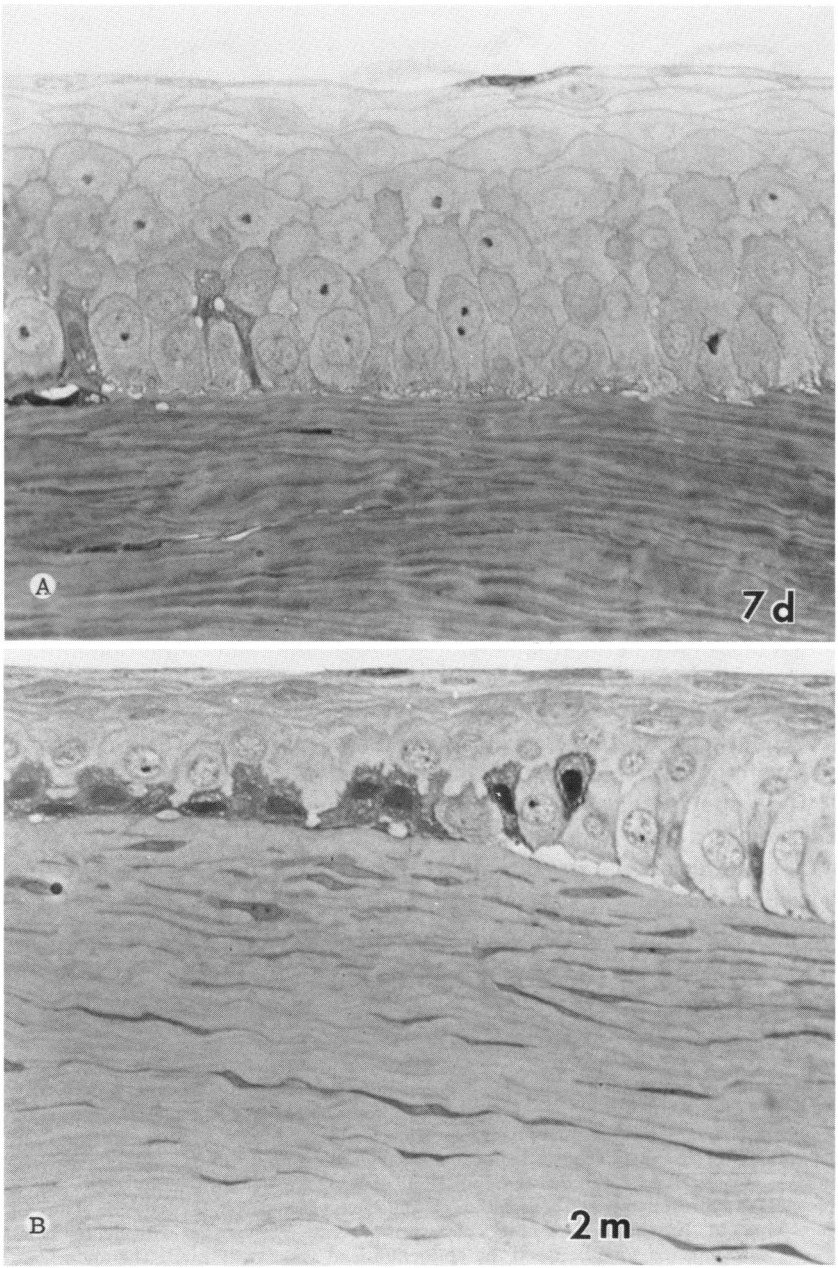
A
7 d
B
2 m

Transmission Electron Microscopy: By 2 to 3 months (Fig 40), the basal epithelial cells had secreted a basement membrane complete with hemidesmosomes and apparent anchoring fibrils. Numerous active fibroblasts were present in the subepithelial zone, exhibiting figures of dilated rough endoplasmic reticulum and Golgi apparatus. The extracellular matrix was generally lamellar in configuration, but not well organized, in contrast to the discrete lamellar organization in the middle and posterior cornea. No changes were seen in the posterior keratocytes, the endothelium, or Descemet's membrane.

Immunohistochemistry: We present here only preliminary results of ongoing immunohistochemical studies. A detailed report of the methods and results will be prepared separately.

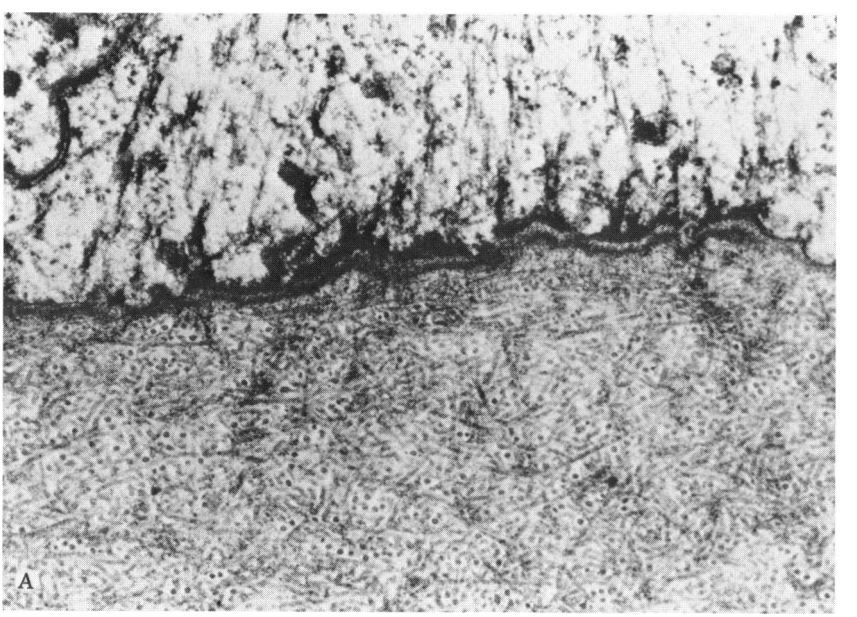

FIGURE 40

Ultrastructure of anterior rhesus monkey corneas 2 to 3 months after excimer laser keratomileusis. A: Unablated zone demonstrates hemidesmosomes, epithelial basement membrane, and underlying Bowman's layer (×20,000). B: Ablated zone demonstrates focal hemidesmosome formation with only spotty secretion of epithelial basement membrane. Bowman's layer is absent. The underlying collagenous stroma has a generally lamellar configuration (×20,000). C: Subepithelial zone is populated by numerous active fibroblasts showing some vacuolization. The extracellular matrix is poorly organized (×20,000). D: Fibroblasts in the anterior stroma show multiple figures of dilated endoplasmic reticulum in the cytoplasm (×20,000). (Courtesy KD Hanna, MD and Y Pouliquen, MD)

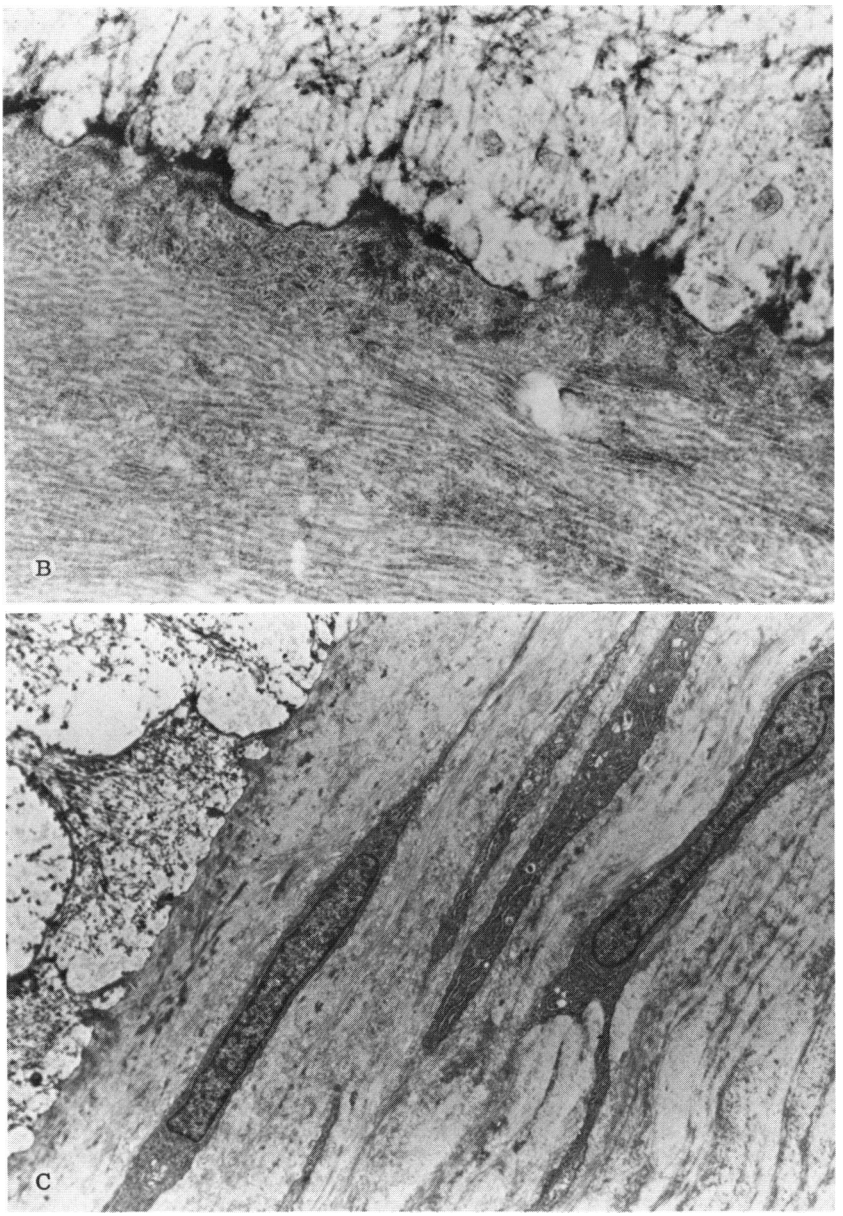
B
C

Fibronectin was present in large amounts in the subepithelial stroma in the first few weeks after ablation and gradually returned to baseline levels by approximately 3 months (Fig 41). Type VII collagen appeared by 2 to 3 weeks in the immediate subepithelial zone and persisted up to 3 months (Fig 42). Type III collagen appeared in the subepithelial anterior stroma at 3 weeks and increased greatly by 3 months (Fig 43).

OBSERVATIONS ON RESULTS OF EXCIMER LASER KERATOMILEUSIS IN THE MONKEY

Although this series of experiments is not yet complete, we can draw some preliminary conclusions from the data presented: (1) epithelial healing occurs uncomplicated in this monkey model, (2) subepithelial opacification is the rule using this laser and delivery system, although some corneas can remain clear. There is no direct correlation between the depth of cornea and the degree of subepithelial opacification. (3) The subepithelial opacities consist of fibroblasts laying down new extracellular matrix that contain some Type III "fetal" collagen and Type VII "an-

FIGURE 41

Immunohistochemical staining for fibronectin after excimer laser keratomileusis in the rhesus monkey. E indicates epithelium. A: Three weeks after ablation, the subepithelial anterior stroma is replete with fibronectin. B: By 12 weeks after ablation, much of the fibronectin has disappeared, leaving only baseline background staining.

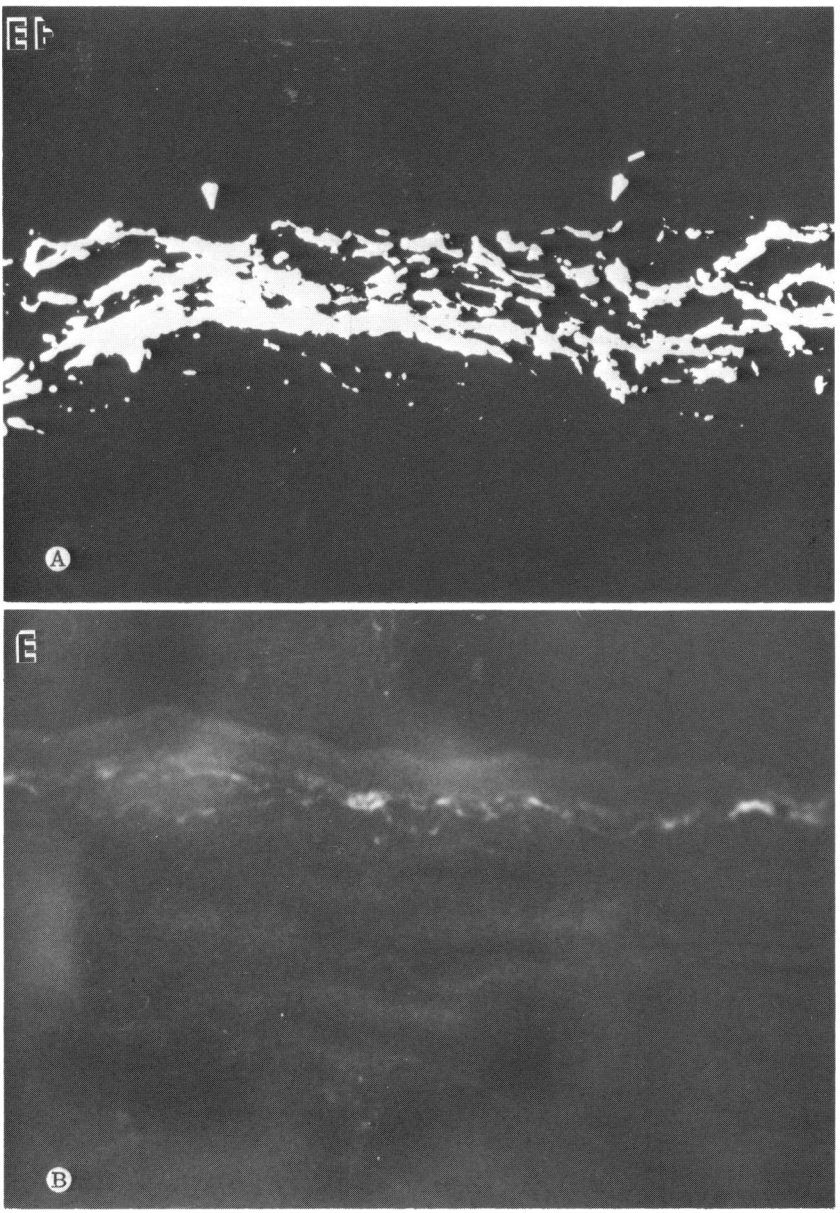
A
B

choring" fibril collagen. (4) Although mild epithelial hyperplasia may persist, the epithelium does not fill in the ablated area and neutralize the refractive effect. (5) Refinements of the laser and delivery system must be made if direct laser keratomileusis is to be successful.

CONCLUSIONS

Attempts over the last 5 years to harness the ArF excimer laser for refractive corneal surgery have progressed from fledgling experiments with crude delivery systems on eye bank eyes to sophisticated protocols using computer-controlled systems on partially sighted human eyes. In spite of this progress, many problems remain to be overcome before excimer laser linear keratectomy or excimer laser keratomileusis can become routinely performed surgery for the correction of refractive errors. The cumulative published and presented experience from other investigators as well as the work from our laboratory presented herein lead to a number of conclusions.

The ArF excimer laser and its delivery systems are expensive, complex, and difficult to harness and maintain for keratomileusis, because of the technical requirements to control the toxic fluorine gas, to create a homogenous beam, to configure the beam in an effective configuration, to measure the beam, and to deliver the beam to the cornea with computer-assisted control.

Deep linear corneal excisions, whether radial for the correction of myopia or transverse for the correction of astigmatism, must be 100 to 150 μ wide and fill an epithelial plug that lasts for months to years. Whether linear laser keratectomy has a different effect on the radius of curvature of the cornea than a diamond knife keratotomy requires further study.

Deep linear corneal excisions, whether radial for the correction of myopia or transverse for the correction of astigmatism, must be 100 to 150 μ wide and fill an epithelial plug that lasts for months to years. Whether linear laser keratectomy has s different effect on the radius of curvature of the cornea than a diamond knife keratotomy requires further study.

Excimer laser keratomileusis is based on the premise that an ArF (193 nm) excimer laser can remove tissue from the central cornea with sub-

FIGURE 42

Immunohistochemical staining for Type VII collagen after excimer laser myopic keratomileusis in the rhesus monkey. E indicates epithelium. A: Type VII collagen appeared in relatively large amounts in the ablated bed on the left side of the figure. *Small arrowhead* indicates the junction between the ablated and unablated cornea. Not enough Type VII collagen is present in the unablated zone to show up with this technique. B: By 3 months after ablation, a dense layer of Type VII collagen is present beneath the epithelium.

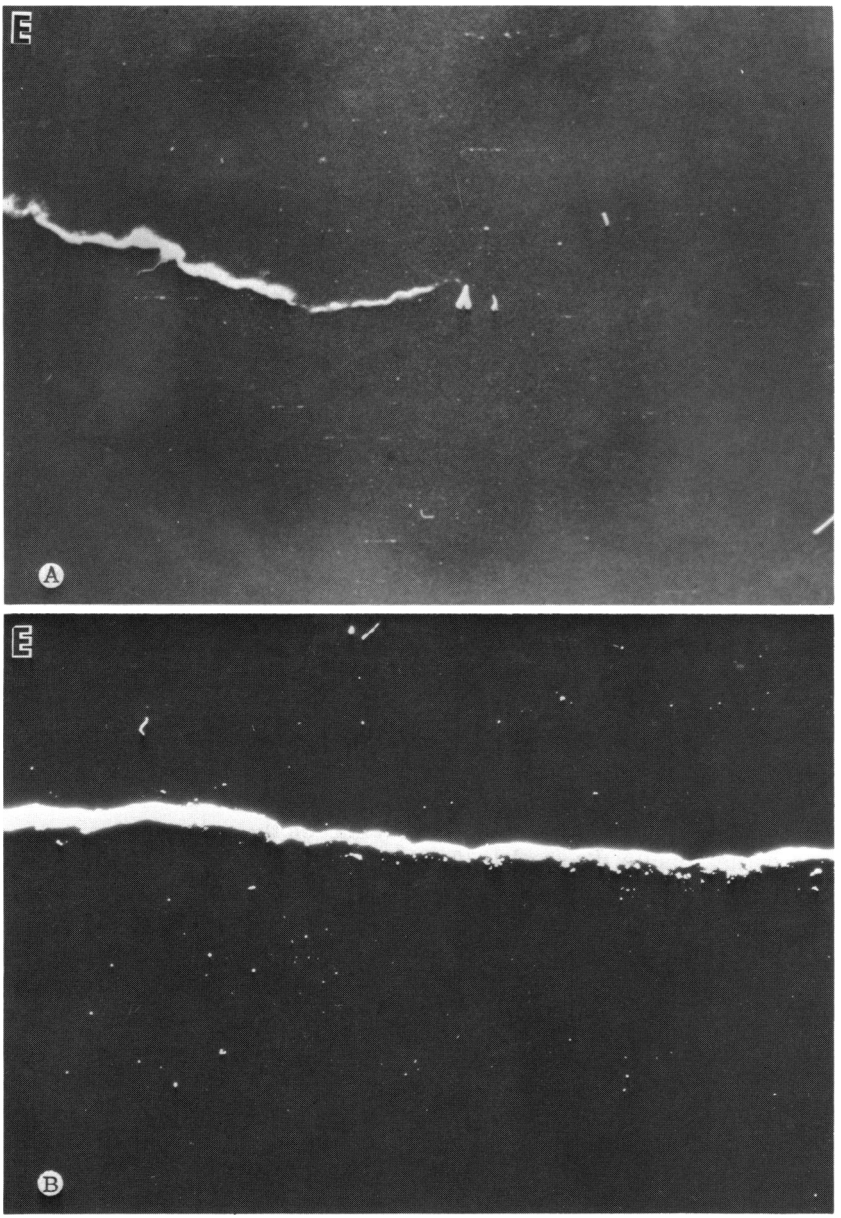
E
A
E
B

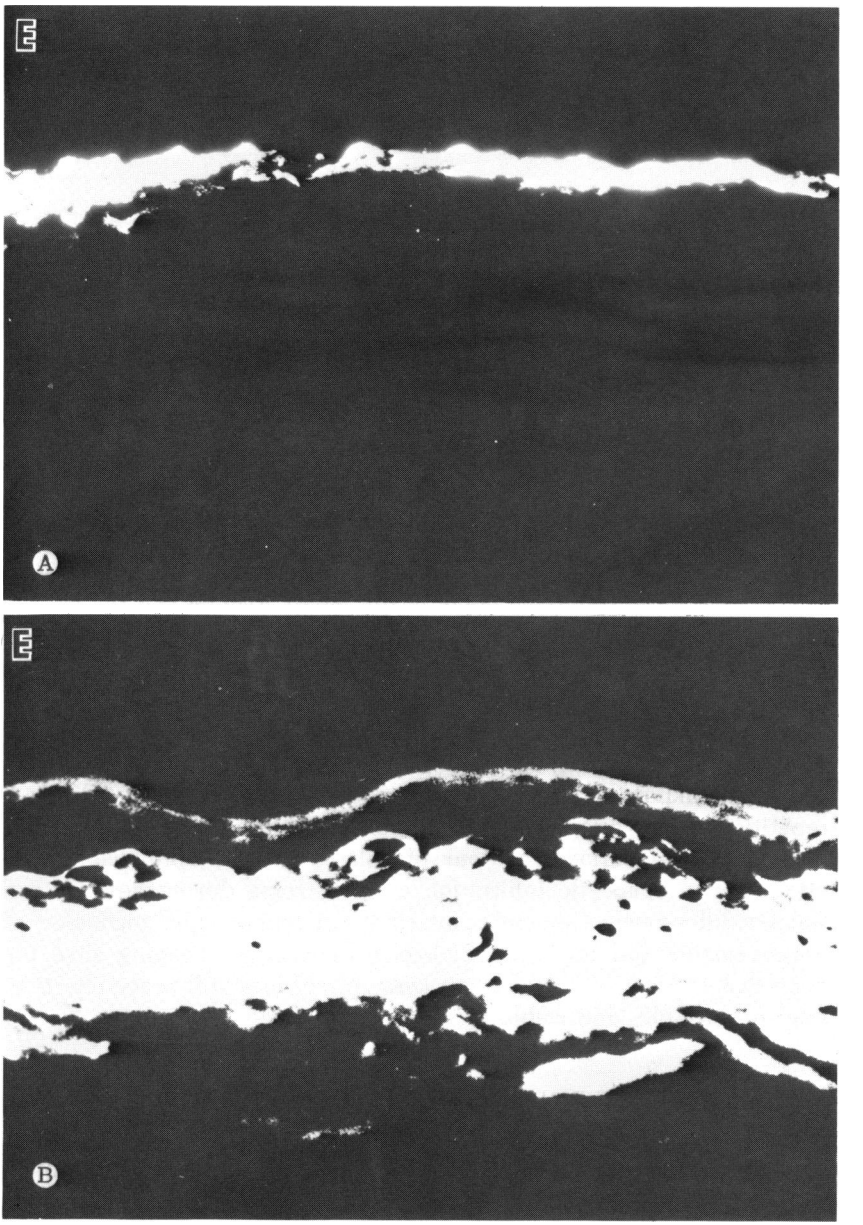
E
A
E
B

FIGURE 43
Immunohistochemical staining for Type III collagen after excimer laser myopic keratomileusis in the rhesus monkey. E indicates epithelium. A: Three weeks after ablation, a moderate amount of Type III collagen is present beneath the epithelium. B: By 6 weeks after ablation, a band of Type III collagen approximately 15 μ thick was present.

micron accuracy in a manner gentle enough that the corneal epithelium and stroma will heal without hyperplasia and the stroma without filling in or scarring; the epithelium is expected to simply resurface the defect over the ablation, leaving the cornea with a new anterior radius of curvature. Published reports and our laboratory results demonstrate that this can occur if the changes in corneal curvature are gradual over the surface. All reported animal and human eyes have demonstrated some subepithelial scarring by slit-lamp microscopy and some regression of the corneal flattening during the postoperative course. However, these events may clear and stabilize at a clinically acceptable level. Histology and ultrastructure have shown both proliferation of fibroblasts in the ablated zone with secretion of new extracellular matrix. This wound healing process may decrease the refractive effect of the initial ablation and the stromal scarring may produce light scattering and image degradation. There is great variability in response from one cornea to another, despite reasonably uniform conditions of ablation; some corneas remain clear.

The factors that affect corneal wound healing after excimer laser ablation are gradually being defined, but the relative role of these factors is presently unknown: radiant exposure, total amount of energy delivered, repetition rate, overlap of successive pulses, beam homogeneity, smoothness of ablated surface, contour of ablated profile, epithelial-stromal interactions, leukocytic infiltration of the stroma during healing, and species differences. Current research is producing rapid technological improvements and increased biological knowledge, keeping alive the hope that excimer laser refractive keratoplasty may still prove effective, safe, predictable, and stable (Fig 44).

EPILOGUE: ADJUSTABILITY IN REFRACTIVE SURGERY

I commenced this thesis by observing that refractive corneal surgery currently has two major weaknesses: lack of accurate and precise predictability and lack of adjustability. Although excimer laser keratomileusis holds forth promise, we have seen that corneal wound healing can certainly undermine the predictability of the surgery at its present level of development. Furthermore, it is likely that repeated ablations of the

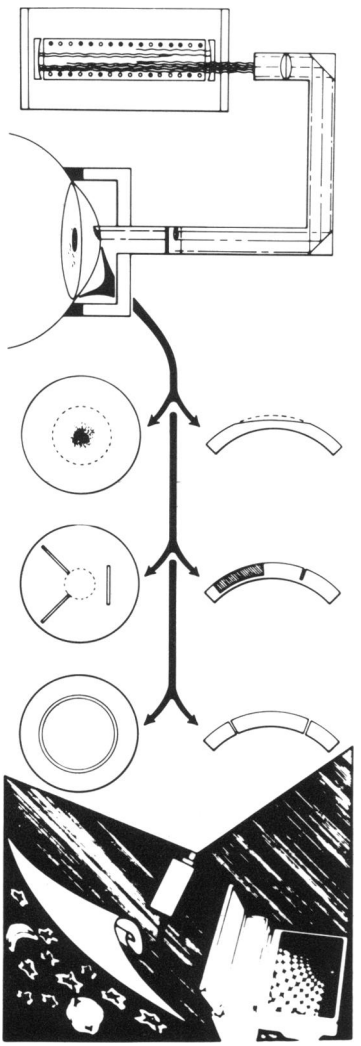

FIGURE 44

The scope of laser corneal surgery is illustrated in a composite montage, read from left to right. An appropriate laser passes through an effective delivery system that is coupled to the eye. Interaction of the laser with the corneal tissue sets the stage for wound healing. Patterns of PRK include laser keratomileusis (surface area ablation) for all ametropias, transverse linear keratectomy for astigmatism, radial keratectomy for myopia, and circular trephination for corneal transplantation. Measurement of the topography and thickness of the cornea allows computation of the effect of refractive surgery, and in conjunction with biomechanical data, computer simulation of surgery. The future is bright, but like the exploration of space, fraught with technical challenges and the unknown.

cornea would be accompanied by increased numbers of complications and possibly by poorer predictability of the outcome. These problems have led us to propose a new approach to refractive surgery: laser adjustable synthetic epikeratoplasty (LASE) (Fig 45).[94]

The attachment of a synthetic epikeratoplasty lenticule to the surface of the cornea would provide an acellular substrate that could be modified repeatedly to change the cornea's refractive power, without disrupting the central structure of the cornea at all. The initial lenticule would be designed to achieve a desired correction, as is currently done with human epikeratoplasty lenticules, but with the advantage that subsequent laser keratomileusis could adjust for inaccuracies in the initial calculation, changes in the configuration of the lenticule with time, changes in the refractive state of the eyes, and the emergence of presbyopia. Should problems arise with the lenticule or should it become too thin, the surgeon could remove or replace it, making LASE a reversible as well as adjustable procedure.

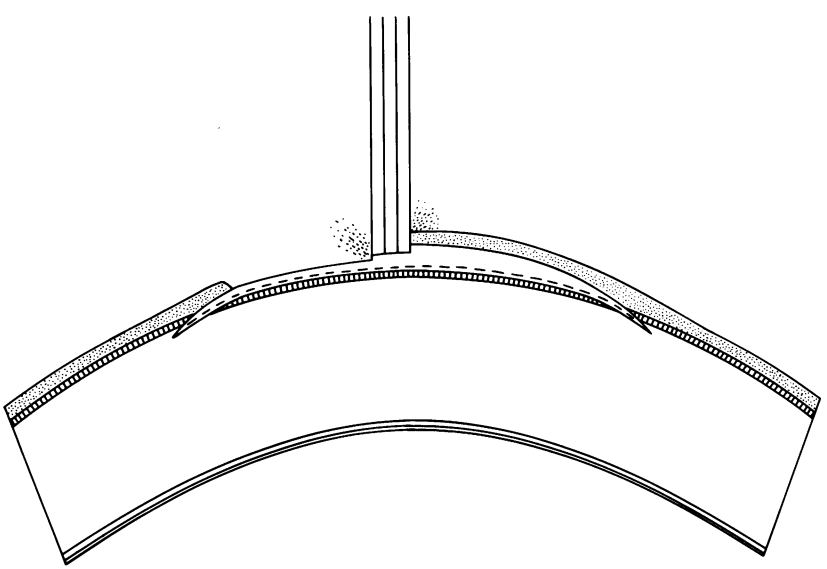

FIGURE 45
Laser adjustable synthetic epikeratoplasty (LASE) consists of the placement of a synthetic epikeratoplasty lenticule with appropriate corrective power on the cornea. If adjustment of the refractive power is necessary, an excimer laser keratomileusis can be performed, repeatedly if necessary, without damaging the patient's central cornea and without concerns about stromal wound healing. There is, however, the challenge of achieving successful epithelial wound healing over a synthetic surface.

The current types of materials under evaluation are cross-linked collagen polymers such as Type IV collagen, coated hydrogels and synthetic co-polymers. We have used Type IV collagen lenticules for epikeratoplasty in rhesus monkeys, securing them in a circular keratotomy wound. We have used an ArF excimer laser to ablate the surface of these lenticules. This research program is in its very early stages.

There are many unsolved problems with this experimental approach, including identification of a suitable biopolymer, stable attachment of the synthetic lenticule to the corneal surface without modifying the underlying shape of the cornea, achievement of rapid and stable epithelialization over a synthetic surface, and maintenance of long-term stability of the material with resistance to enzymatic degradation. The LASE concept is indicative of the resourcefulness of ophthalmic surgeons who seek to develop acceptable techniques to replace glasses and contact lenses as the preferred method of correcting ametropias.

ACKNOWLEDGMENTS

The work reported in this thesis results from the collaborative efforts of numerous individuals. Francisco Fantes, MD, a corneal fellow at the Emory Eye Center from 1987-1989 played a major role in establishing the laser corneal research laboratory and in generating much of the initial data reported herein. Khalil Hanna, MD, Director of Refractive Surgery at Hotel-Dieu Hospital in Paris, France, and Associate Professor of Ophthalmology, part-time, at Emory University in Atlanta, designed the moving slit delivery system used in these experiments, in conjunction with the IBM Scientific Center in Paris, France. The delivery system is on loan to Emory University. Yves Pouliquen, MD, Director of the Ophthalmology Department at Hotel-Dieu Hospital, Paris, established the collaborative research program with Emory, and Ms Michelle Savoldelli did the histologic and electron microscopic studies. Theo Seiler, MD, Professor of Ophthalmology at the Freie Universitat in Berlin has done much of the initial work in laser corneal surgery and provided much of the technical background on which this thesis is based. Keith Thompson, MD, a National Eye Institute Training grant recipient, at Emory University has contributed substantively to the furtherance of this project. Steve Trokel, MD, Clinical Professor of Ophthalmology at Columbia University, New York, provided direction and counsel during the formative stage of this program. Mr Dale Reddick, a Research Associate at the Yerkes Primate Center, has provided valuable technical assistance. The Refractive Corneal Research Laboratory at the Yerkes Primate Center receives constant

support and help from the center staff, whose expertise in caring for the monkeys (and the researchers) is without parallel. Coherent Radiation Corporation provided the laser through its subsidiary, Lambda Physik, along with expert assistance from Jean Phillippe Gay, Theodore Boutacoff, and Ronald Alves, PhD. It is completely appropriate to acknowledge the enormous effort put forth by my staff in completing this thesis. Ms Katherine Lindstrom provided expert editorial support. Ms Brenda Summer, Ms Darla Loga, and Ms Phyllis Lee slogged away with indefatigable secretarial support. Ms Nancy Hayes, Ms Rochelle Kraehe, Dr Ceretha Cartwright, and Ms Edith Barron provided administrative support.

REFERENCES

1. Waring GO: Making sense of keratospeak: A classification of refractive corneal surgery. *Arch Ophthalmol* 1985; 103:1472-1477.
2. ———: Development and evaluation of refractive surgical procedures. I: Five stages in the continuum of development. *J Refract Surg* 1987; 3:142-157.
3. Absten GT, Joffe SN: *Lasers in Medicine*. New York, Chapman Co, 1985.
4. Macruz R, Ribeiro M, Mauro J, et al: Laser surgery in enclosed spaces. *Lasers Surg Med* 1985; 5:199-218.
5. Mainster MA: Ophthalmic applications of infrared laser-thermal considerations. *Invest Ophthalmol Vis Sci* 1979; 18:414-420.
6. O'Shea DC, Callen WR, Rhodes WT: *Introduction to Lasers and their Applications*. Reading, Addison-Wesley Publishing Co, 1977.
7. Mainster MA: Finding your way in the photo forest: Laser effects for clinicians. *Ophthalmology* 1984; 91:886-888.
8. Marshall J, Trokel S, Rothery S, et al: Photoablative reprofiling of the cornea using an excimer laser: Photorefractive keratotomy. *Lasers Ophthalmol* 1986; 1:21-48.
9. Scientific American Readings: *Lasers and Light*. San Francisco, WH Freeman, 1969.
10. Hecht J: Excimer laser update. *Lasers Applic* 1983; 12:43-48.
11. March WF: *Ophthalmic Lasers*. Thorofare, Slack Inc, 1984.
12. Krauss JM, Puliafito CA, Steinert R: Laser interactions with the cornea. *Surv Ophthalmol* 1986; 31:37-53.
13. Beaven GH, Holiday ER: Ultraviolet absorption spectrum of protein and aminoacids. *Adv Protein Chem* 1952; 7:319-386.
14. Tapazto I, Vass Z: Alteration in muchopolysacchalios compounds of team and that of corneal epithelium caused by ultraviolet radiation. *Ophthalmologica* (Suppl) 1969; 5B:343-347.
15. Lee I, Bourow JR, Gould BS, et al: Studies on the ultraviolet absorption spectra of collagen. *Arch Biochem* 1949; 22:406-411.
16. O'Brien WJ: Measurement of DNA content. *Invest Ophthalmol Vis Sci* 1979; 18:518-543.
17. Pirie A: Ascorbic acid content of cornea. *Biochem J* 1946; 40:96-100.
18. Loertscher H, Mandelbaum S, Parrish RK, et al: Preliminary report on corneal incisions created by a hydrogen fluoride laser. *Am J Ophthalmol* 1986; 102-217-221.
19. Dyer PE, Srinivasan R: Nanosecond photoacoustic studies on ultraviolet laser ablation of organic polymers. *Appl Phys Lett* 1986; 48:445-447.
20. Keyes T, Clarke RH: Theory of photoablation and its implication for laser phototherapy. *J Chem Phys* 1985; 89:4194-4196.
21. Lazare S, Srinivasan R: Surface properties of polyethylene terephthalate films modified by far-ultraviolet radiation at 193 nm (laser) and 185 nm (low intensity). *J Phys Chem* 1986; 90:2124-2132.

22. Marshall J, Trokel S, Rothery S, et al: An ultrastructural study of corneal incisions induced by an excimer laser at 193 nm. *Ophthalmology* 1985; 92:749-758.
23. ———: A comparative study of corneal incisions induced by diamond and steel knives and two ultraviolet radiations from an excimer laser. *Br J Ophthalmol* 1986; 70:482-501.
24. Puliafito CA, Steiner RF, Deutsch TF, et al: Excimer laser ablation of the cornea and lens. *Ophthalmology* 1985; 92:741-748.
25. Sutcliffe E, Srinivasan R: Dynamics of the ultraviolet laser ablation of corneal tissue. *Am J Ophthalmol* 1987; 103:470-471.
26. ———: Dynamics of UV laser ablation of organic polymer surfaces. *J Appl Phys* 1986; 60:3315-3322.
27. ———: Time dependent analysis of the UV laser ablation of corneal tissue. *Lasers Ophthalmol* 1987; 2:1201-1208.
28. Srinivasan R, Dyer PE, Braren B: Far-ultraviolet laser ablation of the cornea: Photoacoustic studies. *Lasers Surg Med* 1987; 6:514-519.
29. Srinivasan R: Ablation of polymers and biological tissue by ultraviolet lasers. *Science* 1986; 234:559-565.
30. Srinivasan R, Braren B, Seeger DE, et al: Photochemical cleavage of a polymeric solid: Details of the ultraviolet laser ablation of pol (methymethacrylate) at 193 nm and 248 nm. *Macromolecules* 1986; 19:916-920.
31. Srinivasan R, Braren B, Dreyfus RW, et al: Mechanism of ultraviolet laser ablation of polymethylmethacrylate at 193 and 248 nm: Laser-induced fluorescence analysis, chemical analysis, and doping studies. *J Opt Soc Am* 1986; 3:785-791.
32. Trokel SL, Srinivasan R, Braren BA: Excimer laser surgery of the cornea. *Am J Ophthalmol* 1983; 96:710-715.
33. Searles SK, Hart GA: Stimulated emission at 281 nm XC. *Br Appl Phys Lett* 1975; 27:243-245.
34. Reed RD, Taboada J, Midsell JW: Response of the corneal epithelium to krypton fluoride excimer laser. *Health Phys* 1981; 40:677-683.
35. McDonald M: The future of R and D jeopardized. *J Refract Surg* 1987; 3:207.
36. News Commentary: Patent fight erupts over excimer laser corneal surgery. *Refract Corneal Surg* 1989; 5:3
37. Fine S, Feigen L, McKeen D: Corneal injury threshold to carbon dioxide laser radiation. *Am J Ophthalmol* 1986; 1:1-15.
38. Fine BS, Fine S, Peacock GR, et al: Preliminary observations on ocular effects of high power, continuous CO_2 laser irradiation. *Am J Ophthalmol* 1967; 2:209-222.
39. Beckman H, Rota A, Barraco R: Linbectomies, keratectomies and keratotomies performed with a rapid-pulsed carbon dioxide laser. *Am J Ophthalmol* 1971; 71:1277-1283.
40. Keates RH, Pedrotti L, Weichel H, et al: Carbon dioxide laser beam control for corneal surgery. *Ophthalmic Surg* 1981; 12:117-122.
41. Macdonald JM, Simpson OA, McCarey BE, et al: The CO_2 laser as a tool for corneal surgery. *Proceedings, International Conference on Lasers*, 1987, in press.
42. Seiler T, Marshall J, Rothery S, et al: The potential of an infrared hydrogen fluoride laser on corneal surgery. *Lasers Ophthalmol* 1986; 1:49-60.
43. Loertscher H, Mandelbaum S, Parel JM, et al: Non-contact trephination of the cornea using a pulsed hydrogen fluoride laser. *Am J Ophthalmol* 1987; 104:471-475.
44. Loertscher H, Parel JM, Parrish RK, et al: Laser trephination of the cornea. *Am J Ophthalmol*, in press.
45. ———: Effect of selected beam parameters on corneal incisions produced with a hydrogen fluoride laser. *Am J Ophthalmol*, in press.
46. Troutman RC, Véronneau-Troutman S, Jakobiec FA, et al: A new laser for collagen wounding in corneal and strabismus surgery: A preliminary report. *Trans Am Ophthalmol Soc* 1986; 84:117-332.
47. Rhodes CK: *Excimer Lasers*. New York, Springer-Verlag, 1984.
48. Garrison BJ, Srinivasan R: Microscopic model for the ablative photodecomposition of polymers by far ultraviolet radiation (193 nm). *Appl Phys Lett* 1984; 44:849-851.

49. Puliafito CA, Wong K, Steinert RF: Quantitative and ultrastructural studies of excimer laser ablation of the cornea at 193 and 248 nanometers. *Lasers Surg Med* 1987; 7:155-159.
50. Gaster RN, Binder PS, Coalwell K, et al: Corneal surface ablation by 193 nm excimer laser and wound healing in rabbits. *Invest Ophthalmol Vis Sci* 1989; 30:90-98.
51. Krueger RR, Trokel SL: Quantitation of corneal ablation by ultraviolet laser light. *Arch Ophthalmol* 1985; 103:1741-1742.
52. Seiler T, Wollensak J: In vivo experiments with excimer laser: Technical parameters and healing processes. *Ophthalmologica* 1986; 192:65-70.
53. Lieurance RC, Patel AC, Wan WL, et al: Excimer laser cut lenticules for epikeratophakia. *Am J Ophthalmol* 1987; 103:475-476.
54. Trentacoste J, Thompson K, Parrish RK, et al: Mutagenic potential of a 193 nm excimer laser on fibroblasts in tissue cultures. *Ophthalmology* 1987; 94:125-129.
55. Munnerlyn R, Kooms SJ, Marshall J: Photorefractive keratectomy: A technique for laser refractive surgery. *J Cataract Refract Surg* 1988; 14:46-52.
56. Marshall J, Trokel SL, Rothery S, et al: Long-term healing of the central cornea after photorefractive keratectomy using an excimer laser. *Ophthalmology* 1988; 95:1411-1421.
57. Serdarevic ON, Hanna K, Gribomont A, et al: Excimer laser trephination in penetrating keratoplasty: Morphologic features in wound healing. *Ophthalmology* 1988; 95:493-505.
58. Tenner A, Neuhann T, Schroder E, et al: Excimer laser radial keratotomy in the living human eye: A preliminary report. *J Refract Surg* 1988; 4:5-8.
59. Hanna K, Chastang JC, Pouliquen Y, et al: Excimer laser keratectomy for myopia with a rotating slit delivery system. *Arch Ophthalmol* 1988; 106:245-250.
60. L'Esperance FA, Warner JW, Telfair WB, et al: Excimer laser instrumentation and technique for human corneal surery. *Arch Ophthalmol* 1989; 107:131-139.
61. Hanna K, Pouliquen Y, Waring G, et al: Corneal stromal wound healing in rabbits after 193-nm excimer laser surface ablation. *Arch Ophthalmol* 1989; 107:895-901.
62. Krueger RR, Trokel SS, Shubert H: Interaction of UV light with the cornea. *Invest Ophthalmol Vis Sci* 1985; 26:1455-1464.
63. Peyman GA, Kuszak JR, Weckstrom K, et al: Effects of Xe excimer laser on the eyelid in anterior segment structures. *Arch Ophthalmol* 1986; 104:118-122.
64. Aron-Rosa DS, Boulnoy JL, Carre F, et al: Excimer laser surgery of the cornea: Qualitative and quantitative aspects of photoablation according to the energy density. *J Cataract Refract Surg* 1986; 12:27-33.
65. Seiler T, Bende T, Wollensak J: Laserchinurgie der Hornhaut. *Forstot Ophthalmol* 1987; 84:513-518.
66. Hanna K. Chastang JC, Pouliquen Y, et al: A rotating slit delivery system for excimer laser refractive keratoplasty. *Am J Ophthalmol* 1987; 103:474.
67. McDonald MB, Beuerman R, Falzoni W, et al: Refractive surgery with excimer laser. *Am J Ophthalmol* 1987; 103:469.
68. Trokel S, Munnerlyn CF: Excimer laser ophthalmic delivery systems. *Ophthalmology*, in press.
69. Schroder E, Dardenne MU, Neuhann T, et al: An ophthalmic excimer laser for corneal surgery. *Am J Ophthalmol* 1987; 103:472-473.
70. Bende T, Seiler T, Wollensak J: Side effect in excimer corneal surgery: Corneal thermal gradients. *Albrecht Von Graefes Arch Klin Exp Ophthalmol* 1988; 226:277-280.
71. Nuss RC, Puliafito CA, Dehm E: Unscheduled DNA synthesis following excimer laser ablation of the cornea in vivo. *Invest Ophthalmol Vis Sci* 1987; 28:287-294.
72. Seiler T, Bende T, Winckler K, et al: Side effects in excimer corneal surgery: DNA damage as a result of 193 nm excimer laser radiation. *Albrecht Von Graefes Arch Klin Exp Ophthalmol*, in press.
73. Cotlier AM, Shubert HD, Mandel E, et al: Excimer laser keratotomy. *Ophthalmology* 1985; 92:206-208.

74. Stern D, Lin W, Puliafito CA, et al: Femtosecond optical ranging of corneal incision depth. *Invest Ophthalmol Vis Sci* 1989; 30:99-104.
75. Sanders DR (ed): *Radial Keratotomy Surgical Techniques*. Thorofare, Slack, Inc, 1986, pp 99-130.
76. Kerr-Muir MG, Trokel SL, Marshall J: Ultrastructural comparison of conventional surgical and argon fluoride excimer laser keratectomy. *Am J Ophthalmol* 1987; 103: 448-453.
77. Stephenson G, Salmeron B, McDonald M, et al: Healing characteristics and power predictability of freeze/lyophilized epikeratophakia tissue lenses and non-freeze epikeratophakia tissue lenses. *Invest Ophthalmol Vis Sci* (Suppl) 1988; 29:282.
78. Aron-Rosa DS, Boerner CF, Bath P, et al: Corneal would healing after laser keratotomy in a human eye. *Am J Ophthalmol* 1987; 103:44-464.
79. L'Esperance FA, Taylor DM, Warner JW: Human excimer laser keratectomy: Short-term histopathology. *J Refract Surg* 1988; 4:118-124.
80. Cotten KL, Tripoli NK: Tissue fit and corneal shape after transplantation. *Invest Ophthalmol Vis Sci* (Suppl) 1987; 28:276.
81. Tuft S, Marshall J, Rothery S: Stromal remodeling following photorefractive keratectomy. *Lasers Ophthalmol* 1987; 1:177-183.
82. Waring GO, Rodrigues MM: Patterns of pathologic response in the cornea. *Surv Ophthalmol* 1987; 31:262-266.
83. Gipson IK: Hemidesmosome formation in vitro. *J Cell Biol* 1983; 97:849.
84. Steinert RF, Wagoner MD: Long-term comparison of epikeratoplasty and penetrating keratoplasty for keratoconus. *Arch Ophthalmol* 1988; 106:493-496.
85. Barraquer E, Loertscher HP, Davis J, et al: Corneal wound healing following laser excisions. *Invest Ophthalmol Vis Sci* 1988; 29:390.
86. Hanna K, Chastang C, Asfar L, et al: Scanning slit delivery system. *J Cataract Refract Surg* 1989; 15:390-396.
87. Fantes FE, Waring GO: Effect of excimer laser radiant exposure on uniformity of ablated corneal surface. *Lasers Surg Med*, in press.
88. Hanna KD, Jouve FE, Bercovier MH, et al: Computer simulation of lamellar keratectomy and laser myopic keratomileusis. *J Refract Surg* 1988; 4:222-231.
89. Hanna K, Jouve F, Waring G, et al: Computer simulation of arcuate and radial incisions involving the corneoscleral limbus. *Eye* 1989; 3:227-239.
90. Hanna K, Jouve F, Waring G: Preliminary computer simulation of the effects of radial keratotomy. *Arch Ophthalmol* 1989; 107:911-918.
91. Melki T, Cavanagh HD, Jester JV, et al: Effects of correlation of *in vivo* confocal tandem scanning microscopy (TSM) observations of effects of thromboxain antagonist Ag 23848 B (Galxco, Gr Brit) and ouabain on rabbit corneal endothelium with scanning and transmission electron microscopy and lanthanum penetration studies. *Invest Ophthalmol Vis Sci* (Suppl) 1988; 29:257.
92. Zabel R, Tuft S, Marshall J: Excimer laser photorefractive keratectomy: Endothelial morphology following area ablation of the cornea *Invest Ophthalmol Vis Sci* (Suppl) 1988; 29:390.
93. Fantes F, Hanna K, Waring G, et al: Myopic laser keratomileusis on monkeys: Clinical microscopic and ultrastructural observations. *Invest Ophthalmol Vis Sci* (Suppl) 1989; 30:217.
94. Thompson K, Hanna K, Waring G: Emerging technologies for refractive surgery: Laser adjustable synthetic epikeratoplasty. *Ref Corneal Surg* 1989; 5:46-49.